71 Ferroelectric and antiferroelectric liquid crystals

Liquid crystals are grouped into two: 71A which exhibits the ferroelectric hysteresis loops as shown in Fig. IB-1 in Introduction, and 71B which exhibits the antiferroelectric hysteresis loops as in Fig. IB-2. Triple hysteresis loops appear in some phases in the group 71B. Such phases are often called "ferrielectric" and indicated by F′ in this section.

71A Ferroelectric liquid crystals

No. 71A-1 DOBAMBC and analogues

(A) $C_nH_{2n+1}O$–⬡–CH=N–⬡–CH=CHCOOCH$_2$CH(CH$_3$)C$_2$H$_5$

n = 5: POBAMBC (*p*-pentyloxybenzylidene *p′*-amino 2-methylbutyl cinnamate)
n = 6: HOBAMBC (*p*-hexyloxybenzylidene *p′*-amino 2-methylbutyl cinnamate)
n = 7: HpOBAMBC (*p*-heptyloxybenzylidene *p′*-amino 2-methylbutyl cinnamate)
n = 8: OOBAMBC (*p*-octyloxybenzylidene *p′*-amino 2-methylbutyl cinnamate)
n = 9: NOBAMBC (*p*-nonyloxybenzylidene *p′*-amino 2-methylbutyl cinnamate)
n = 10: DOBAMBC (*p*-decyloxybenzylidene *p′*-amino 2-methylbutyl cinnamate)
n = 12: DDOBAMBC (*p*-dodecyloxybenzylidene *p′*-amino 2-methylbutyl cinnamate)
n = 14: TDOBAMBC (*p*-tetradecyloxybenzylidene *p′*-amino 2-methylbutyl cinnamate)

1a Possibility of the ferroelectric activity of *L*-DOBAMBC in the smectic C* phase was reported by Meyer et al. in 1975. 75Mey
Ferroelectric hysteresis loops were observed in the smectic C* and the H* phases by Yoshino et al. in 1977. 77Yos

b

phase		IV	III	II	I	I′
		crystalline solid	smectic H* (Sm H*)	smectic C* (Sm C*)	smectic A (Sm A)	isotropic liquid
state			F	F	P	
Θ [°C]	n = 5	55.5	79	81		
	6	62.5	76	86		
	7	75	(71)	94		
	8	74.5	(68)	93	118	
	9	75	(65)	95.5		
	10	76	(63)	92		
	12		60	87		
	14	72.5		86		( ): cooling

76Kel, 79Yos, 80Kon

Phase diagram of mixtures:
(DOBAMBC)–(PAA): Fig. 71A-1-001.
(DOBAMBC)–(DOBA-1-MPC): Fig. 71A-1-002.
(DOBAMBC)–(HDOBAMBC): Fig. 71A-1-003.
(DOBAMBC)–(4-methoxybenzylidene aminocinnamic acid n-butyl ester): see Phase diagram in external magnetic field: Fig. 71A-1-004; 82Ima
see also Fig. 71A-1-057 in subsection 12.

3b Tilt angle and helical pitch in the Sm C* phase: Fig. 71A-1-005, Fig. 71A-1-006, Fig. 71A-1-007, Fig. 71A-1-008, Fig. 71A-1-009 , Fig. 71A-1-010, Fig. 71A-1-011, Fig. 71A-1-012, Fig. 71A-1-013, Fig. 71A-1-014, Fig. 71A-1-015;
see also Fig. 71A-1-032, Fig. 71A-1-033, Fig. 71A-1-034 in subsection 5c.

5a	Dielectric constant: Fig. 71A-1-016, Fig. 71A-1-017. Dielectric dispersion: Fig. 71A-1-018, Fig. 71A-1-019, Fig. 71A-1-020, Fig. 71A-1-021, Fig. 71A-1-022, Fig. 71A-1-023, Fig. 71A-1-024. Dielectric constant of $(DOBAMBC)_{1-x}(PAA)_x$: Fig. 71A-1-025. κ' vs. T under various pressures: Fig. 71A-1-026. κ'' vs. T under various pressures: see Phase diagram in regard to hydrostatic pressure: Fig. 71A-1-027, Fig. 71A-1-028.	85Yas
b	Effects of measuring electric field and dc bias field: Fig. 71A-1-029, Fig. 71A-1-030.	
c	Spontaneous polarization: Fig. 71A-1-031, Fig. 71A-1-032, Fig. 71A-1-033, Fig. 71A-1-034; see also Spontaneous polarization of mixtures: Fig. 71A-1-035, Fig. 71A-1-036; see also Effect of hydrostatic pressure on P_s: Fig. 71A-1-037. Coercive field: Fig. 71A-1-038.	84Tak 82Ima
d	Pyroelectric coefficient: see Fig. 71A-1-034. Relaxation time of pyroelectric response: Fig. 71A-1-039.	
6a	Heat capacity: Fig. 71A-1-040, Fig. 71A-1-041.	
7a	Shear flow induced voltage: Fig. 71A-1-042, Fig. 71A-1-043.	
9a	Refractive indices: Fig. 71A-1-044. Birefringence: Fig. 71A-1-045. Transmission: Fig. 71A-1-046, Fig. 71A-1-047.	
b	Effect of E_{bias} on transmission of light: Fig. 71A-1-048. Threshold field of electro-optic effect: Fig. 71A-1-049. Response time of electro-optic effect: see	78Yos, 79Iwa, 80Cla, 79Yos, 84Yos1, 84Yos2, 85Oza
c	Acoustical phenomena: see	84Kap
d	Optical activity: Fig. 71A-1-050, Fig. 71A-1-051, Fig. 71A-1-052, Fig. 71A-1-053.	
e	SHG: Fig. 71A-1-054. Nonlinear optical susceptibility under applied electric field: Fig. 71A-1-055; see also	87Yos
11	Electrical conductivity: Fig. 71A-1-056.	
12	Phase diagram for magnetic field: Fig. 71A-1-057.	
13a	NMR of ^{13}C: Fig. 71A-1-058, Fig. 71A-1-059.	
14b	Phason dispersion by light scattering: Fig. 71A-1-060.	

(B) $C_2H_{2n+1}O$–⬡–CH=N–⬡–CH=CHCOOCH(CH_3)C_mH_{2m+1}

***p*-alkoxybenzylidene *p′*-amino-1-methylalkyl cinnamate**

n = 10, m = 2: DOBA-1-MPC

n = 10, m = 3: DOBA-1-MBC

n = 10, m = 4: DOBA-1-MPeC

1b

phase		IV	III [a])	II	I	I′
		crystalline solid	smectic* (Sm*)	smectic C* (Sm C*)	smectic A (Sm A)	isotropic liquid
state			F	F	P	
Θ [°C]						
m = 2	n = 6	75	80	98	119	
	10 [b])	41	61	89	106	
	14	58		86	98	
	18	61		62	83	
m = 3	n = 8	76		82	86	
	10	73		83	85	
	14	63			79	

[a]) Undefined chiral smectic phase.

[b]) See also Fig. 71A-1-002.

84Sak

3b Helical pitch: Fig. 71A-1-061.
Tilt angle: see Fig. 71A-1-067 in subsection 5c and also 90Lev

5a Dielectric constant: Fig. 71A-1-062, Fig. 71A-1-063, Fig. 71A-1-064.

c Spontaneous polarization: Fig. 71A-1-065, Fig. 71A-1-066, Fig. 71A-1-067; see also 90Lev

6a Heat capacity: Fig. 71A-1-068.

(C) $C_nH_{2n+1}O$–⬡–CH=N–⬡–$COOCH_2CH(CH_3)C_2H_5$

2-methylbutyl 4-(4′-alkoxybenzylidene-amino) benzoate

1b

phase		III	II	I	I′
		crystalline solid	smectic C* (Sm C*)	smectic A (Sm A)	isotropic liquid
state			F	P	
Θ [°C]	n = 7	46.1	(35.2)	61.4	
	8	41.3	(39.3)	66.0	
	9	59.8	(41.6)	66.0	
	10	52.0	(42.2)	68.0	
	12	47.5	(40.6)	68.5	( ): cooling

85Kon

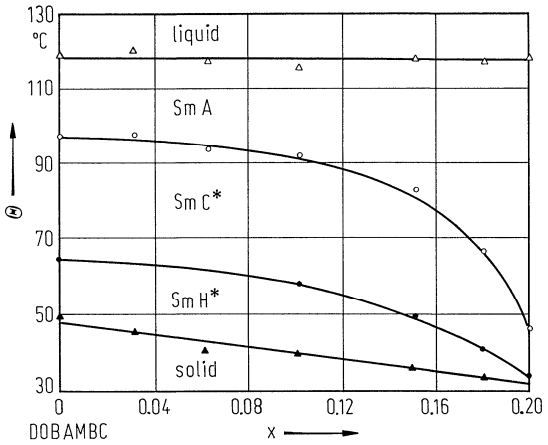

Fig. 71A-1-001. $(DOBAMBC)_{1-x}(PAA)_x$. Θ vs. x [80Uem]. PAA: *p*-azoxyanisole.

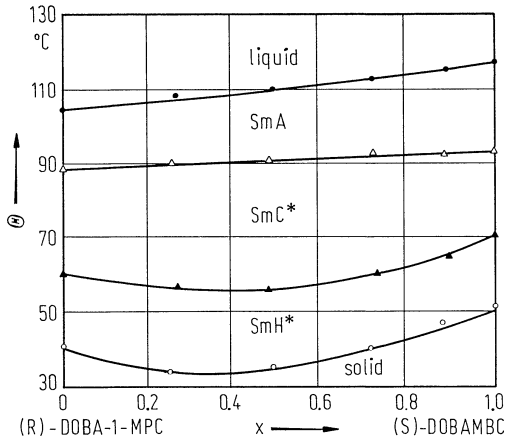

Fig. 71A-1-002. $(DOBAMBC)_x(DOBA\text{-}1\text{-}MPC)_{1-x}$. Θ vs. x [85Sak].

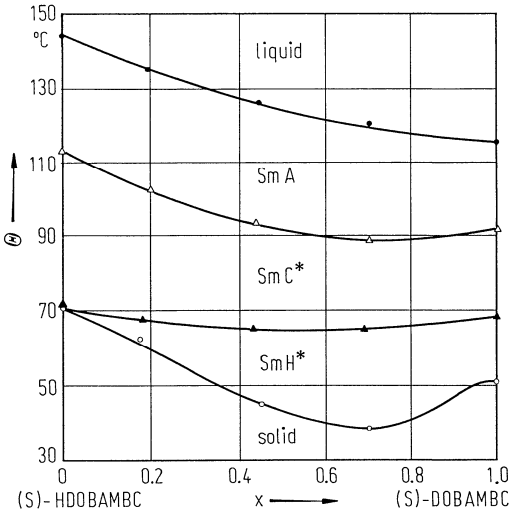

Fig. 71A-1-003. $(DOBAMBC)_x(HDOBAMBC)_{1-x}$. Θ vs. x [85Sak].

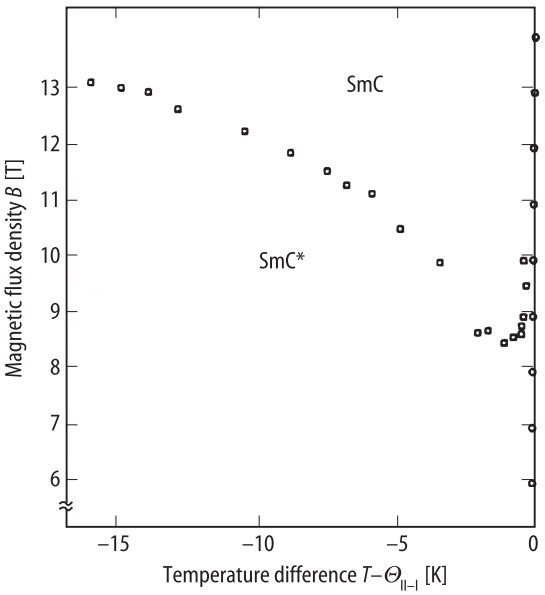

Fig. 71A-1-004. DOBAMBC. Phase diagram for *B* [84Bli]. *B*: magnetic flux density. Unmodulated SmC phase is induced in the high *B* region.

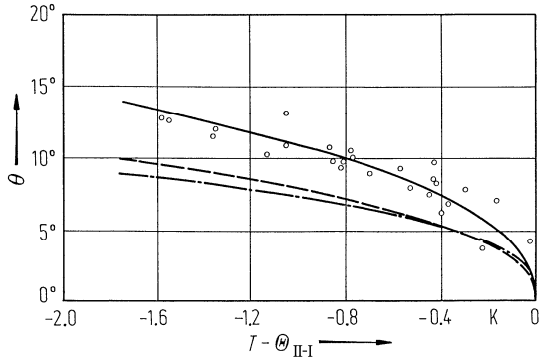

Fig. 71A-1-005. DOBAMBC. θ vs. $T - \Theta_{II–I}$ near $\Theta_{II–I}$ [81Mar]. θ: tilt angle. Full line and open circle: homeotropic geometry (optical measurement). Dashed line: homogeneous geometry (optical). Dot-dashed line: homogeneous geometry (X-ray).

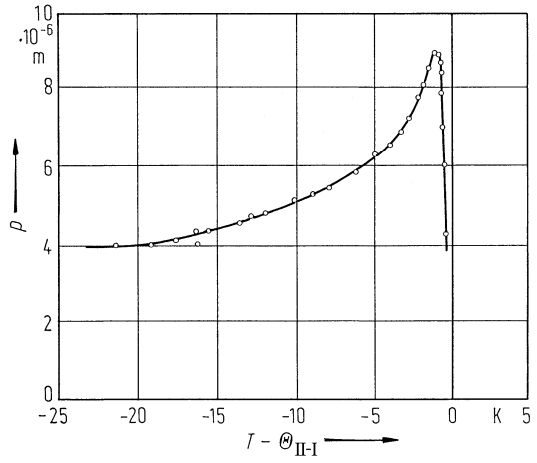

Fig. 71A-1-006. DOBAMBC. p vs. $T - \Theta_{I-I}$ [78Ost1]. p: helical pitch.

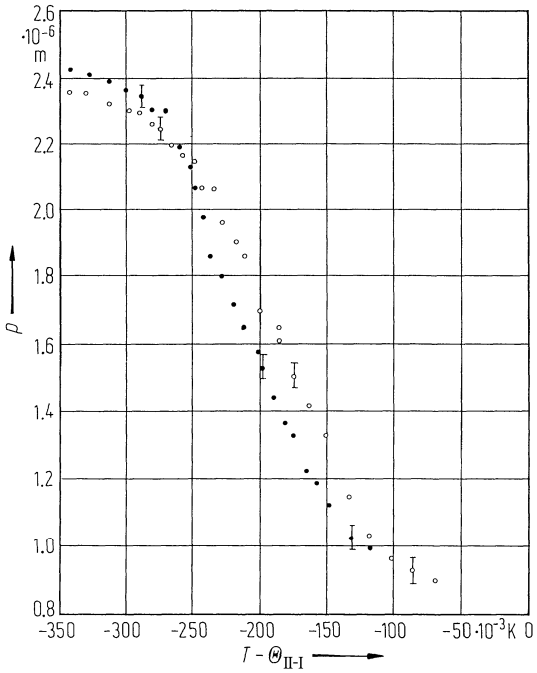

Fig. 71A-1-007. DOBAMBC. p vs. $T - \Theta_{I-I}$ [84Mus]. p: helical pitch. λ: wavelength of light. Full circle: λ = 647.1 nm. Open circle: λ = 647.1 nm.

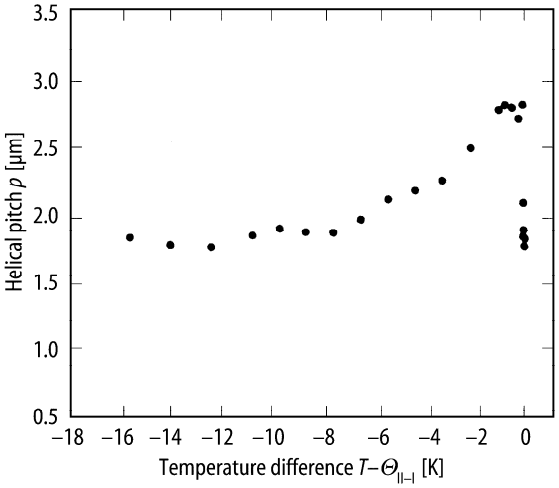

Fig. 71A-1-008. DOBAMBC. p vs. $T - \Theta_{II-I}$ [90Lev]. p: helical pitch.

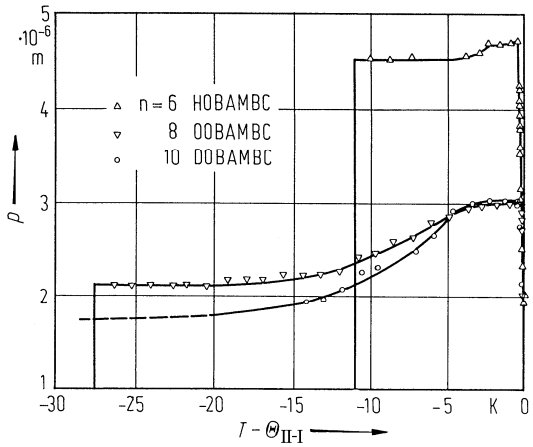

Fig. 71A-1-009. DOBAMBC, OOBAMBC, HOBAMBC. p vs. $T - \Theta_{II-I}$ [80Kon]. p: helical pitch.

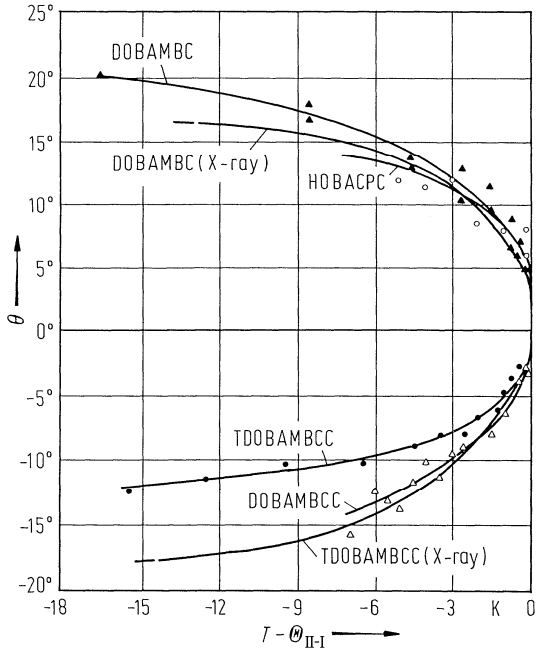

Fig. 71A-1-010. DOBAMBC, DOBAMBCC, TDOBAMBCC, HOBACPC. θ vs. $T - \Theta_{II–I}$ in monodomain specimen [76Mar]. θ: tilt angle. Full line and open circle: homeotropic.

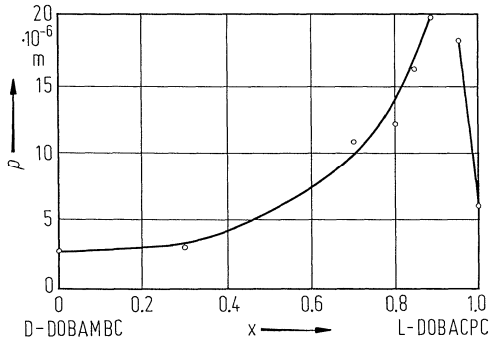

Fig. 71A-1-011. $(DOBAMBC)_{1–x}(DOBACPC)_x$. p vs. x at $T = \Theta_{II–I} – 1$ K [80Yos]. p: helical pitch. x: molar fraction of L-DOBACPC in the mixture with D-DOBAMBC.

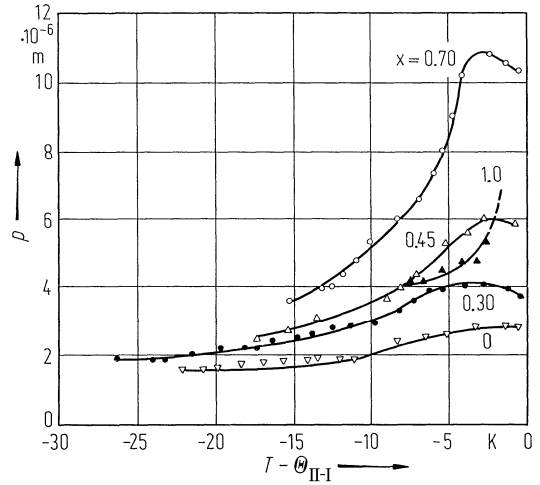

Fig. 71A-1-012. $(DOBAMBC)_{1-x}(DOBACPC)_x$. p vs. $T - \Theta_{II-I}$ [81Uem]. p: helical pitch. Parameter: x. x: molar fraction of DOBACPC in the mixture with DOBAMBC.

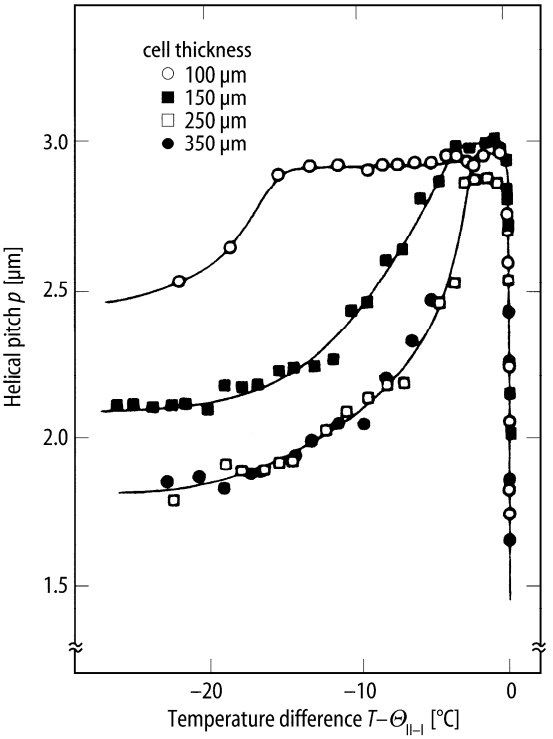

Fig. 71A-1-013. OOBAMBC. p vs. $T - \Theta_{II-I}$ [84Tak]. Parameter: cell thickness. p: helical pitch.

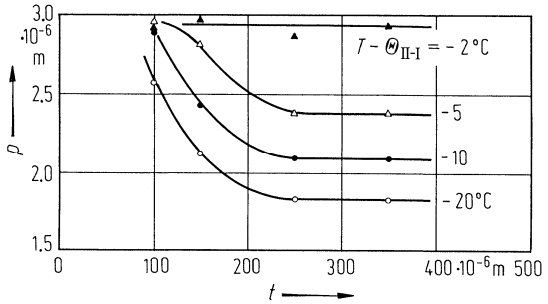

Fig. 71A-1-014. OOBAMBC. p vs. t [82Kon]. Parameter: $T - \Theta_{II–I}$. p: helical pitch. t: cell thickness.

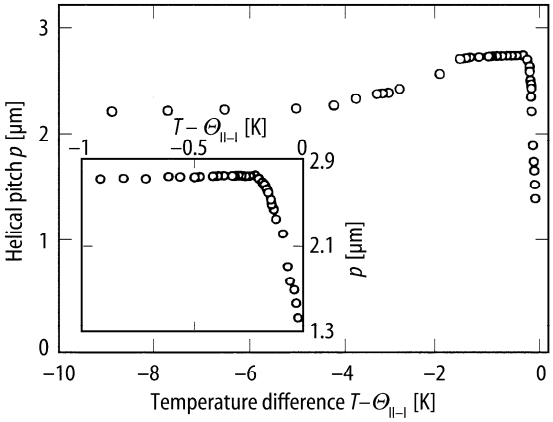

Fig. 71A-1-015. OOBAMBC. p vs. $T - \Theta_{II–I}$ near $\Theta_{II–I}$ [91Pra]. p: helical pitch. Insert shows the data in close vicinity of $\Theta_{II–I}$.

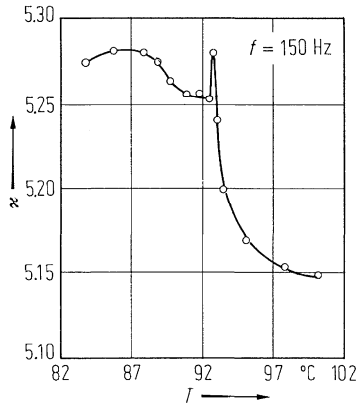

Fig. 71A-1-016. DOBAMBC. κ vs. T [77Yos]. f = 150 Hz.

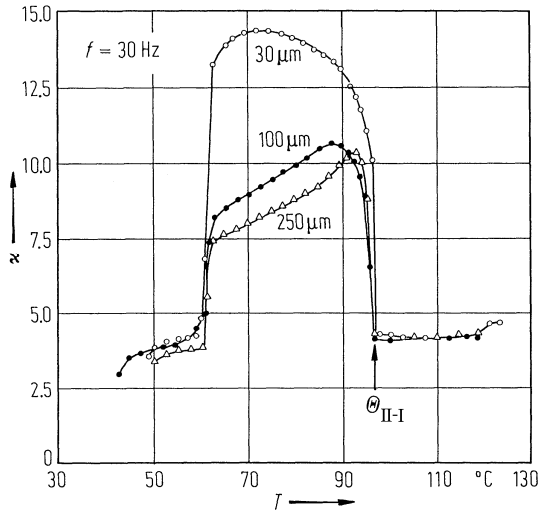

Fig. 71A-1-017. DOBAMBC. κ vs. T [83Yos]. Parameter: cell thickness. f = 30 Hz.

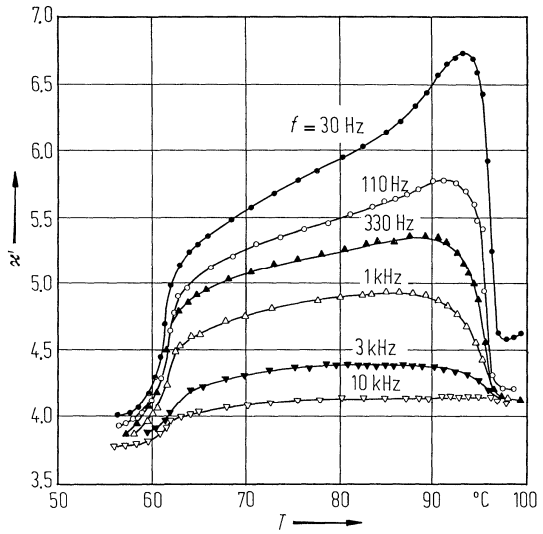

Fig. 71A-1-018. DOBAMBC. κ' vs. T between 30 Hz and 10 kHz [83Yos]. Parameter: f. Cell thickness: 2.3 µm.

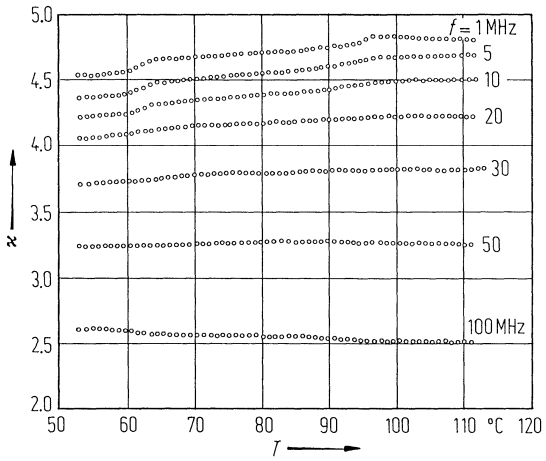

Fig. 71A-1-019. DOBAMBC. κ vs. T between 1 MHz and 100 MHz [84Mar]. Parameter: f.

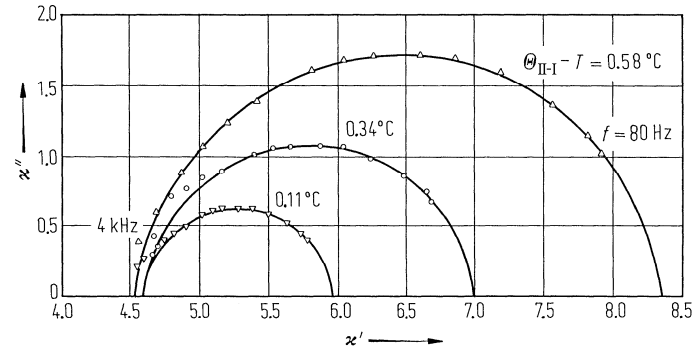

Fig. 71A-1-020. DOBAMBC. κ' vs. κ'' (Cole-Cole diagram) [79Lev]. Parameter: $\Theta_{II-I} - T$.

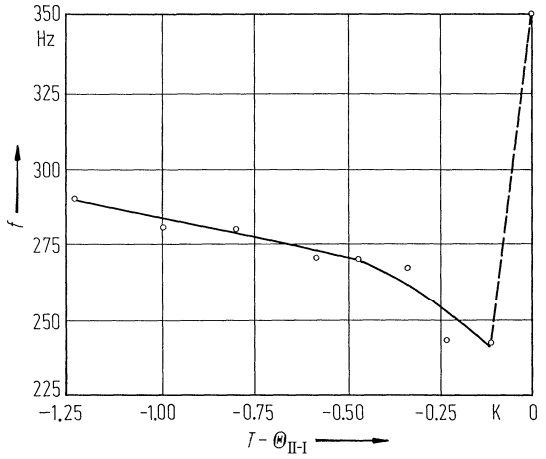

Fig. 71A-1-021. DOBAMBC. f vs. $T - \Theta_{II-I}$ near Θ_{II-I} [79Lev]. f: relaxation frequency of dielectric dispersion.

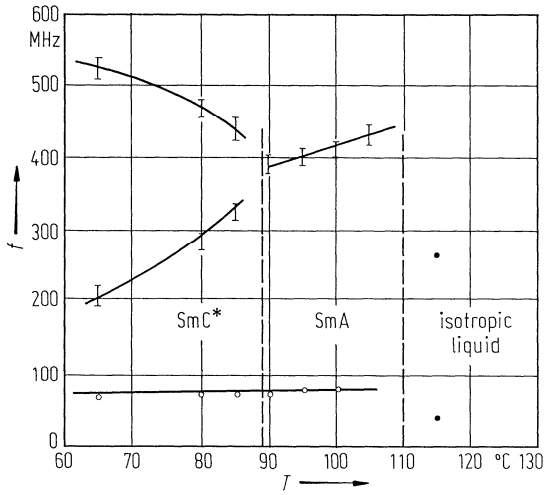

Fig. 71A-1-022. DOBAMBC. f vs. T [82Ben]. f: relaxation frequency of dielectric dispersion.

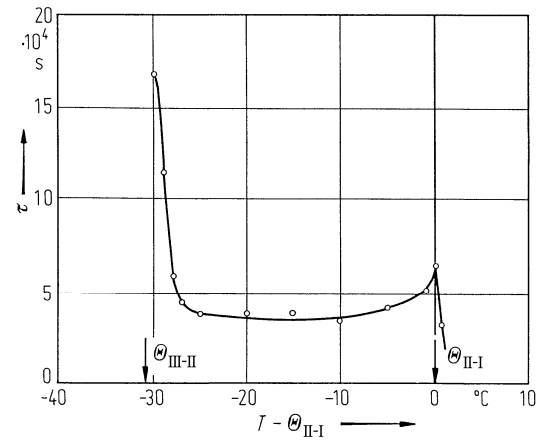

Fig. 71A-1-023. DOBAMBC. τ vs. $T - \Theta_{II-I}$ [78Hof]. τ: dielectric relaxation time.

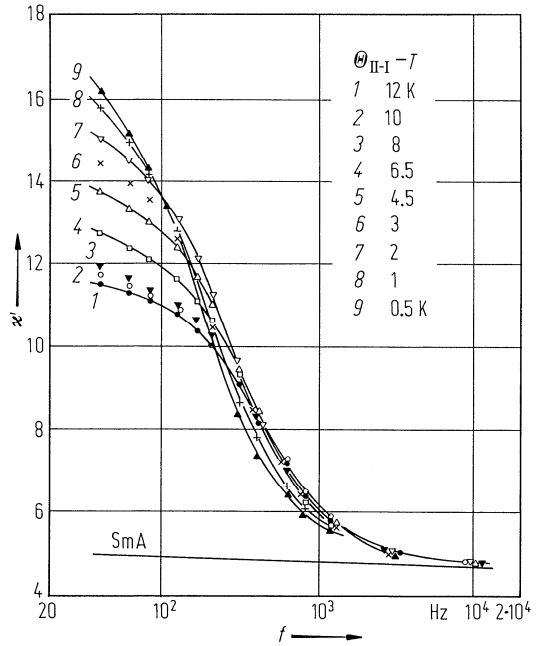

Fig. 71A-1-024. DOBAMBC. κ' vs. f [78Ost2]. Parameter: $\Theta_{I-I} - T$. f: measuring frequency.

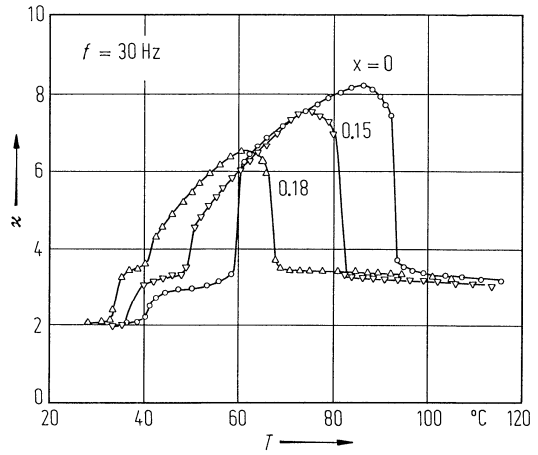

Fig. 71A-1-025. $(DOBAMBC)_{1-x}(PAA)_x$. κ vs. T [80Uem]. Parameter: x. f = 30 Hz. PAA: *p*-azoxyanisole.

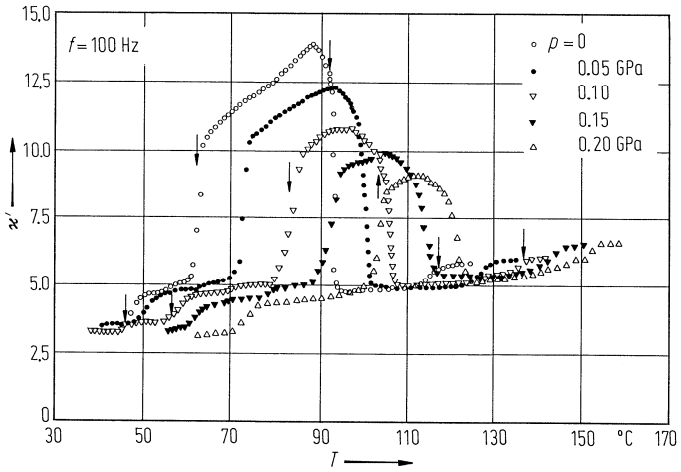

Fig. 71A-1-026. DOBAMBC. κ' vs. T [85Yas]. Parameter: p. f = 100 Hz. Arrows indicate transitions.

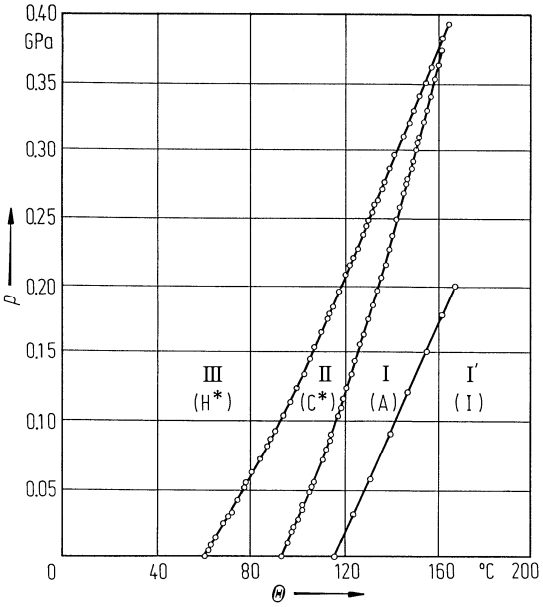

Fig. 71A-1-027. DOBAMBC. p vs. Θ [84Pra]. p: hydrostatic pressure. Θ: phase transition temperature.

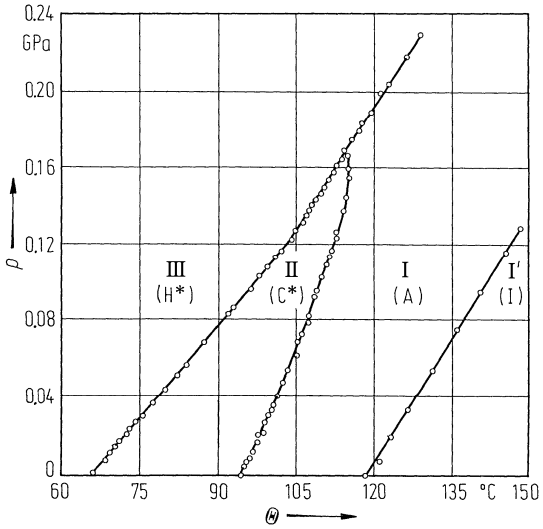

Fig. 71A-1-028. OOBAMBC. p vs. Θ [84Pra]. p: hydrostatic pressure. Θ: phase transition temperature.

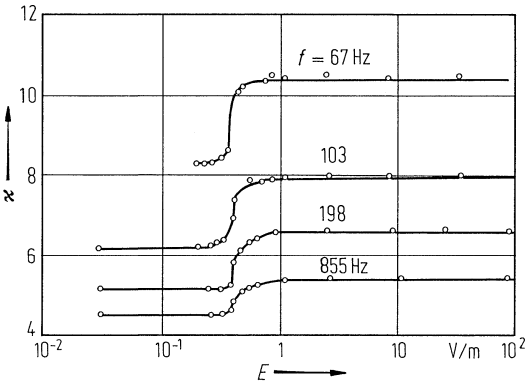

Fig. 71A-1-029. DOBAMBC. κ vs. E [84Mar]. Parameter: f. E: measuring electric field. T = 82 °C.

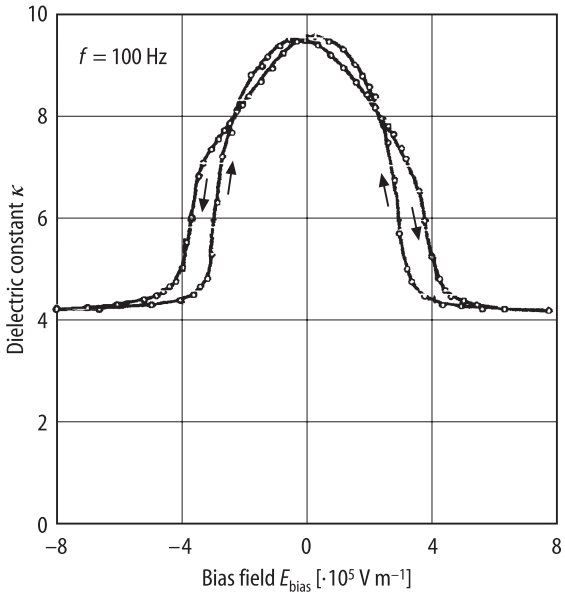

Fig. 71A-1-030. DOBAMBC. κ vs. E_{bias} [79Yos]. E_{bias}: dc biasing electric field. Cell thickness: 100 µm. T = 82 °C. f = 100 Hz.

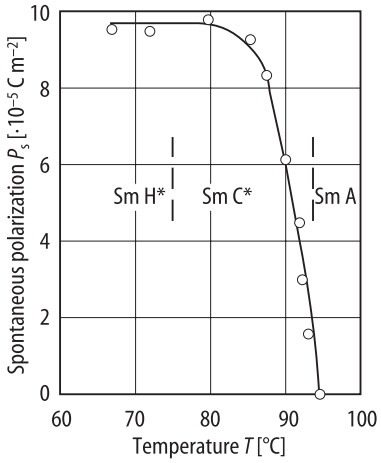

Fig. 71A-1-031. DOBAMBC. P_s vs. T [77Yos].

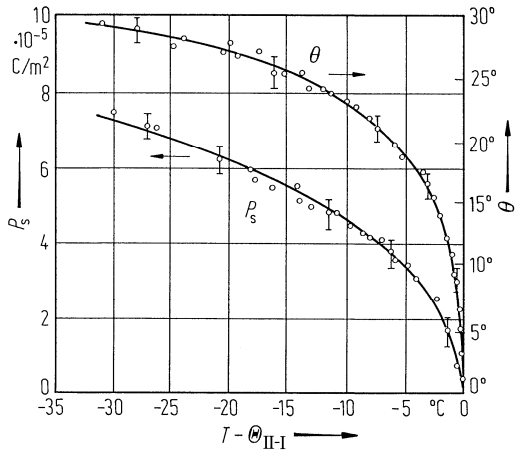

Fig. 71A-1-032. DOBAMBC. P_s, θ vs. $T - \Theta_{II-I}$ [77Ost1]. θ: tilt angle.

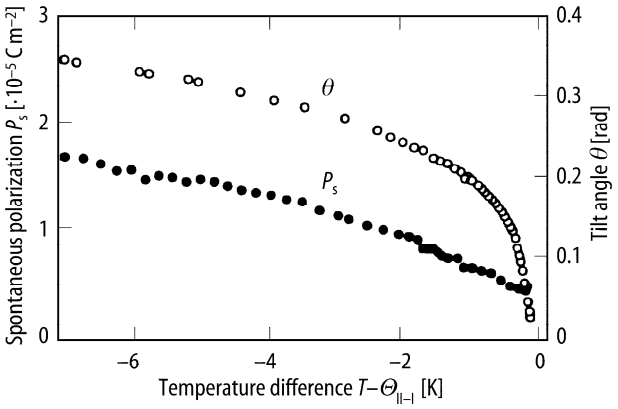

Fig. 71A-1-033. OOBAMBC. P_s, θ vs. $T - \Theta_{II-I}$ [91Pra]. θ: tilt angle.

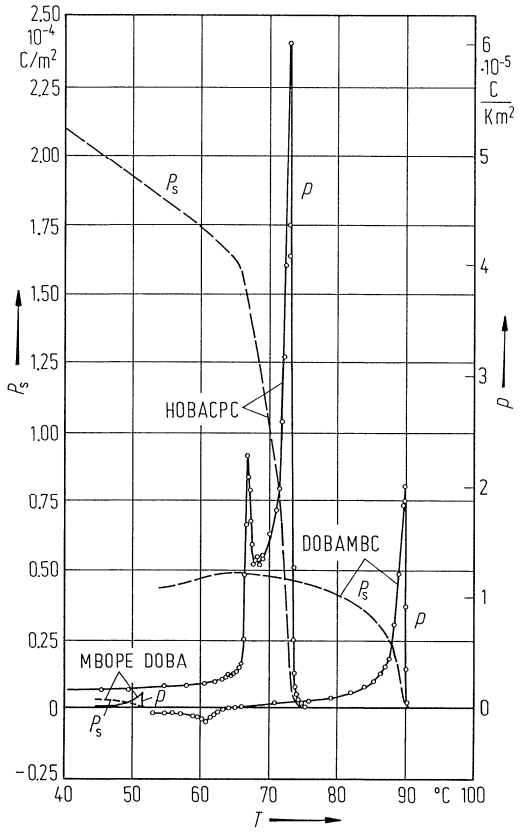

Fig. 71A-1-034. DOBAMBC, HOBACPC, MBOPE DOBA. P_s, p vs. T [81Ber]. p: pyroelectric coefficient. MBOPE DOBA: *d*-4-(2-methylbutoxy)-phenyl ester of 4-decyloxybenzoic acid.

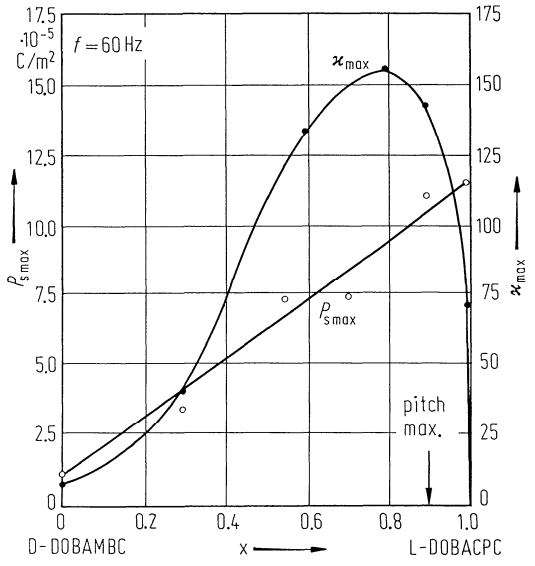

Fig. 71A-1-035. $(DOBAMBC)_{1-x}(DOBACPC)_x$. $P_{s\,max}$, κ_{max} vs. x [81Yos]. $P_{s\,max}$,: maximum spontaneous polarization. κ_{max}: maximum dielectric constant. x: molar fraction of L-DOBACPC in the mixture with D-DOBAMBC. f = 60 Hz.

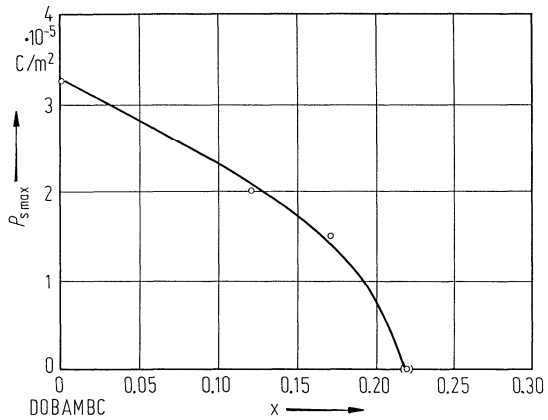

Fig. 71A-1-036. $(DOBAMBC)_{1-x}(PAA)_x$. $P_{s\,max}$ vs. x [80Uem]. $P_{s\,max}$,: maximum spontaneous polarization. PAA: *p*-azoxyanisole.

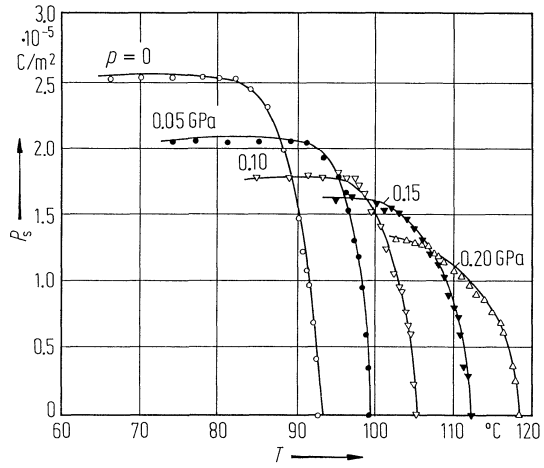

Fig. 71A-1-037. DOBAMBC. P_s vs. T [85Yas]. Parameter: p.

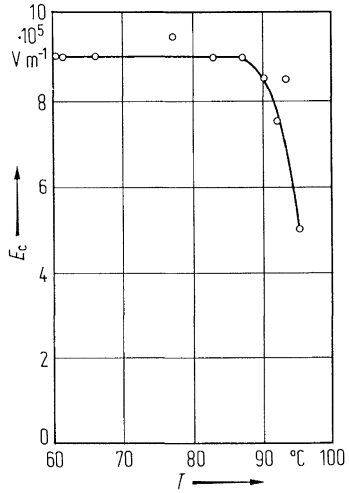

Fig. 71A-1-038. DOBAMBC. E_c vs. T [77Yos].

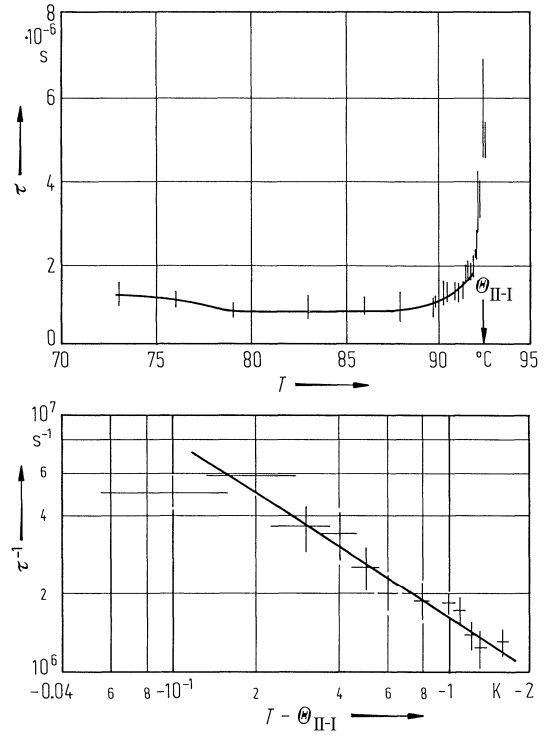

Fig. 71A-1-039. DOBAMBC. τ vs. T, τ^{-1} vs. $T - \Theta_{II-I}$ [79Bli]. τ: relaxation time determined from pyroelectric current measurement.

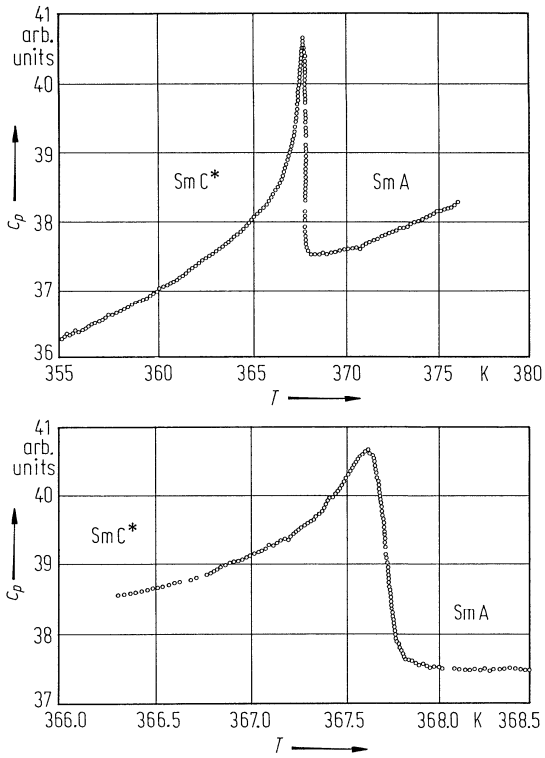

Fig. 71A-1-040. DOBAMBC. c_p vs. T [86Dum]. c_p: specific heat capacity at constant pressure.

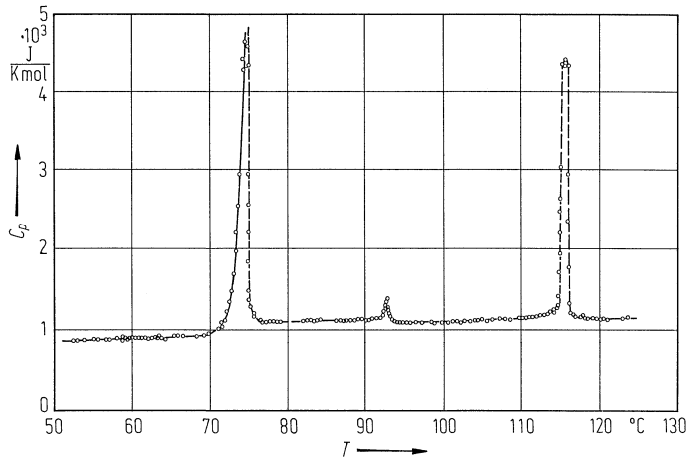

Fig. 71A-1-041. DOBAMBC. C_p vs. T [77Ost2]. C_p: molar heat capacity at constant pressure.

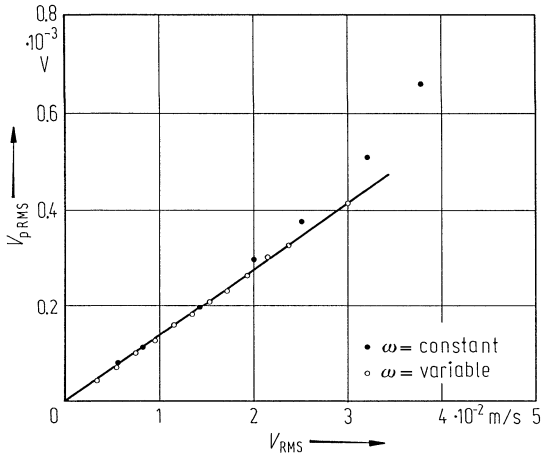

Fig. 71A-1-042. DOBAMBC. V_{pRMS} vs. V_{RMS} [75Pie]. V_{pRMS}: shear flow induced voltage. V_{RMS}: shear rate. T = 84 °C. ω: angular frequency of the sinewave velocity of the glass plate in the flow cell.

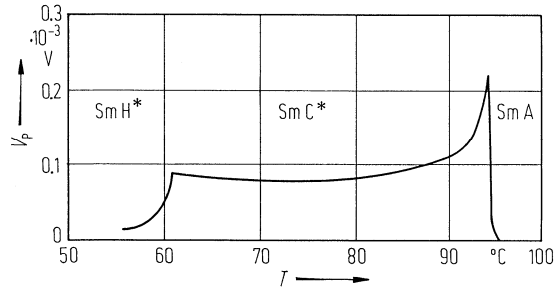

Fig. 71A-1-043. DOBAMBC. V_p vs. T [75Pie]. V_p: shear flow induced voltage. Shear rate: $7.58 \cdot 10^{-3}$ ms^{-1}.

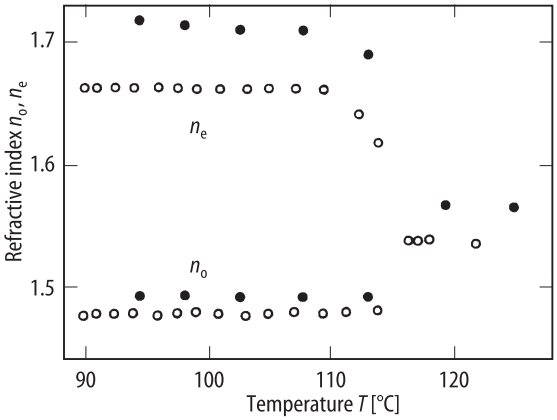

Fig. 71A-1-044. DOBAMBC. n_o, n_e vs. T [84Tak]. Open circle: λ = 2.68 µm. Full circle: λ = 633 nm.

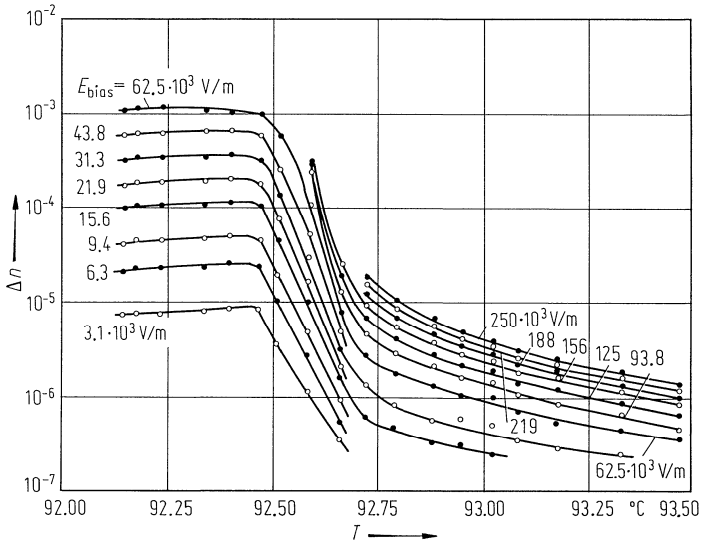

Fig. 71A-1-045. DOBAMBC. Δn vs. T [78Tak]. Parameter: E_{bias}. Δn: birefringence induced by applied field. λ = 632.8 nm.

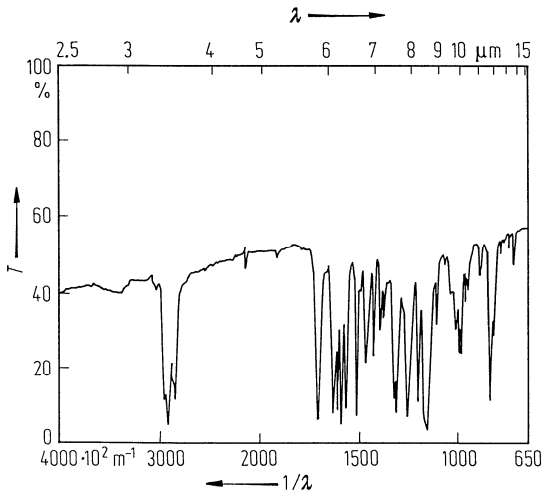

Fig. 71A-1-046. DOBAMBC. T vs. $1/\lambda$ at RT [85Yos]. T: transmission.

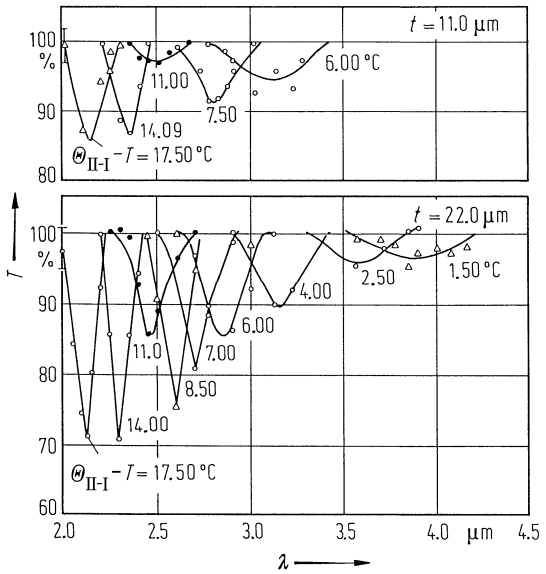

Fig. 71A-1-047. DOBAMBC. T vs. λ [85Abd]. T: transmission. t: cell thickness: Parameter: $\Theta_{\text{II–I}} - T$.

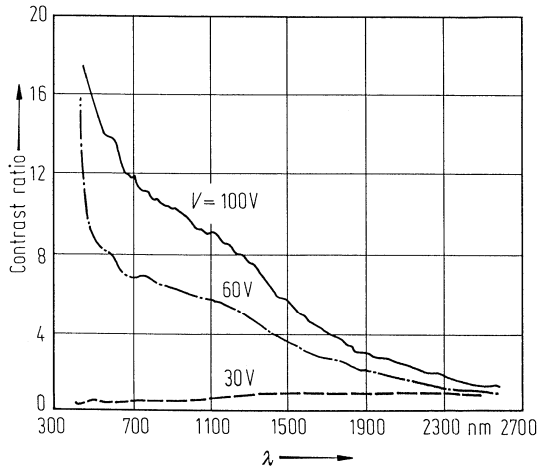

Fig. 71A-1-048. DOBAMBC. Contrast ratio vs. λ [85Yos]. Parameter: V. V: applied electric field. Cell thickness: 100 μm. T = 80 °C.

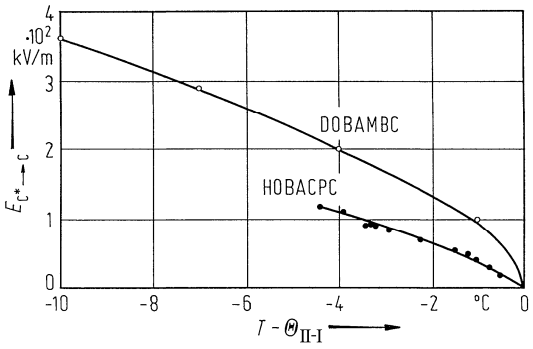

Fig. 71A-1-049. DOBAMBC, HOBACPC. $E_{C^* \rightarrow C}$ vs. $T - \Theta_{II-I}$ [84Yos2]. $E_{C^* \rightarrow C}$: threshold field of Sm C* → Sm C transition.

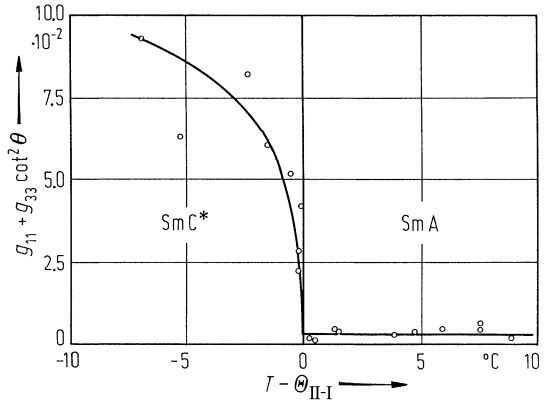

Fig. 71A-1-050. DOBAMBC. $g_{11} + g_{33} \cot^2 \theta$ vs. $T - \Theta_{II-I}$ [81Ues]. g_{11}, g_{33}: gyration tensor components. θ: tilt angle.

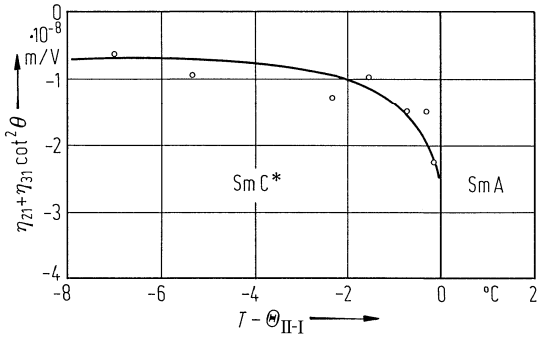

Fig. 71A-1-051. DOBAMBC. $\eta_{21} + \eta_{31} \cot^2 \theta$ vs. $T - \Theta_{II–I}$ [81Ues]. η_{21}, η_{31}: electro-gyration coefficients for E. θ: tilt angle.

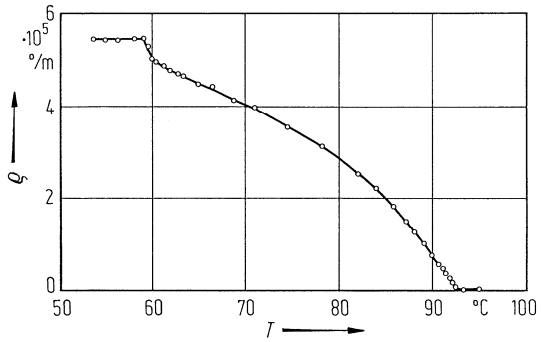

Fig. 71A-1-052. DOBAMBC. ρ vs. T [78Tak]. ρ: rotatory power. λ = 632.8 nm.

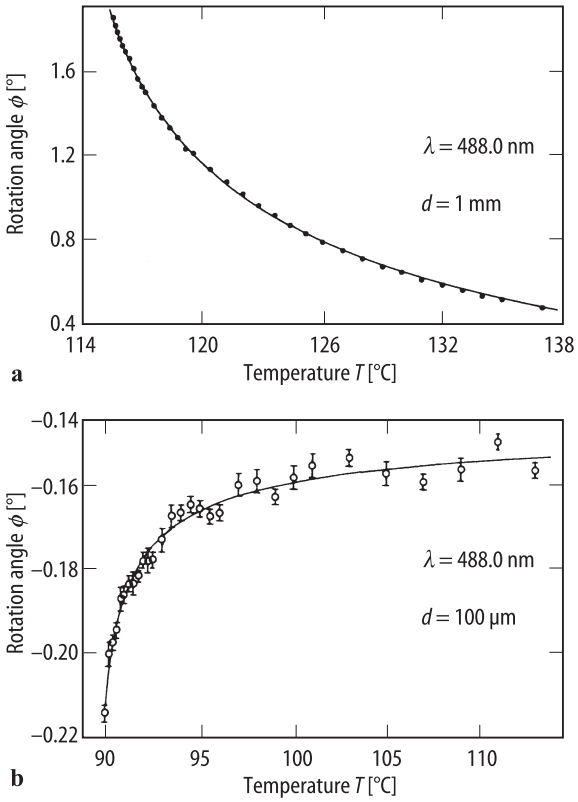

Fig. 71A-1-053. DOBAMBC. ϕ vs. T [91Fra]. ϕ: angle of optical rotation. λ = 488.0 nm. (**a**) isotropic phase; sample thickness: 1 mm. (**b**) Sm A phase, for light propagating parallel to the director; sample thickness: 100 µm.

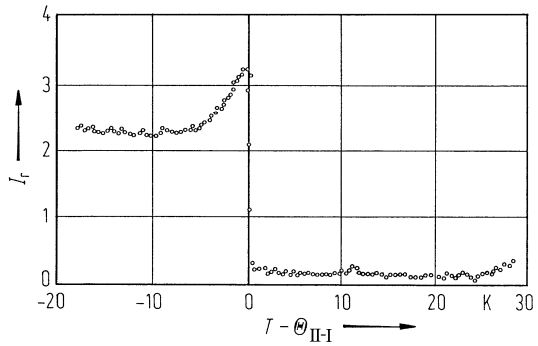

Fig. 71A-1-054. DOBAMBC. I_r vs. $T - \Theta_{II-I}$ [81Vty]. I_r: relative intensity of second harmonic generation. Oriented field E = 100 kV m^{-1}.

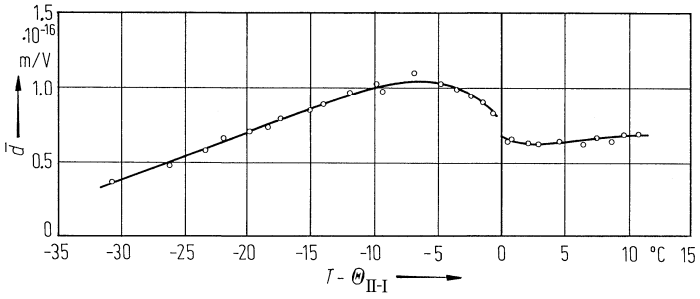

Fig. 71A-1-055. DOBAMBC. $\bar{d}$ vs. $T - \Theta_{II-I}$ [85Sht]. $\bar{d}$: effective nonlinear susceptibility.

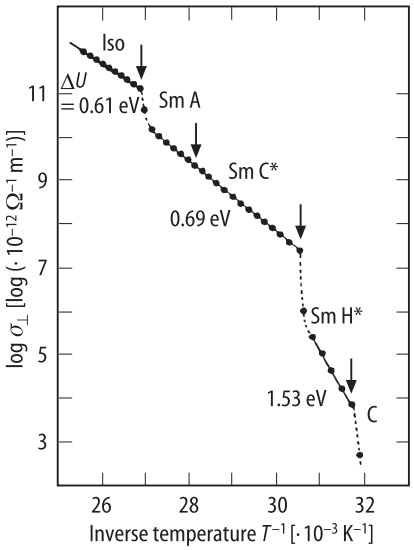

Fig. 71A-1-056. DOBAMBC. log $\sigma_\perp$ vs. $1/T$ [88Jub]. $\sigma_\perp$: dc electric conductivity [$\cdot 10^{-12}\ \Omega^{-1}\ m^{-1}$] of magnetic field oriented specimen perpendicular to magnetic field. ΔU: activation energy for electric conduction. Iso: isotropic.

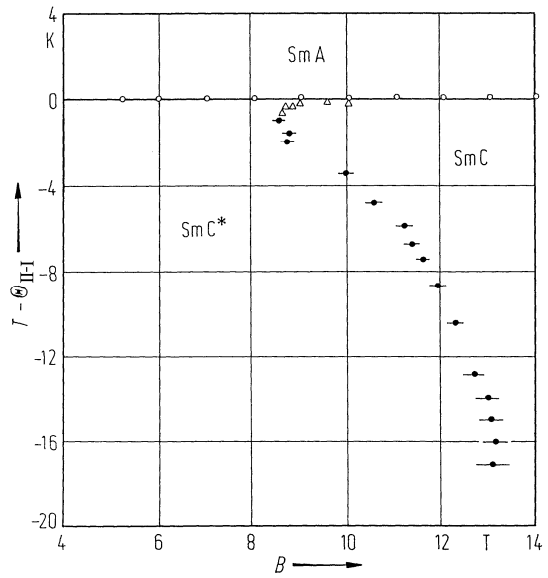

Fig. 71A-1-057. DOBAMBC. $T - \Theta_{II-I}$ vs. B [82Mus]. B: magnetic flux density.

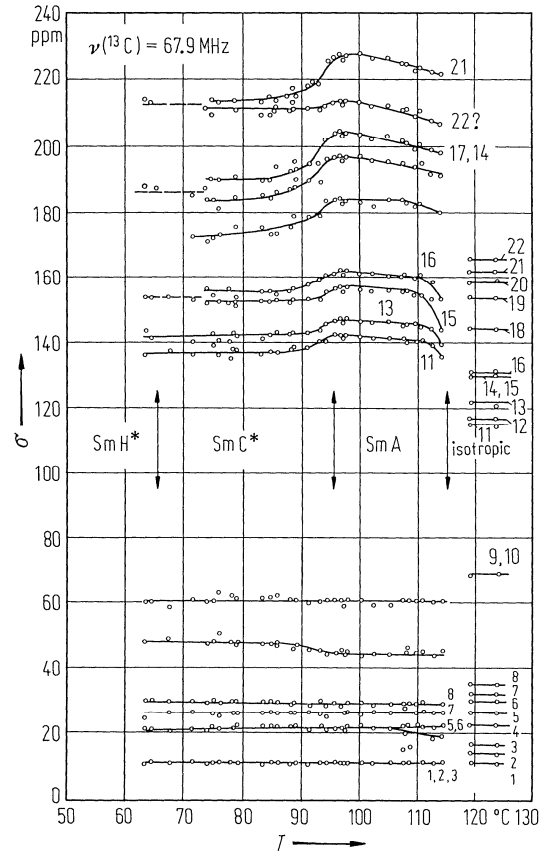

Fig. 71A-1-058. DOBAMBC. σ vs. T [80Luz]. σ: chemical shift of ^{13}C. Numerals from 1 to 22 denote different carbons in the molecule.

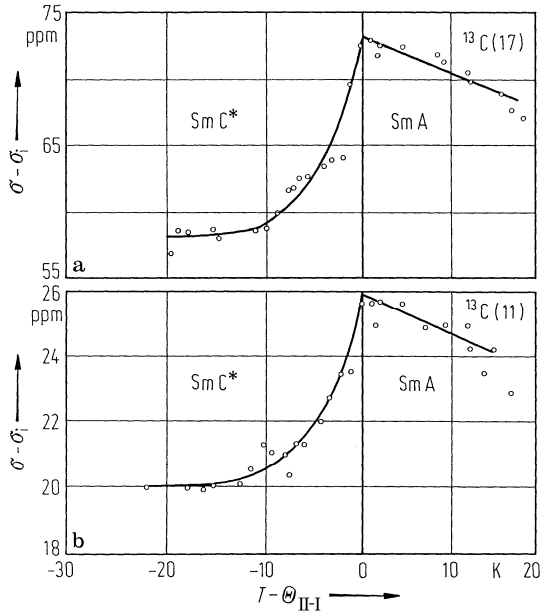

Fig. 71A-1-059. DOBAMBC. $\sigma - \sigma_i$ vs. $T - \Theta_{II-I}$ [84Luz]. σ: chemical shift of ^{13}C. ***H*** is normal to the smectic layer. $\sigma_i = (\mathrm{Tr}\ \sigma)/3$. (**a**) para-position. (**b**) ortho-position.

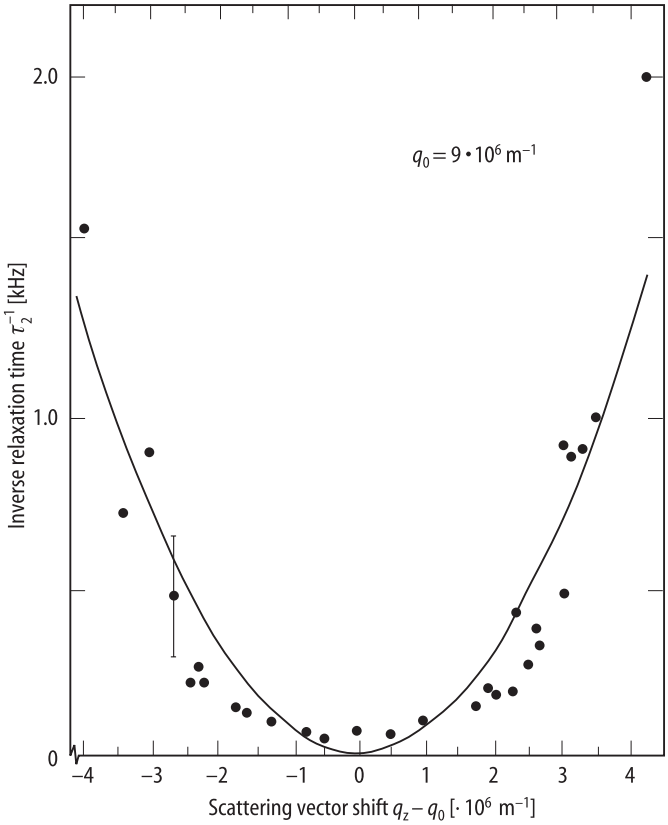

Fig. 71A-1-060. DOBAMBC. τ_2^{-1} vs. $q_z - q_0$ [88Mus]. τ_2: slow mode (phason) relaxation time determined by optical-mixing spectroscopy. The scattering vector q_z is || to the helical axis. q_0: position of the diffraction spot. $\Theta_{I-I} - T = 0.1$ K.

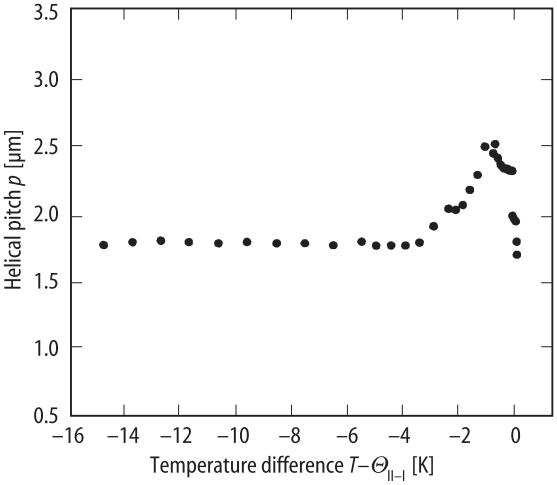

Fig. 71A-1-061. DOBA-1-MPC. p vs. $T - \Theta_{I-I}$ [90Lev]. p: helical pitch.

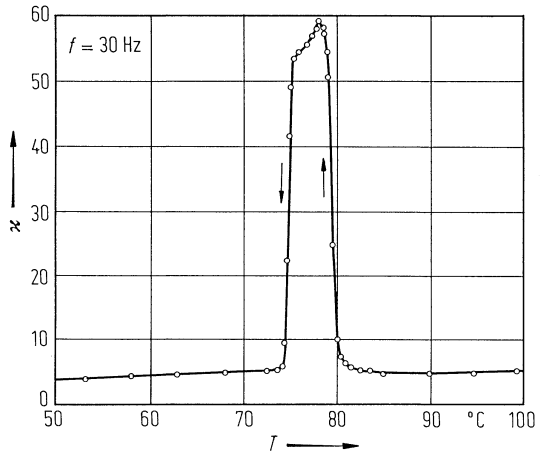

Fig. 71A-1-062. DOBA-1-MBC. κ vs. T [84Yos3]. f = 30 Hz. Cell thickness: 50 µm.

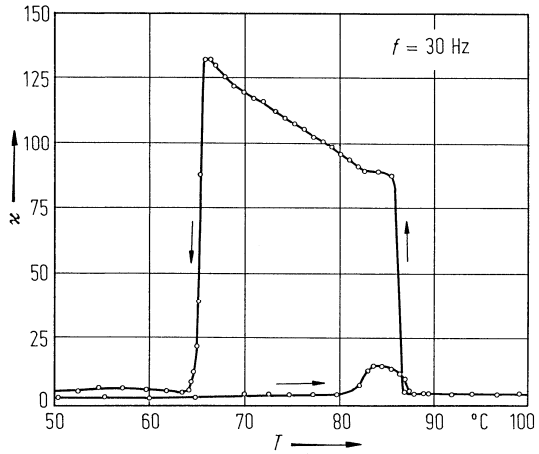

Fig. 71A-1-063. DOBA-1-MPC. κ vs. T [84Yos3]. f = 30 Hz. Cell thickness: 50 µm.

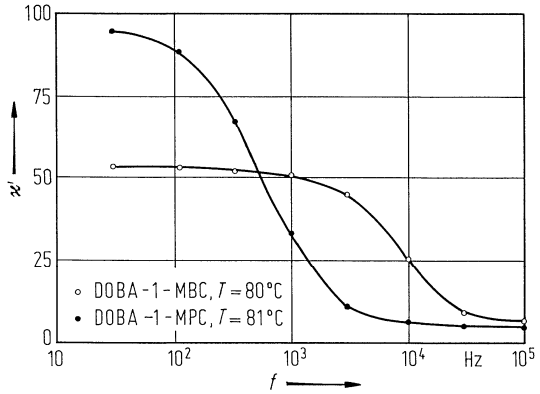

Fig. 71A-1-064. DOBA-1-MPC, DOBA-1-MBC. κ' vs. f [84Yos3]. f: measuring frequency.

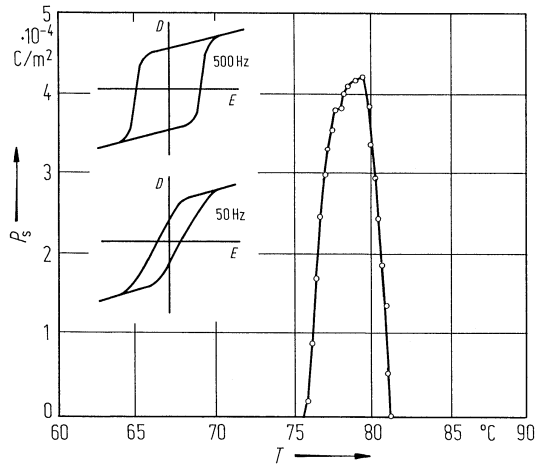

Fig. 71A-1-065. DOBA-1-MBC. P_s vs. T [84Yos3]. f = 500 Hz. Cell thickness: 50 µm. Insert indicates typical hysteresis loops at 500 Hz and 50 Hz.

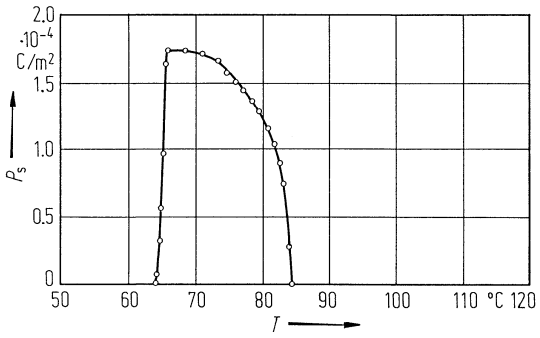

Fig. 71A-1-066. DOBA-1-MPC. P_s vs. T [84Yos3]. f = 100 Hz. Cell thickness: 50 µm.

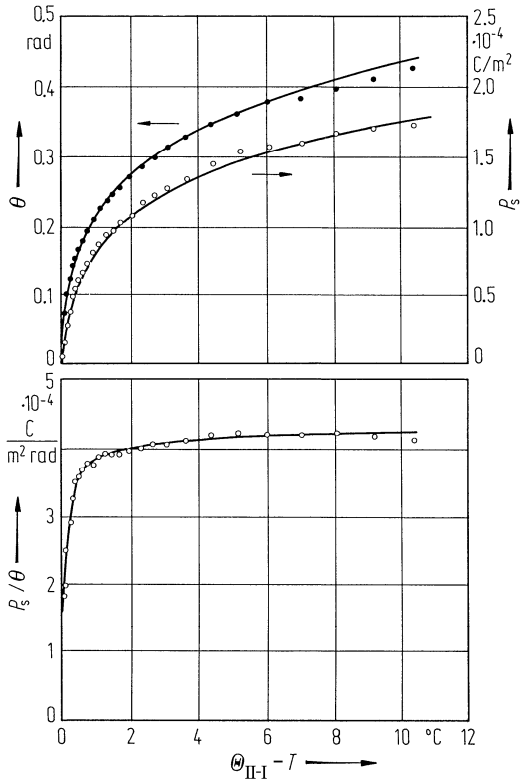

Fig. 71A-1-067. DOBA-1-MPC. P_s, θ, P_s/θ vs. $\Theta_{II–I} – T$ [87Hua]. θ: tilt angle.

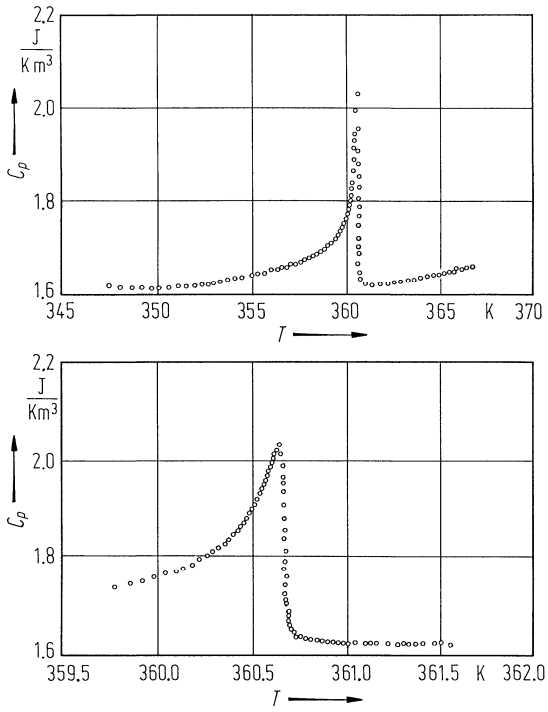

Fig. 71A-1-068. DOBA-1-MPC. C_p vs. T [87Hua]. C_p: heat capacity per unit volume at constant pressure.

References

75Mey Meyer, R.B., Liebert, L., Strzelecki, L., Keller, P.: J. Phys. (Paris) Lett. **36** (1975) L69.
75Pie Pieranski, P., Guyon, E., Keller, P.: J. Phys. (Paris) **36** (1975) 1005.
76Kel Keller, P., Liebert, L., Strzelecki, L.: J. Phys. (Paris) Colloq. **37** (1976) C3, 27.
76Mar Martinot-Lagarde, Ph.; J. Phys. (Paris) Colloq. **37** (1976) C3, 129.
77Ost1 Ostrovskii, B.I., Rabinovich, A.Z., Sonin, A.S., Strukov, B.A., Chernova, N.I.: Pis'ma Zh. Eksp. Teor. Fiz. **25** (1977) 80; JETP Lett. (English Transl.) **25** (1977) 70.
77Ost2 Ostrovskii, B.I., Taraskin, S.A., Strukov, B.A., Rabinovich, A.Z., Sonin, A.S., Chernova, N.I.: Fiz. Tverd. Tela **19** (1977) 3686; Sov. Phys. Solid State (English Transl.) **19** (1977) 2153.
77Yos Yoshino, K., Uemoto, T., Inuishi, Y.: Jpn. J. Appl. Phys. **16** (1977) 571.
78Hof Hoffman, J., Kuczynski, W., Malecki, J.: J. Mol. Cryst. Liquid Cryst. **14** (1978) 287.
78Ost1 Ostrovskii, B.I., Rabinovich, A.Z., Sonin, A.S., Strukov, B.A., Taraskin, S.A.: Ferroelectrics **20** (1978) 189.
78Ost2 Ostrovskii, B.I., Rabinovich, A.Z., Sonin, A.S., Strukov, B.A.: Zh. Eksp. Teor. Fiz. **74** (1978) 1748; Sov. Phys. JETP (English Transl.) **47** (1978) 912.
78Tak Takezoe, H., Furuhata, K., Nakagiri, T., Fukuda, A., Kuze, E.: Jpn. J. Appl. Phys. **17** (1978) 1219.
78Yos Yoshino, K., Balakrishnan, K.G., Uemoto, T., Iwasaki, Y., Inuishi, Y.: Jpn. J. Appl. Phys. **17** (1978) 597.
79Bli Blinov, L.M., Beresnev, L.A., Shtykov, N.M., Elashvili, Z.M.: J. Phys. (Paris) Colloq. **40** (1979) C3, 269.
79Iwa Iwasaki, Y., Yoshino, K., Uemoto, T., Inuishi, Y.: Jpn. J. Appl. Phys. **18** (1979) 2323.
79Lev Levstik, A., Žekš, B., Levstik, I., Blinc, R., Filipic, C.: J. Phys. (Paris) Colloq. **40** (1979) C3, 303.
79Yos Yoshino, K., Iwasaki, Y., Uemoto, T., Inuishi, Y.: Jpn. J. Appl. Phys. **18** (1979) Suppl. 18–1, 427.
80Cla Clark, N.A., Lagerwall, S.T.: Appl. Phys. Lett. **36** (1980) 899.
80Kon Kondo, K., Kobayashi, F., Takezoe, H., Fukuda, A., Kuzue, E.: J. Appl. Phys. **19** (1980) 2293.
80Luz Luzar, M., Rutar, V., Seliger, J., Burgar, M., Blinc, R.: Ferroelectrics **24** (1980) 215.
80Uem Uemoto, T., Yoshino, K., Inuishi, Y.: Jpn. J. Appl. Phys. **19** (1980) 1467.
80Yos Yoshino, K., Uemoto, T., Iwasaki, Y., Yanagida, S., Inuishi, Y.: J. Phys. Soc. Jpn. **49** (1980) Suppl. B, p. 116.
81Ber Beresnev, L.A., Blinov, L.M.: Ferroelectrics **33** (1981) 129.
81Mar Martinot-Lagarde, Ph., Duke, R., Durand, G.: Mol. Cryst. Liq. Cryst. **75** (1981) 249.
81Uem Uemoto, T., Yoshino, K., Inuishi, Y.: Mol. Cryst. Liq. Cryst. **66** (1981) 793.
81Ues Uesu, Y., Kobayashi, J., Matsumoto, T., Strukov, B.A., Kawabe, T.: Ferroelectrics **39** (1981) 1253.
81Vty Vtyurin, A.N., Ermakov, V.P., Ostrovskii, B.I., Shabanov, V.F.: Phys. Status Solidi (b) **107** (1981) 397.
81Yos Yoshino, K., Inuishi, Y.: Jpn. J. Appl. Phys. **20** (1981) Suppl. 20–4, p. 3.
82Ben Benguigui, L.: J. Phys. (Paris) **43** (1982) 915.
82Ima Imasaki, M., Fujimoto, T., Nishihara, T., Yoshioka, T., Narushige, Y.: Jpn. J. Appl. Phys. **21** (1982) 1100.
82Kon Kondo, K., Takezoe, H., Fukuda, A., Kuze, E.: Jpn. J. Appl. Phys. **21** (1982) 224.
82Mus Muševic, I., Žekš, B., Blinc, R., Rasing, Th., Wyder, P.: Phys. Rev. Lett. **48** (1982) 192.
83Yos Yoshino, K., Urabe, T., Inuishi, Y.: Jpn. J. Appl. Phys. **22** (1983) Suppl. 22–2, p. 115.
84Bli Blinc, R., Žekš, B., Musevic, I., Levstik, A.: Mol. Cryst. Liq. Cryst. **114** (1984) 189.
84Kap Kapustina, O.A.: Mol. Cryst. Liq. Cryst. **112** (1984) 1.
84Luz Luzer, M., Rutar, V., Seliger, J., Blinc, R.: Ferroelectrics **58** (1984) 115.
84Mar Maruyama, N.: Ferroelectrics **58** (1984) 187.
84Mus Muševic, I., Žekš, B., Blinc, R., Jansen, L., Seppen, A., Wyder, P.: Ferroelectrics **58** (1984) 71.
84Pra Prasad, S.K., Ratna, B.R., Shashidhar, R. Surendranath, V.: Ferroelectrics **58** (1984) 101.
84Sak Sakurai, T., Sakamoto, K., Honma, M., Yoshino, K., Ozaki, M.: Ferroelectrics **58** (1984) 21.
84Tak Takezoe, H., Kondo, K., Miyasato, K., Abe, S., Tsuchiya, T., Fukuda, A., Kuze, E.: Ferroelectrics **58** (1984) 55.
84Yos1 Yoshino, K., Ozaki, M.: Jpn. J. Appl. Phys. **23** (1984) L385.

84Yos2 Yoshino, K., Ozaki, M., Agawa, H., Shigeno, Y.: Ferroelectrics **58** (1984) 283.
84Yos3 Yoshino, K., Ozaki, M., Sakurai, T., Sakamoto, K., Honma, M.: Jpn. J. Appl. Phys. **23** (1984) L175.
85Abd Abdulhalim, I., Benguigui, L., Weil, R.: J. Phys. (Paris) **46** (1985) 1429.
85Kon Kondo, K., Era, S., Isogai, M., Mukoh, A.: Jpn. J. Appl. Phys. **24** (1985) 1389.
85Oza Ozaki, M., Kishio, S., Shigeno, Y., Yoshino, K.: Jpn. J. Appl. Phys. **24** (1984) Suppl. 24–2, p. 63.
85Sak Sakurai, T., Mikami, N., Yoshino, K.: Jpn. J. Appl. Phys. **24** (1985) Suppl. 24–3, p. 56.
85Sht Shtykov, N.M., Barnik, M.I., Beresnev, L.A., Blinov, L.M.: Mol. Cryst. Liq. Cryst. **124** (1985) 379.
85Yas Yasuda, N., Fujimoto, S., Funado, S.: J. Phys. D **18** (1985) 521.
85Yos Yoshino, K., Ozaki, M., Kishio, S.: Jpn. J. Appl. Phys. **24** (1985) Suppl. 24–3, p. 45.
86Dum Dumrongrattana, S., Huang, C.C., Nounesis, G., Lien, S.C., Viner, J.M.: Phys. Rev. A **34** (1986) 5010.
87Hua Huang, C.C., Dumrongrattana, S., Nounesis, G., Stofko Jr., J.J., Arimilli, P.A.: Phys. Rev. A **35** (1987) 1460.
87Yos Yoshino, K., Kishino, S., Ozaki, M., Yokotani, A., Sasaki, Y., Yamanaka, C.: Tech. Rept. Osaka Univ. **37** (1987) 283.
88Jub Jubindo, M.P., Ezcurra, A., de la Fuente, M.R., Santamaria, C., Etxebaria, J., Serramo, J.L., Marcos, M: Ferroelectrics **85** (1988) 199.
88Mus Muševic, I., Blinc, R., Žekš, B., Filipic, C., Copic, M., Seppen, A., Wyder, P., Levanyuk, A.: Phys. Rev. Lett. **60** (1988) 1530.
90Lev Levstik, A., Kutnjak, Z., Filipic, C., Levstik, I., Bregar, Z., Žekš, B., Carlsson, T.: Phys. Rev. A **42** (1990) 2204.
91Fra Frame, K.C., Walker, J.L., Collins, P.J.: Mol. Cryst. Liq. Cryst. **198** (1991) 91.
91Pra Prasad, S.K., Nair, G.G.: Mol. Cryst. Liq. Cryst. **202** (1991) 91.

No. 71A-2 AOBACPC and analogues

(A) $C_nH_{2n+1}O$–⬡–CH=N–⬡–CH=CHCOOCH$_2$CHClCH$_3$

AOBACPC (*p*-alkoxybenzylidene *p′*-amino-2-chloropropyl cinnamate)
n = 6: HOBACPC (*p*-hexyloxybenzylidene *p′*-amino-2-chloropropyl cinnamate)
n = 8: OOBACPC (*p*-octyloxybenzylidene *p′*-amino-2-chloropropyl cinnamate)
n = 10: DOBACPC (*p*-decyloxybenzylidene *p′*-amino-2-chloropropyl cinnamate)

1b n = 6 (HOBACPC) 85Cla

phase	VI	V	IV	III	II	I	I′
	crystalline solid	smectic X (Sm X)	smectic G′* (Sm G′*)	smectic I* (Sm I*)	smectic C* (Sm C*)	smectic A (Sm A)	isotropic liquid
state			F	F	F	P	
Θ [°C]	heating: 19.9	58	68.0	74.8	82	136.3	
	cooling:	58	66.8	73.8	82	133.5	

3b Smectic layer spacing: Fig. 71A-2-001.
Helical pitch of HOBACPC: Fig. 71A-2-002.
Helical pitch of DOBACPC: see Fig. 71A-1-011, 71A-1-012 in No. 71A-1.
Critical field for helical to unwinded structure: Fig. 71A-2-003.
Tilt angle of HOBACPC: see Fig. 71A-1-010 in No. 71A-1.

5a Dielectric constant: Fig. 71A-2-004, 71A-2-005, Fig. 71A-2-006, 71A-2-007.
Phase diagram in regard to hydrostatic pressure: 71A-2-008.
Maximum dielectric constant of (DOBAMBC)–(DOBACPC): see Fig. 71A-1-035 in No. 71A-1.

c Spontaneous polarization: 71A-2-009.
Spontaneous polarization of HOBACPC: see 71A-1-034 in No. 71A-1.
Spontaneous polarization of HOBACPC, OOBACPC, DOBACPC: see 80Yos2
Spontaneous polarization of (DOBAMBC)–(DOBACPC): see Fig. 71A-1-035 in No. 71A-1.

6a Heat capacity: 71A-2-010, 71A-2-011.
Transition heat of HOBACPC: see 85Cla
Differential scanning calorimetry: Fig. 71A-2-012.

9a Birefringence of (MBRA 7)$_{0.95}$(HOBACPC)$_{0.05}$: see Fig. 71A-3-014 in No. 71A-3.
Threshold field of electro-optic effect: see Fig. 71A-1-049 in No. 71A-1.

(B) $C_nH_{2n+1}O$–⬡–CH=N–⬡–CH=CHCOOCH$_2$CHClCH(CH$_3$)C$_2$H$_5$

AOBAC-3-MPC ((2S,3S)-*p*-alkoxybenzylidene *p′*-amino-2-chloro-3-methylpentyl cinnamate)

n = 1: MOBAC-3-MPC
n = 5: POBAC-3-MPC
n = 6: HOBAC-3-MPC
n = 10: DOBAC-3-MPC
n = 14: TDOBAC-3-MPC

1b	phase	IV	III	II	I	I′	I″	86Sak
		crystalline solid	unidentified smectic	smectic C* (Sm C*)	smectic A (Sm A)	nematic	isotropic liquid	
	state		F	F	P	P		
	Θ [°C] n = 1	72				73	74	
	5	22			36		96	
	6	24	52		63		101	
	10		43		80		104	
	14		54		77		89	
5c	Spontaneous polarization of DOBAC-3-MPC: Fig. 71A-2-013.							

(C) $C_nH_{2n+1}O$–⬡–CH=N–⬡–CH=C(CH$_3$)COOCH$_2$CHClCH(CH$_3$)C$_2$H$_5$

AOBAC-3-MPCM ((2S,3S)-*p*-alkoxybenzylidene *p′*-amino-2-chloro-3-methylpentyl-methyl cinnamate)

n = 10: DOBAC-3-MPCM

1b	phase	III	II	I	I′	86Sak
		crystalline solid	smectic C* (Sm C*)	smectic A (Sm A)	isotropic liquid	
	state		F	P		
	Θ [°C]	31	54	79		

(D) $C_nH_{2n+1}O$–⬡–CH=N–⬡–CH=CHCOOCH$_2$CHBrCH(CH$_3$)C$_2$H$_5$

AOBAB-3-MPC ((2S,3S)-*p*-alkoxybenzylidene *p′*-amino-2-bromo-3-methylpentyl cinnamate)

n = 10: DOBAB-3-MPC

1b	phase	III	II	I	I′	86Sak
		crystalline solid	smectic C* (Sm C*)	smectic A (Sm A)	isotropic liquid	
	state		F	P		
	Θ [°C]	45	65	88		

(E) $C_nH_{2n+1}O$–⬡–CH=N–⬡–CH=CHCOOCH$_2$CHClCH$_2$CH(CH$_3$)$_2$

AOBAC-4-MPC ((2S)-*p*-alkoxybenzylidene *p′*-amino-2-chloro-4-methylpentyl cinnamate)

n = 5: POBAC-4-MPC
n = 6: HOBAC-4-MPC
n = 10: DOBAC-4-MPC
n = 14: TDOBAC-4-MPC
n = 18: ODOBAC-4-MPC

1b	phase	IV	III	II	I	I′	86Sak
		crystalline solid	unidentified smectic	smectic C* (Sm C*)	smectic A (Sm A)	isotropic liquid	
	state		F	F	P		
	Θ [°C] n = 5	22	40	63	87		
	6	34	51	75	104		
	10		49	80	94		
	14		60	78	99		
	18		59	69	73		

(F) $C_nH_{2n+1}O$–⬡–CH=N–⬡–CH=CHCOOCH$_2$CHClCH(CH$_3$)$_2$

AOBAC-3-MBC ((2S)-*p*-alkoxybenzylidene *p′*-amino-2-chloro-3-methylbutyl cinnamate)

n = 5: POBAC-3-MBC
n = 6: HOBAC-3-MBC
n = 10: DOBAC-3-MBC
n = 14: TDOBAC-3-MBC

1b	phase	IV	III	II	I	I′	86Sak
		crystalline solid	unidentified smectic	smectic C* (Sm C*)	smectic A (Sm A)	isotropic liquid	
	state		F	F	P		
	Θ [°C] n = 5	44		81	100		
	6	45	65	83	110		
	10		59	78	105		
	14		60	83	99		

(G) $C_nH_{2n+1}O$–⬡–CH=N–⬡–CH=CHCOOCH$_2$CHClCH$_2$–⬡

AOBAC-3-PPC ((2S)-*p*-alkoxybenzylidene *p′*-amino-2-chloro-3-phenylpropyl cinnamate)

n = 10: DOBAC-3-PPC

1b	phase	II	I	I′	86Sak
		crystalline solid	nematic	isotropic liquid	
	state		P		
	Θ [°C]	44	62		

(H) $C_nH_{2n+1}O$–⬡–CH=N–⬡–CH=CHCOOCH$_2$CH$_2$CHClCH$_3$

AOBA-3-CBC ((3S)-*p*-alkoxybenzylidene *p′*-amino-3-chlorobutyl cinnamate)

n = 10: DOBA-3-CBC

1b	phase	IV	III	II	I	I′	86Sak
		crystalline solid	unidentified smectic	smectic C* (Sm C*)	smectic A (Sm A)	isotropic liquid	
	state		F	F	P		
	Θ [°C]	43	80	93	113		

(I) $C_nH_{2n+1}O$–⬡–CH=N–⬡–CH=C(CN)COOCH$_2$CH(CH$_3$)C$_2$H$_5$

AOBAMBCC (*p*-alkoxybenzylidene- *p′*-amino-2-methylbutyl-cyano cinnamate)

n = 10: DOBAMBCC (*p*-decyloxybenzylidene- *p′*-amino-2-methylbutyl-cyano cinnamate)

n = 14: TDOBAMBCC (*p*-tetradecyloxybenzylidene- *p′*-amino-2-methylbutyl-cyano cinnamate)

1b	phase		III	II	I	I′	I″	76Kel
			crystalline solid	smectic C* (Sm C*)	smectic A (Sm A)	chiral nematic	isotropic liquid	
	state			F [a])	P	P		[a]) 81Mar
	Θ [°C]	n = 7	65	87	94	95		
		8	(71)	88		98.5		
		9	(75.5)	90		100.5		
		10	(70)	92		104		
		14	(71)	78		105		
							( ): cooling	
3b	Helical pitch: Fig. 71A-2-014, Fig. 71A-2-015. Tilt angle: see Fig. 71A-1-010 in No. 71A-1.							

(J) $C_nH_{2n+1}O$–⬡–CH=N–⬡–CH=CClCOOCH$_2$CH(CH$_3$)C$_2$H$_5$

AOBAMBClC (*p*-alkoxybenzylidene- *p′*-amino-2-methylbutyl-chloro cinnamate)

1b	phase		III	II	I	I′	76Kel
			crystalline solid	smectic C* (Sm C*)	smectic A (Sm A)	isotropic liquid	
	state			F [a])	P		[a]) 81Mar
	Θ [°C]	n = 6	(32)	47	62		
		8	(38)	41	64		
		10	(45)	51	71		
		14	(41)	50.5	79	( ): cooling	

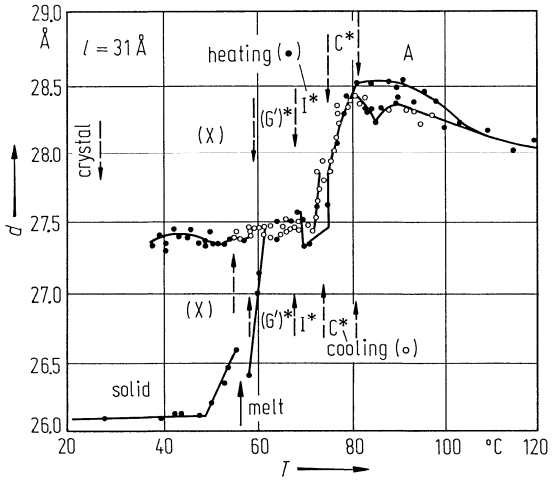

Fig. 71A-2-001. HOBACPC. d vs. T [85Cla]. d: smectic layer spacing. l = 31 Å: length of fully extended HOBACPC molecule.

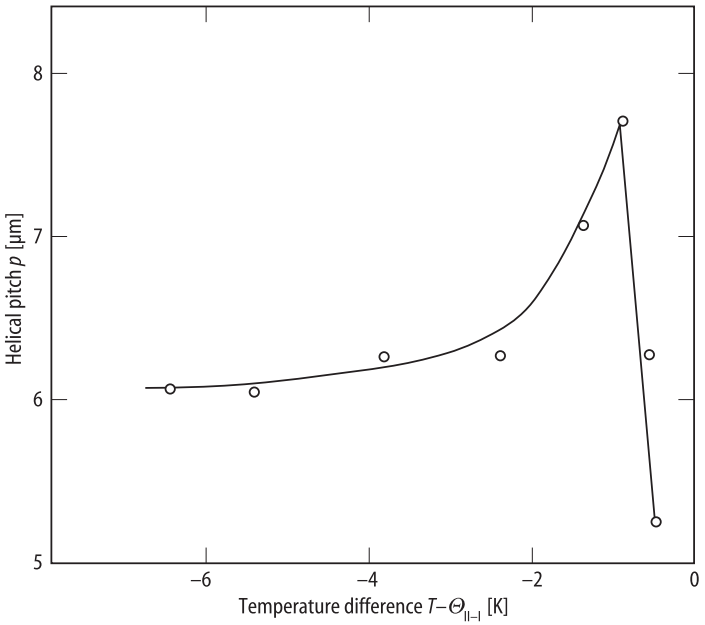

Fig. 71A-2-002. HOBACPC. p vs. $T - \Theta_{II–I}$ [83Par]. p: helical pitch. Sample thickness: 20 µm.

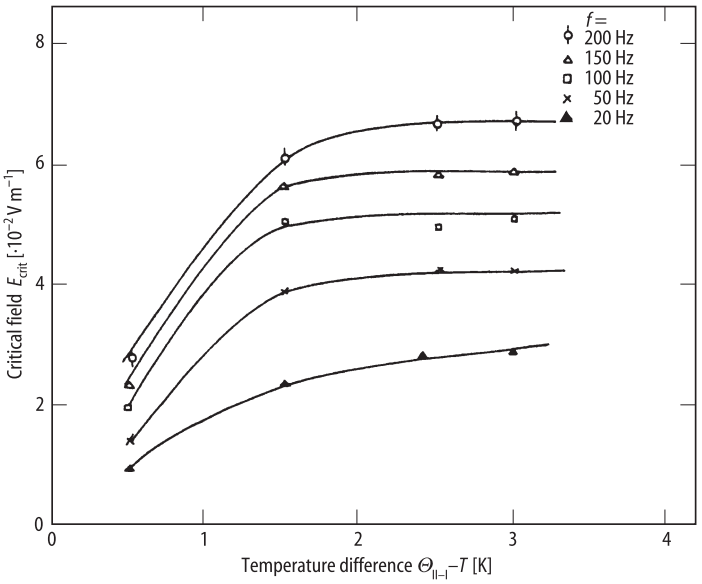

Fig. 71A-2-003. HOBACPC. E_{crit} vs. $\Theta_{II-I} - T$ [83Par]. E_{crit}: critical ac electric field for helical to unwinded structure. Parameter: f, frequency of E_{crit}. Sample thickness: 18 µm.

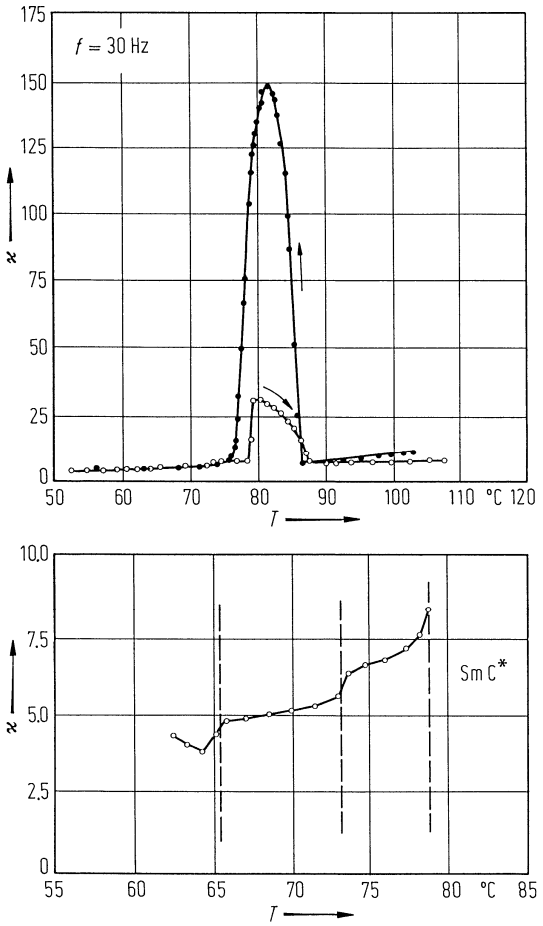

Fig. 71A-2-004. HOBACPC. κ vs. T [80Yos1]. Cell thickness: 100 µm. f = 30 Hz.

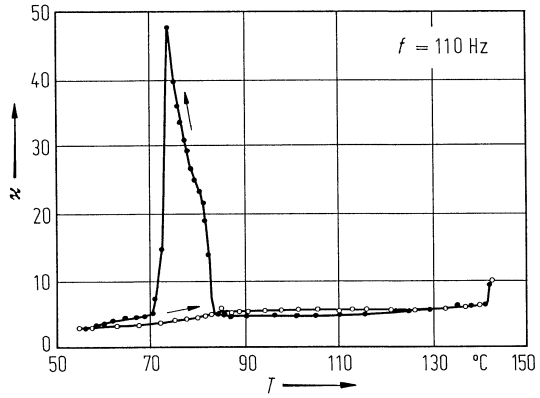

Fig. 71A-2-005. OOBACPC. κ vs. T [80Yos2]. Cell thickness: 100 µm. f = 110 Hz.

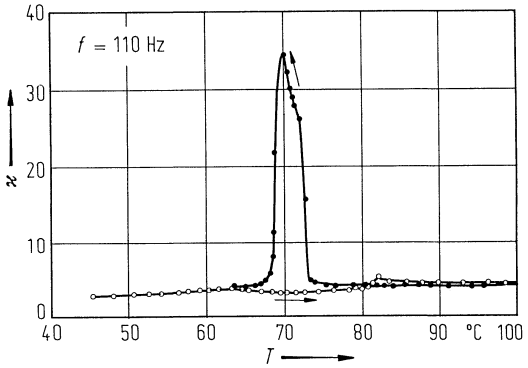

Fig. 71A-2-006. DOBACPC. κ vs. T [80Yos2]. Cell thickness: 100 µm. f = 110 Hz.

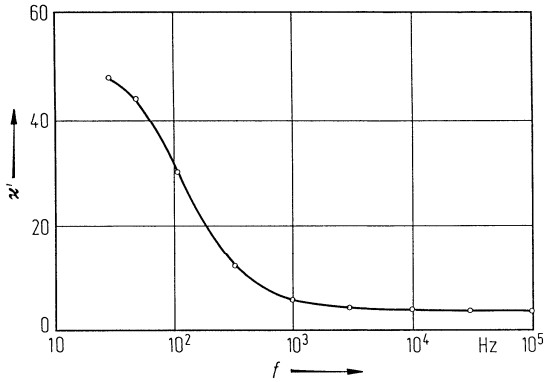

Fig. 71A-2-007. HOBACPC. κ' vs. f [80Yos2]. Cell thickness: 100 µm. T = 79 °C.

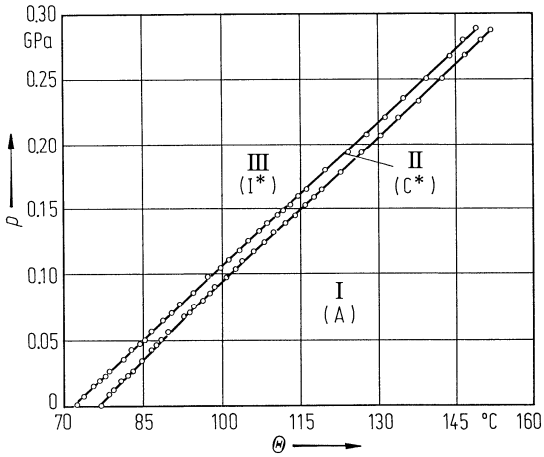

Fig. 71A-2-008. HOBACPC. p vs. Θ [84Pra]. p: hydrostatic pressure. I(A): smectic A. II(C^*): smectic C^*. III(I^*): smectic I^*.

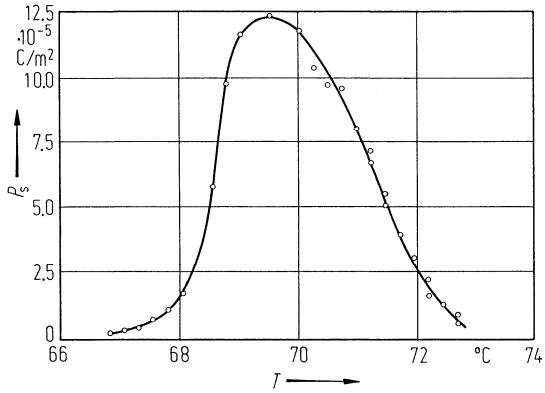

Fig. 71A-2-009. DOBACPC. P_s vs. T [80Yos1]. Cell thickness: 100 µm. f = 60 Hz.

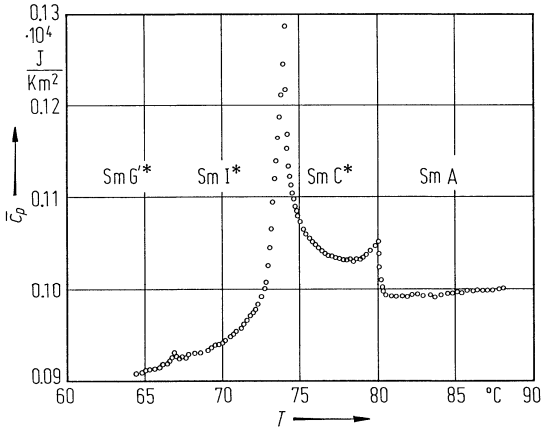

Fig. 71A-2-010. HOBACPC. $\bar{c}_p$ vs. T [83Lie]. $\bar{c}_p$: total heat capacity of sample and sample cell per unit area. On cooling.

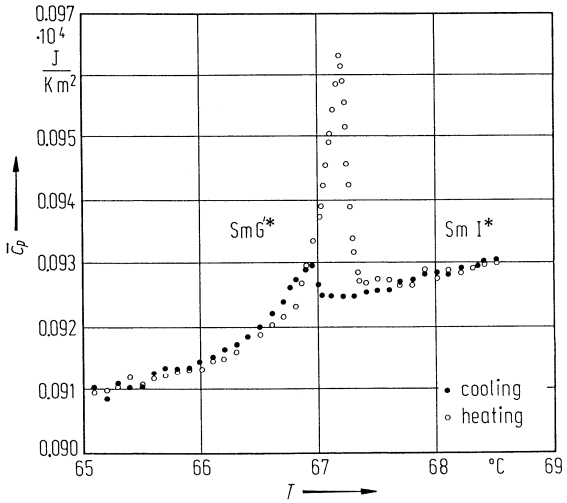

Fig. 71A-2-011. HOBACPC. $\bar{c}_p$ vs. T around $\Theta_{\mathrm{II–I}}$ [83Lie]. $\bar{c}_p$: total heat capacity of sample and sample cell per unit area.

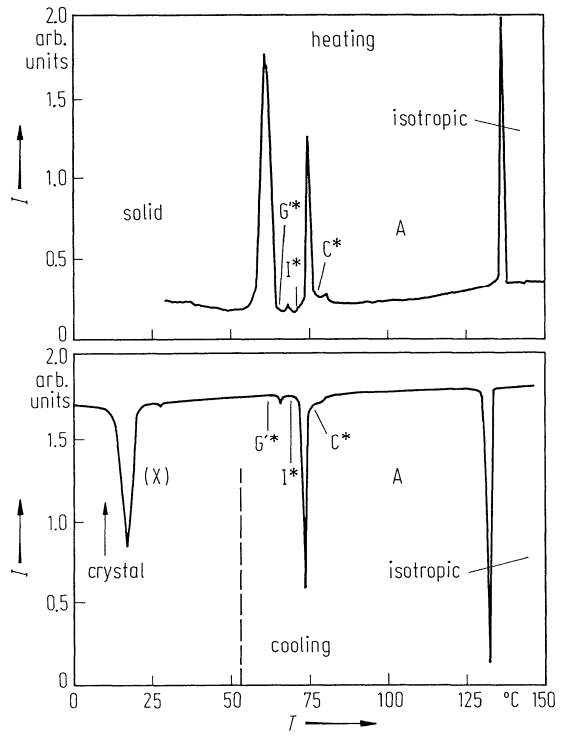

Fig. 71A-2-012. HOBACPC. I vs. T [85Cla]. I: intensity of DSC signal.

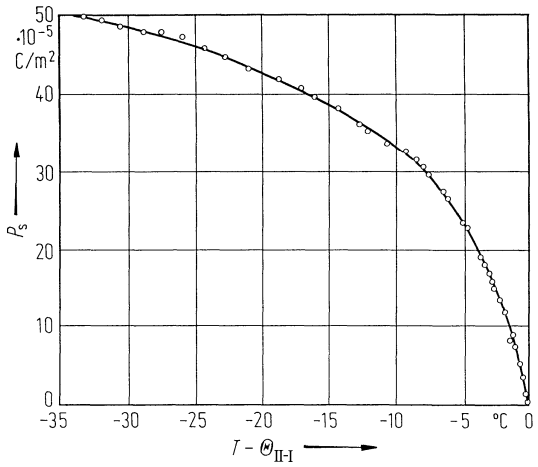

Fig. 71A-2-013. DOBAC-3-MPC. P_s vs. $T - \Theta_{II-I}$ [86Sak]. Cell thickness: 50 µm. f = 60 Hz.

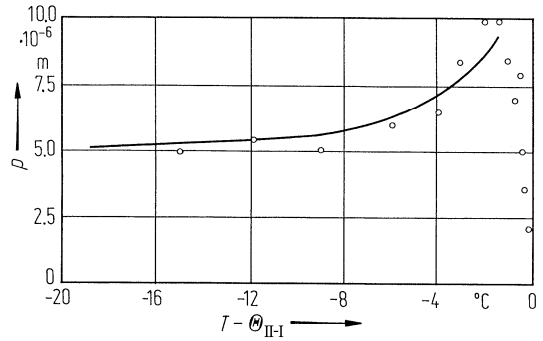

Fig. 71A-2-014. TDOBAMBCC. p vs. $T - \Theta_{II-I}$ [76Mar]. p: helical pitch.

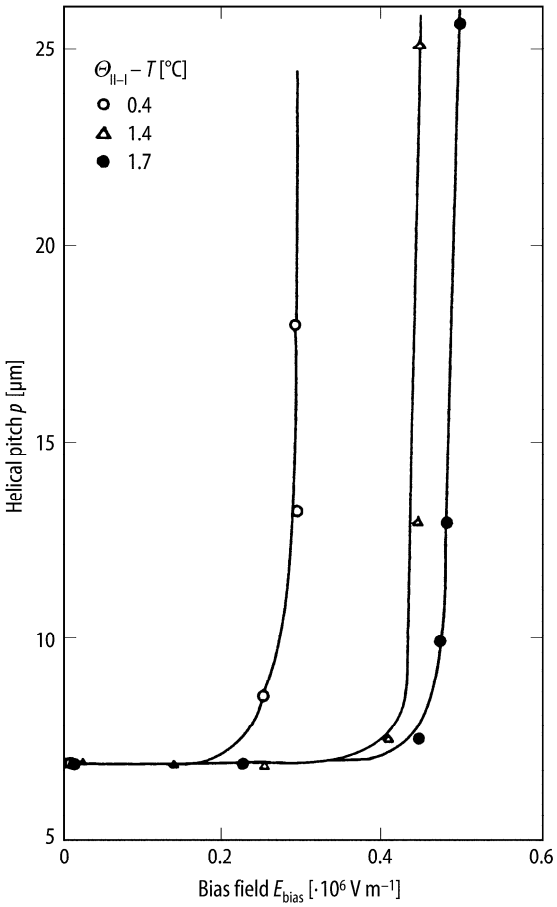

Fig. 71A-2-015. DOBAMBCC. p vs. E_{bias} [83Par]. p: helical pitch. Parameter: $\Theta_{I-I} - T$. Sample thickness: 18 µm.

References

76Kel Keller, P., Liebert, I., Strzelecki, L.: J. Phys. (Paris) Colloq. **37** (1976) C3, 27.

76Mar Martinot-Lagarde, Ph.: J. Phys. (Paris) Colloq. **37** (1976) C3, 129.

80Yos1 Yoshino, K., Iwasaki, Y., Uemoto, T., Inuishi, Y., Yanagida, S., Okahara, M.: Jpn. J. Appl. Phys. **19** (1980) 1439.

80Yos2 Yoshino, K., Iwasaki, Y., Uemoto, T., Yanagida, S., Okahara, M.: Oyo Buturi **49** (1980) 876.

81Mar Martinot-Lagarde, Ph., Duke, R., Durand, G.: Mol. Cryst. Liq. Cryst. **75** (1981) 249.

83Lie Lien, S.C., Viner, J.M., Huang, C.C., Clark, N.A.: Mol. Cryst. Liq. Cryst. **100** (1983) 145.

83Par Parmar, D.S., Raina, K.K., Shankar, J.: Mol. Cryst. Liq. Cryst. **103** (1983) 77.

84Pra Prasad, K.S., Ratna, B.R., Shashidhar, R., Surendranath, V.: Ferroelectrics **58** (1984) 101.

85Cla Claids, P.E., Brand, H.R., Keller, P., Finn, P.L.: J. Phys. (Paris) **46** (1985) 2151.

86Sak Sakurai, T., Mikami, N., Ozaki, M., Yoshino, K.: J. Chem Phys. **85** (1986) 585.

No. 71A-3 HAOBAMBC and analogues

(A) 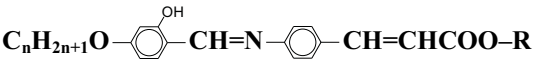

R: $CH_2CH(CH_3)C_2H_5$

HAOBAMBC (2-hydroxy-4-alkoxybenzylidene-4′-amino-2-methylbutyl cinnamate)

n = 6: HHOBAMBC

n = 8: HOOBAMBC

n = 10: HDOBAMBC

n = 14: HTDOBAMBC

R: $CH(CH_3)C_2H_5$

HAOBA-1-MPC (2-hydroxy-4-alkoxybenzylidene-4′-amino-1-methylpropyl cinnamate)

R: $CH(CH_3)COOC_2H_5$

n = 10: HDOBACEEC (2-hydroxy-4-decyloxybenzylidene-4′-amino-1-carboethoxyethyl cinnamate)

1b

phase	III	II	I	I′	84Sak
	crystalline solid	smectic C* (Sm C*)	smectic A (Sm A)	isotropic liquid	
state		F	P		
Θ [°C]					
HAOBAMBC					
n = 4	72		181		
	(76)		(179)		
6	96	106	154		
	(86)	(105)	(151)		
10 [a])	88	114	145		
	(72)	(114)	(145)		
14	76	95	135		
18	64	76	124		
HAOBA-1-MPC					
n = 4			163		
	(125)		(162)		
6			151		
	(127)		(148)		
10	124		135		
	(108)	(118)	(130)		
14	101		123		
	(101)	(111)	(122)		
HDOBACEEC					
n = 10	31	78	98		89Ezc

[a]) see also Fig. 71A-1-003 in No. 71A-1. ( ): cooling.

5a Dielectric constant of HAOBAMBC: Fig. 71A-3-001, Fig. 71A-3-002, Fig. 71A-3-003.
Dielectric constant of HDOBACEEC: Fig. 71A-3-004, Fig. 71A-3-005, Fig. 71A-3-006.

c Spontaneous polarization of HAOBAMBC: Fig. 71A-3-007, Fig. 71A-3-008, Fig. 71A-3-009.
Spontaneous polarization of HDOBACEEC: Fig. 71A-3-010.

(B) 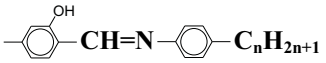

m = 1, n = n: MBRA n ((S)-4-o-(2-methyl)butyl-resorcylidene-4′-alkylaniline)
m = 5, n = n: MORA n ((S)-4-o-(6-methyl)octyl-resorcylidene-4′-alkylaniline)

1b	phase	IV	III	II	I	I′	I″	82Hal
		unidentified smectic	unidentified smectic	smectic C* (Sm C*)	smectic A (Sm A)	nematic	isotropic liquid	86Bil
	state		F	P				
	Θ [°C]							
	MBRA							
	n = 4		18			43	69	
	8			28	57		64	
	12				41		70	
	MORA							
	n = 4			35		62	70	
	8			12			97	
	12			35			93	

3b Helical pitch and tilt angle: Fig. 71A-3-011, Fig. 71A-3-012.

c Spontaneous polarization: Fig. 71A-3-013.

9a Birefringence of $(MBRA)_{0.95}(HOBACPC)_{0.05}$: Fig. 71A-3-014.

(C) 

HAOBAC-3-MPC ((2S,3S)-2-hydroxy-4-alkoxybenzylidene *p′*-amino-2-chloro-3-methylpentyl cinnamate)
n = 1: HMOBAC-3-MPC
n = 5: HPOBAC-3-MPC
n = 9: HNOBAC-3-MPC
n = 10: HDOBAC-3-MPC
n = 18: HODOBAC-3-MPC

1b	phase	III	II	I	I′	I″	86Sak
		crystalline solid	smectic C* (Sm C*)	smectic A (Sm A)	nematic	isotropic liquid	
	state		F	P	P		
	Θ [°C] n = 1		113	122	124		
	5	49	117		133		
	9	43	120		126		
	10	41	105		136		
	15	57	84		126		

5a Dielectric constant: Fig. 71A-3-015.

c Spontaneous polarization: Fig. 71A-3-016.

(D) 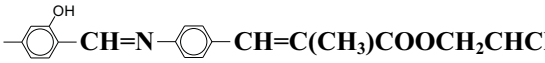

HAOBAC-3-MPCM ((2S,3S)-2-hydroxy-4-alkoxybenzylidene *p′*-amino-2-chloro-3-methylpentyl-methyl cinnamate)

n = 10: HDOBAC-3-MPCM

1b	phase	III	II	I	I′	86Sak
		crystalline solid	smectic C* (Sm C*)	smectic A (Sm A)	isotropic liquid	
	state		F	P	P	
	Θ [°C]	48	77	98		

(E) 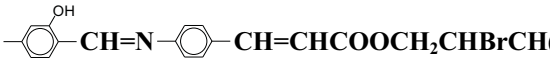

HAOBAB-3-MPC ((2S,3S)-2-hydroxy-4-alkoxybenzylidene *p′*-amino-2-bromo-3-methylpentyl cinnamate)

n = 10: HDOBAB-3-MPC

1b	phase	III	II	I	I′	86Sak
		crystalline solid	smectic C* (Sm C*)	smectic A (Sm A)	isotropic liquid	
	state		F	P	P	
	Θ [°C]	33	88	113		
5c	Spontaneous polarization: Fig. 71A-3-017.					

(F) 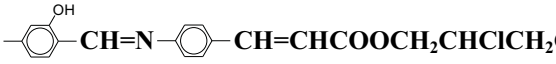

HAOBAC-4-MPC ((2S)-2-hydroxy-4-alkoxybenzylidene *p′*-amino-2-chloro-4-methylpentyl cinnamate)

n = 5: HPOBAC-4-MPC

n = 6: HHOBAC-4-MPC

n = 14: HTDOBAC-4-MPC

1b	phase	III	II	I	I′	86Sak
		crystalline solid	smectic C* (Sm C*)	smectic A (Sm A)	isotropic liquid	
	state		F	P	P	
	Θ [°C] n = 5	78	108	138		
	6	76	117	133		
	14	58	100	124		

(G) 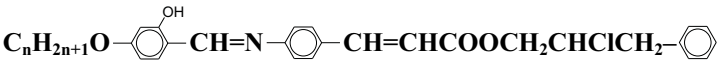

HAOBAC-3-PPC ((2S)-2-hydroxy-4-alkoxybenzylidene *p′*-amino-2-chloro-3-phenylpropyl cinnamate)

n = 10: HDOBAC-3-PPC

1b	phase	III	II	I	I′	86Sak
		crystalline solid	smectic C* (Sm C*)	smectic A (Sm A)	isotropic liquid	
	state		F	P	P	
	Θ [°C]	53	65	89		

(H) 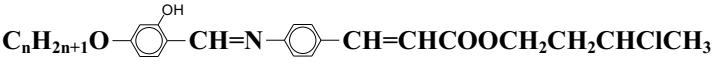

HAOBA-3-CBC ((2S)-2-hydroxy-4-alkoxybenzylidene *p′*-amino-3-chlorobutyl cinnamate)

n = 10: HDOBA-3-CBC

1b	phase	III	II	I	I′	86Sak
		crystalline solid	smectic C* (Sm C*)	smectic A (Sm A)	isotropic liquid	
	state		F	P	P	
	Θ [°C]	51	105	148		

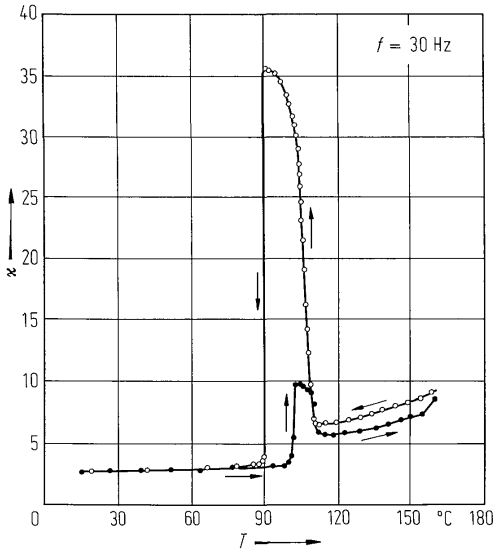

Fig. 71A-3-001. HHOBAMBC. κ vs. T [84Sak]. Cell thickness: 50 µm. f = 30 Hz.

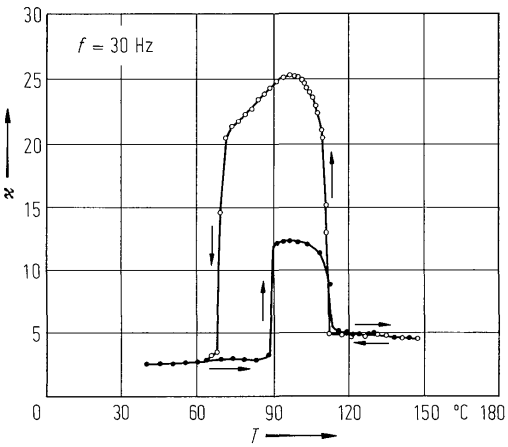

Fig. 71A-3-002. HDOBAMBC. κ vs. T [84Sak]. Cell thickness: 100 µm. f = 30 Hz.

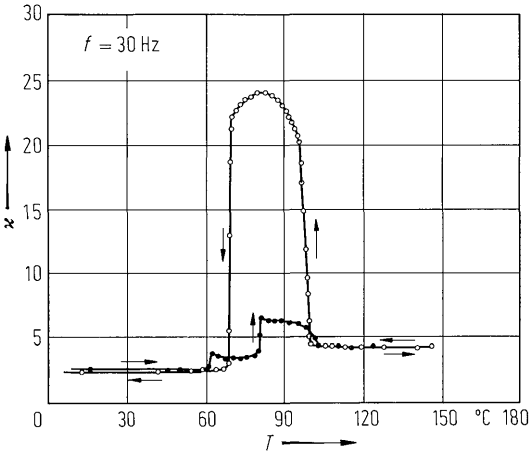

Fig. 71A-3-003. HTDOBAMBC. κ vs. T [84Sak]. Cell thickness: 50 µm. f = 30 Hz.

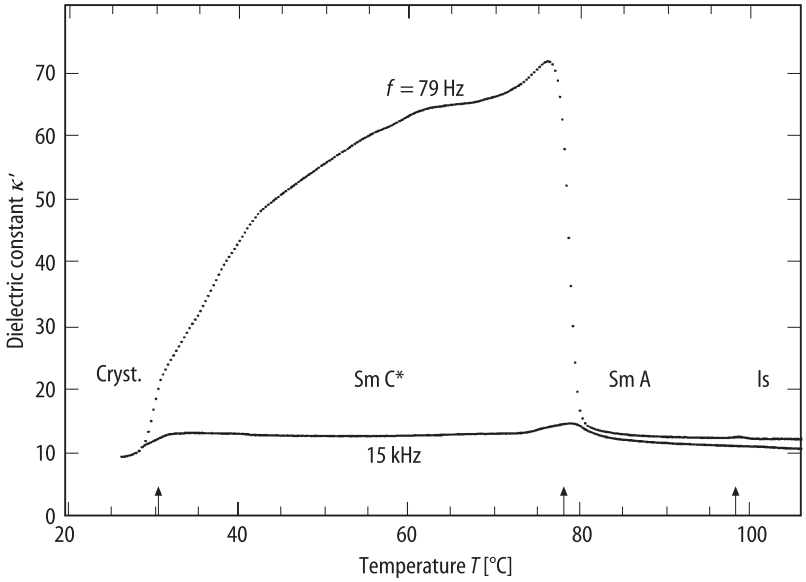

Fig. 71A-3-004. HDOBACEEC. κ' vs. T [89Ezc]. Parameter: f. Is: isotropic liquid. Cryst.: crystalline solid.

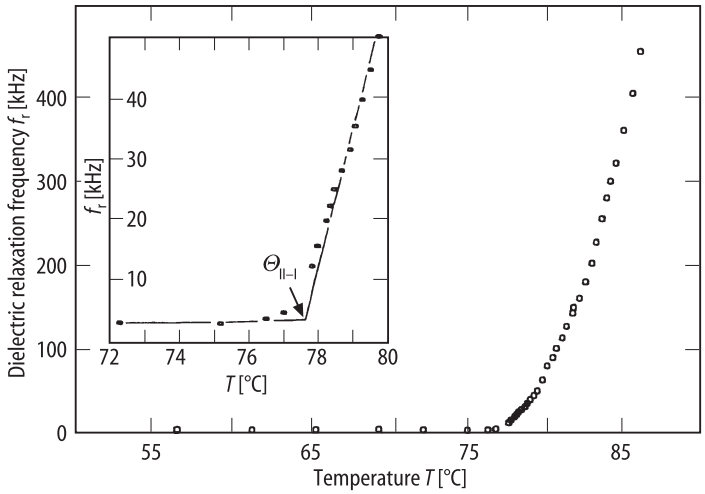

Fig. 71A-3-005. HDOBACEEC. f_r vs. T [89Ezc]. f_r: dielectric relaxation frequency.

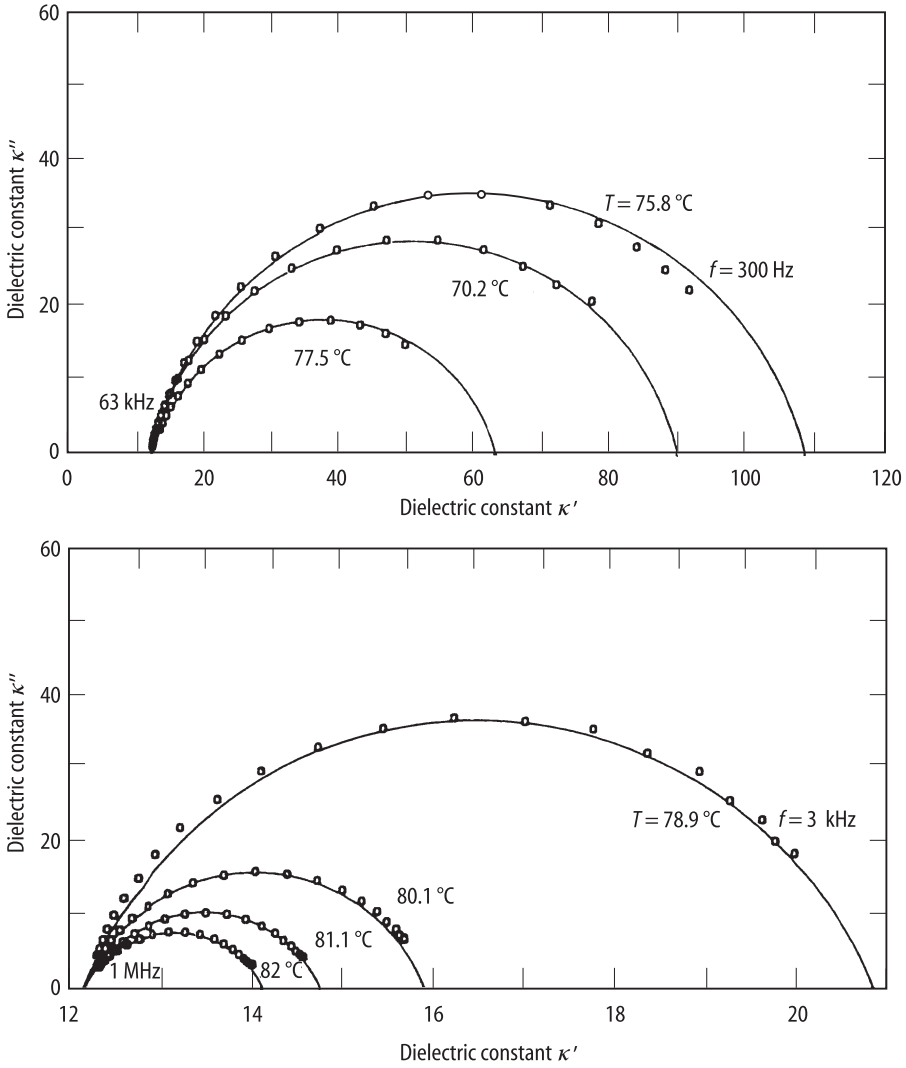

Fig. 71A-3-006. HDOBACEEC. κ' vs. κ'' (Cole-Cole plot) [89Ezc]. Parameter: T.

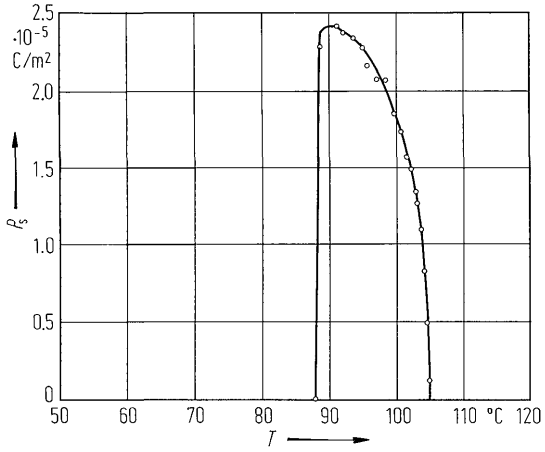

Fig. 71A-3-007. HHOBAMBC. P_s vs. T [84Sak]. Cell thickness: 50 µm. f = 100 Hz.

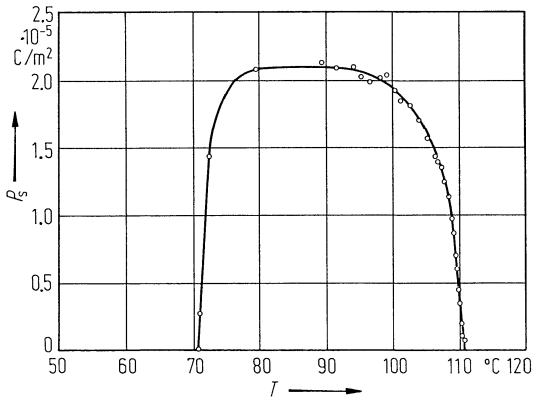

Fig. 71A-3-008. HDOBAMBC. P_s vs. T [84Sak]. Cell thickness: 50 µm. f = 100 Hz.

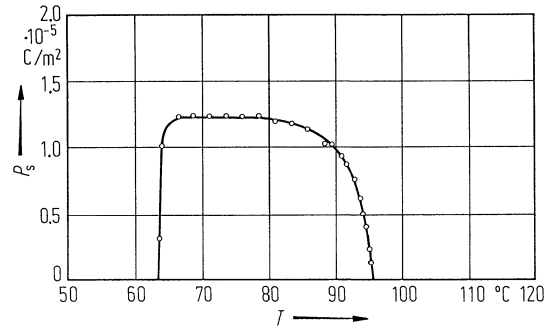

Fig. 71A-3-009. HTDOBAMBC. P_s vs. T [84Sak]. Cell thickness: 50 µm. f = 100 Hz.

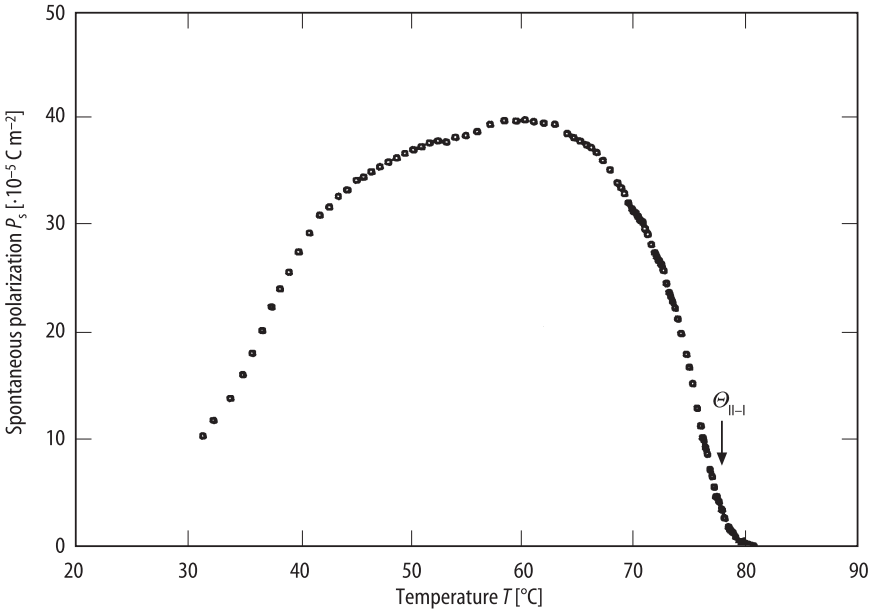

Fig. 71A-3-010. HDOBACEEC. P_s vs. T [89Ezc].

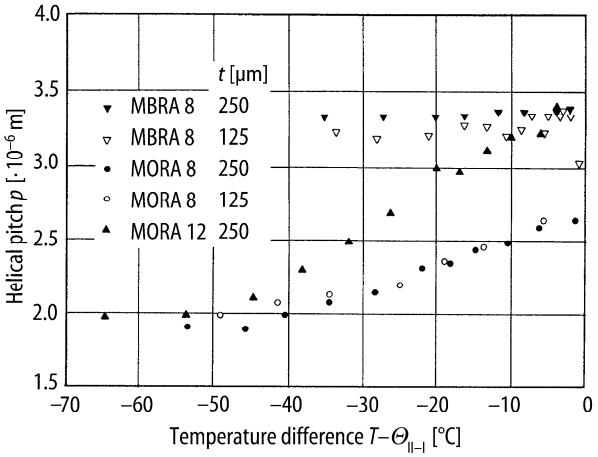

Fig. 71A-3-011. MBRA 8, MORA 8, MORA 12. p vs. $T - \Theta_{II-I}$ [83Ska]. Parameter: t, cell thickness. p: helical pitch.

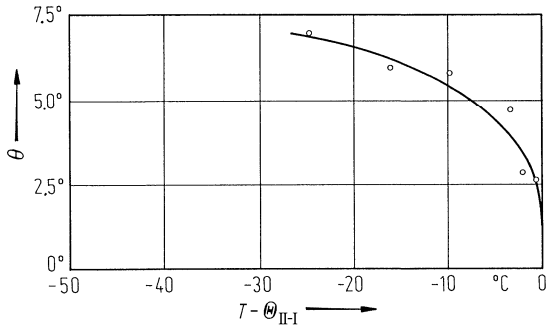

Fig. 71A-3-012. MBRA 8. θ vs. $T - \Theta_{II-I}$ [83Ska]. θ: tilt angle.

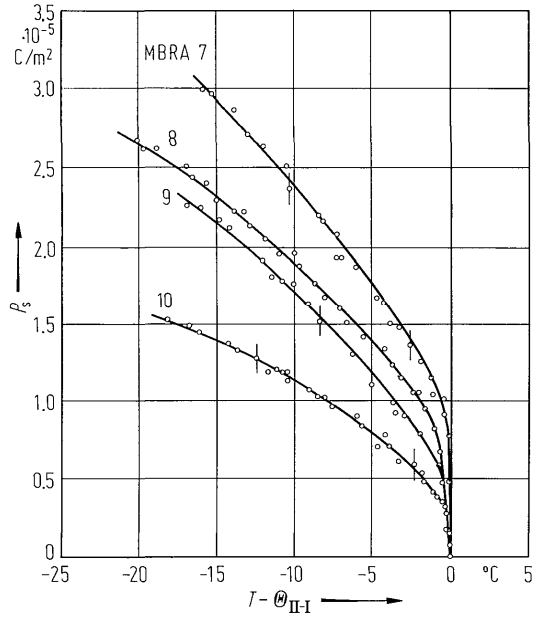

Fig. 71A-3-013. MBRA n (n = 7, 8, 9, 10). P_s vs. $T - \Theta_{II-I}$ [80Ost].

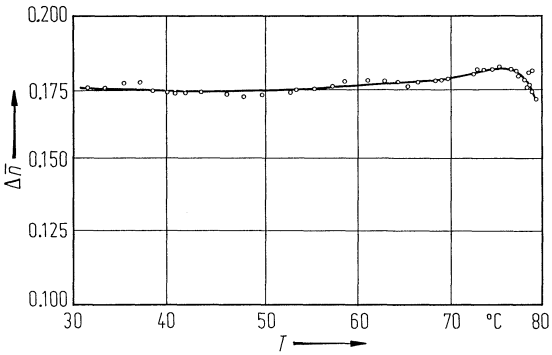

Fig. 71A-3-014. $(MBRA\ 7)_{0.95}(HOBACPC)_{0.05}$. $\Delta\bar{n}$ vs. T [85Bai]. $\Delta\bar{n}$: birefringence under applied electric field. Cell thickness: 8.6 µm. Applied voltage: 50 V.

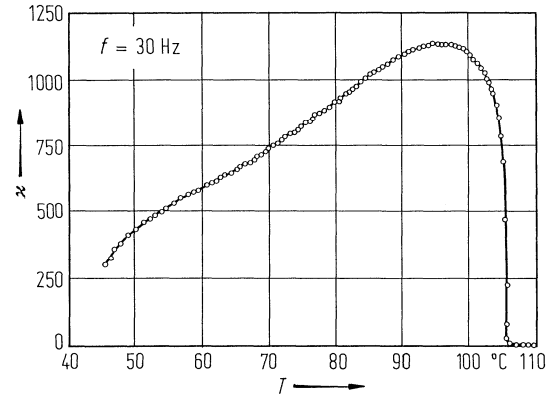

Fig. 71A-3-015. HDOBAC-3-MPC. κ vs. T [86Sak]. Cell thickness: 100 µm. f = 30 Hz.

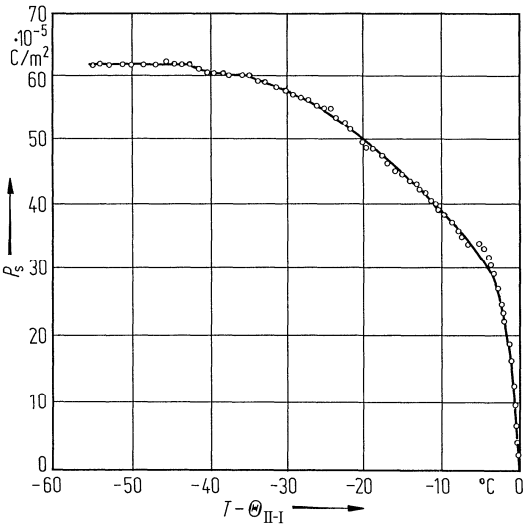

Fig. 71A-3-016. HDOBAC-3-MPC. P_s vs. $T - \Theta_{II-I}$ [86Sak]. Cell thickness: 100 µm. f = 60 Hz.

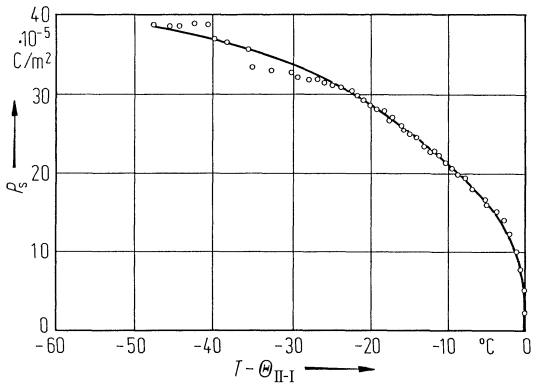

Fig. 71A-3-017. HDOBAB-3-MPC. P_s vs. $T - \Theta_{II-I}$ [86Sak]. Cell thickness: 50 µm. f = 60 Hz.

References

80Ost Ostrovskii, B.I., Rabinovich, A.Z., Sonin, A.S., Sorkin, E.L., Strukov, B.A., Taraskin, S.A.: Ferroelectrics **24** (1980) 309.

82Hal Hallsby, A., Nilsson, M., Otterholm, B.: Mol. Cryst. Liq. Cryst. (Lett.) **82** (1982) 61.

83Ska Skarp, K., Flatischler, K., Kondo, K., Sato, Y., Miyasato, K., Takezoe, H., Fukuda, A., Kuzue, E.: Jpn. J. Appl. Phys. **22** (1983) 566.

84Sak Sakurai, T., Sakamoto, K., Honma, M., Yoshino, K., Ozaki, M.: Ferroelectrics **58** (1984) 21.

85Bai Baikalov, V.A., Beresnev, L.A., Bilnov, L.M.: Mol. Cryst. Liq. Cryst. **127** (1985) 397.

86Bil Billard, J., Dahlgren, A., Flatischler, K., Lagerwall, S.T., Otterholm, B.: Mol. Cryst. Liq. Cryst. **135** (1986) 265.

86Sak Sakurai, T., Mikami, N., Ozaki, M., Yoshino, K.: J. Chem. Phys. **85** (1986) 585.

89Ezc Ezcurra, A., Pérez Jubindo, M.A., Etxebarría, J., de la Fuente, M.R., Sierra, M.T.: Ferroelectrics **92** (1989) 325.

No. 71A-4 B-8 and analogues

(A) $C_nH_{2n+1}O$– 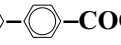 –$COOCH_2CH(CH_3)C_2H_5$

B-n: 2-methylbutyl-4-(4′-alkoxyphenyl)-benzoate

1b n = 8 (B-8):

phase	III	II	I	I′
	crystalline solid	smectic C* (Sm C*)	smectic A (Sm A)	isotropic liquid
state		F	P	
Θ [°C]	46.1	(43.7)	64.1	( ): cooling

85Kon

Phase diagram of mixture with S-8 (2-methylbutyl-4-(4′-octyloxybenzylidene amino)-benzoate): Fig. 71A-4-001.

3b Tilt angle and helical pitch of mixture with S-8: Fig. 71A-4-002.

5c Spontaneous polarization: Fig. 71A-4-003.

9a Birefringence: Fig. 71A-4-004.

(B) $C_nH_{2n+1}COO$– 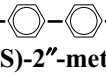 –$COOCH_2CH(CH_3)C_2H_5$

2MBACBC ((S)-2″-methylbutyl-4′-*n*-alkylcarbonyloxy-(1,1′-biphenyl)-4-carboxylate)

n = 7: 2MBHpCBC
n = 8: 2MBOCBC
n = 9: 2MBNCBC
n = 10: 2MBDCBC
n = 11: 2MBUDCBC
n = 12: 2MBDDCBC
n = 13: 2MBTDCBC

1b

phase		III	II	I	I′
		crystalline solid	smectic C* (Sm C*)	smectic A (Sm A)	isotropic liquid
state			F	P	
Θ [°C]	n = 7		35	58	
		(17)	(33)	(58)	
	8	0	40	49	
		(10)	(17)	(49)	
	9	38.4	46.2	61.5	
		(21)	(46.6)	(61.1)	
	10	24	49	62	
		(29)	(47)	(62)	
	11	37	51	63	
		(34)	(50)	(63)	
	12	46	48.5	62	
		(35)	(48.5)	(62)	
	13		50	64	
		(46)	(51)	(64)	( ): cooling

86Mik

3b	Tilt angle and helical pitch: Fig. 71A-4-005, Fig. 71A-4-006 .
5a	Dielectric constant: Fig. 71A-4-007, Fig. 71A-4-008. Effect of hydrostatic pressure on dielectric constant: Fig. 71A-4-009.
b	Effect of applied voltage on dielectric constant: Fig. 71A-4-010.
c	Spontaneous polarization: Fig. 71A-4-011, Fig. 71A-4-012; see also Fig. 71A-4-005 in 3b.

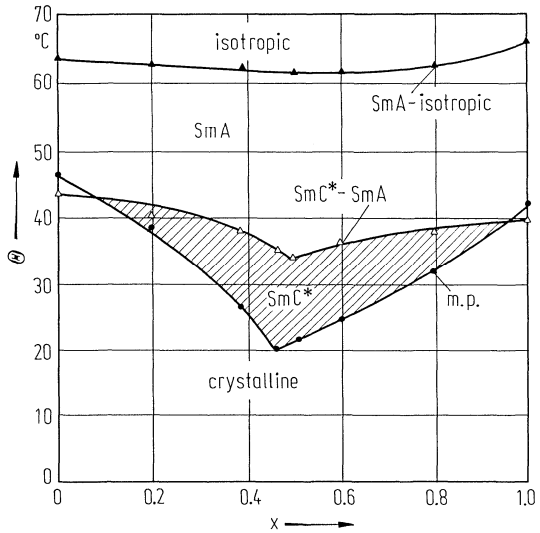

Fig. 71A-4-001. $(B\text{-}8)_{1-x}(S\text{-}8)_x$. Θ vs. x [85Kon]. S-8: 2-methylbutyl-4-(4′-octyloxybenzylidene amino)-benzoate. m.p.: mesophase-crystal boundary.

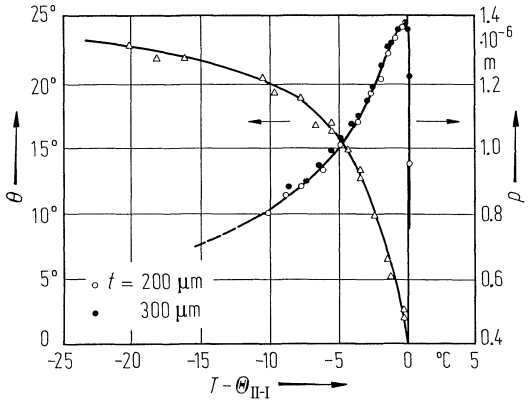

Fig. 71A-4-002. $(B\text{-}8)_{0.5}(S\text{-}8)_{0.5}$. θ, p vs. $T - \Theta_{II-I}$ [85Kon]. θ: tilt angle. p: helical pitch. S-8: 2-methylbutyl-4-(4′-octyloxybenzylidene amino)-benzoate. t: cell thickness.

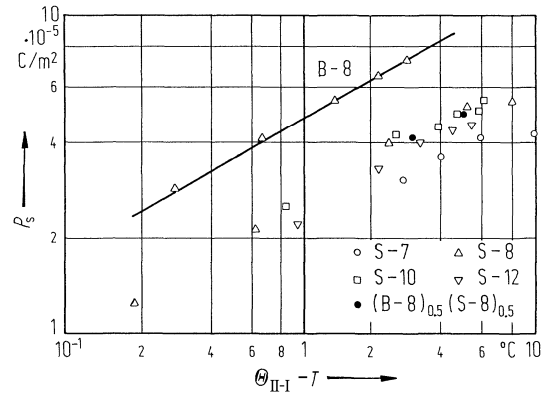

Fig. 71A-4-003. B-8, S-n, $(B\text{-}8)_{0.5}(S\text{-}8)_{0.5}$. P_s vs. $\Theta_{II-I} - T$ [85Kon]. S-n: 2-methylbutyl-4-(4′-alkoxybenzylidene amino)-benzoate.

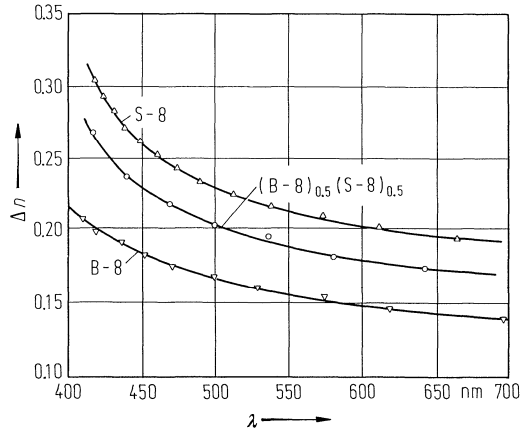

Fig. 71A-4-004. B-8, S-8, $(B\text{-}8)_{0.5}(S\text{-}8)_{0.5}$.. Δn vs. λ [85Kon]. S-8: 2-methylbutyl-4-(4′-octyloxybenzylidene amino)-benzoate.

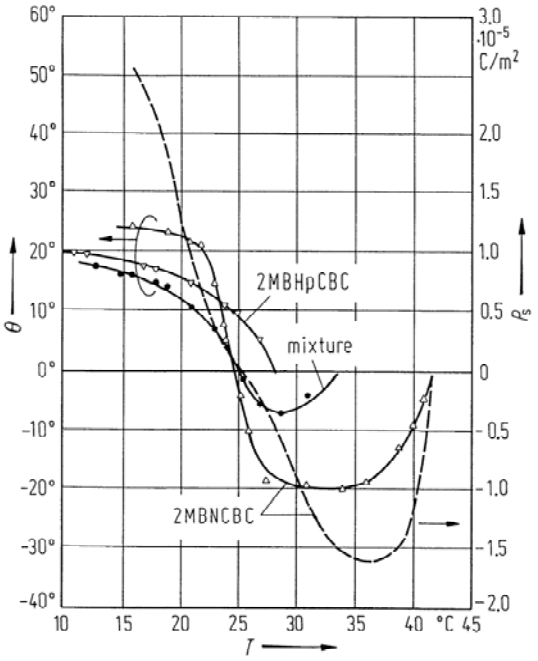

Fig. 71A-4-005. 2MBHpCBC, 2MBNCBC. θ, P_s vs. T [86Mik]. θ: tilt angle.

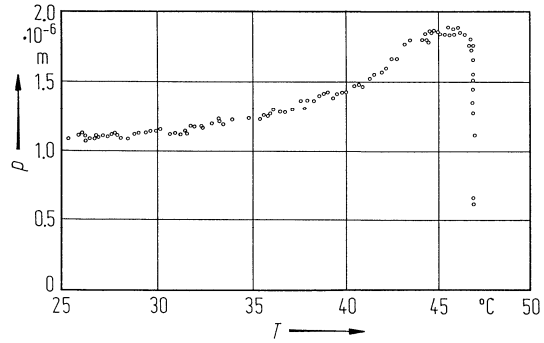

Fig. 71A-4-006. 2MBNCBC. p vs. T [87Nak]. p: helical pitch. Cell thickness: 250 μm.

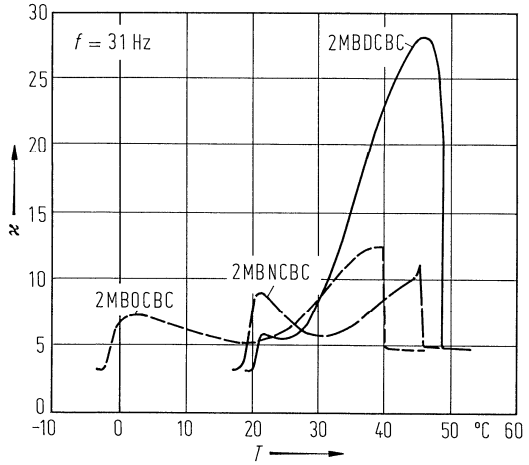

Fig. 71A-4-007. 2MBOCBC, 2MBNCBC, 2MBDCBC. κ vs. T [87Nak]. Cell thickness: 50 µm. f = 31 Hz.

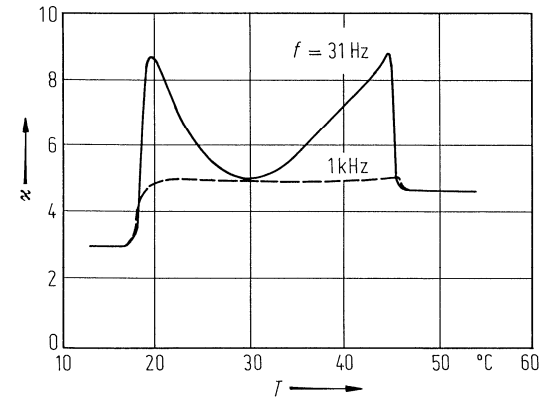

Fig. 71A-4-008. 2MBNCBC. κ vs. T [86Mik]. Parameter: f.

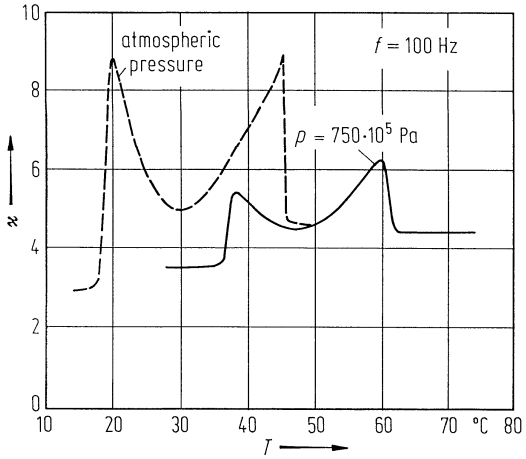

Fig. 71A-4-009. 2MBNCBC. κ vs. T [87Oza]. Parameter: p, hydrostatic pressure. f = 100 Hz.

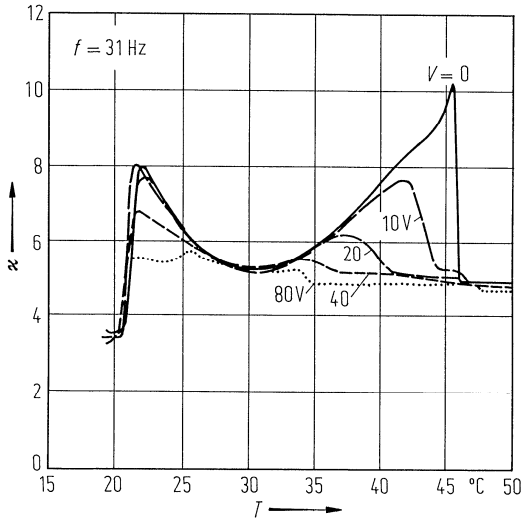

Fig. 71A-4-010. 2MBNCBC. κ vs. T [87Nak]. Parameter: applied voltage. Cell thickness: 50 µm. f = 31 Hz.

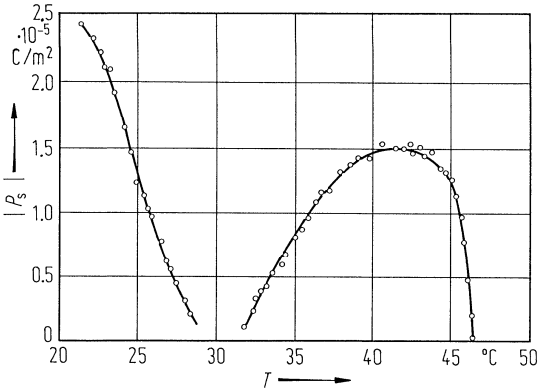

Fig. 71A-4-011. 2MBNCBC. | P_s | vs. T [86Mik]. | P_s |: magnitude of spontaneous polarization.

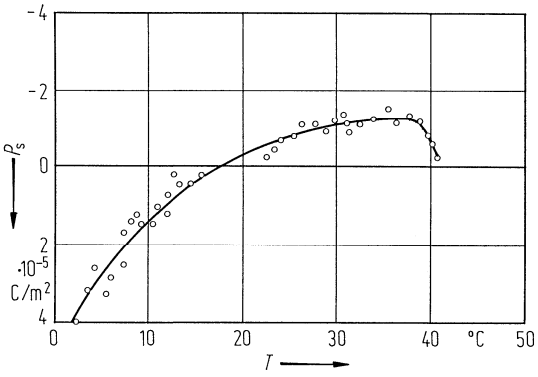

Fig. 71A-4-012. 2MBOCBC. P_s vs. T [87Nak]. Cell thickness: 6 µm.

References

85Kon Kondo, K., Era, S., Isogai, M., Mukoh, A.: Jpn. J. Appl. Phys. **24** (1985) 1389.
86Mik Mikami, N., Higuchi, R., Sakurai, T., Ozaki, M., Yoshino, K.: Jpn. J. Appl. Phys. **25** (1986) L833.
87Nak Nakao, K., Ozaki, M., Yoshino, K.: Jpn. J. Appl. Phys. **26** (1987) Suppl. 26–2, p.104.
87Oza Ozaki, M., Yasuda, N., Yoshino, K.: Jpn. J. Appl. Phys. **26** (1987) L1927.

No. 71A-5 3M2CPAOB and analogues

(A) $C_nH_{2n+1}O$–⬡–⬡–$OCOCHClCH(CH_3)C_2H_5$

3M2CPAOB ((2S,3S)-3-methyl-2-halopentanoic acid 4′,4″-alkoxybiphenyl ester)

n = 5: 3M2CPPOB
n = 6: 3M2CPHOB
n = 7: 3M2CPHpOB
n = 8: 3M2CPOOB
n = 9: 3M2CPNOB
n = 10: 3M2CPDOB
n = 12: 3M2CPDDOB

1b	phase		III	II	I	I′	87Oza1
			crystalline solid	smectic C* (Sm C*)	smectic A (Sm A)	isotropic liquid	
	state			F	P		
	Θ [°C]	n = 5	50	55	64		
		6	47	57	62		
		7	44	56	63		
		8	30	53	66		
		9	41	54	67		
		10	48	52	67		
		12	62	66	67		

5a Dielectric constant: Fig. 71A-5-001, Fig. 71A-5-002, Fig. 71A-5-003.
Dielectric dispersion: Fig. 71A-5-004, Fig. 71A-5-005, Fig. 71A-5-006, Fig. 71A-5-007; see also Fig. 71A-5-014 in 5b.
Dielectric constant under hydrostatic pressure: Fig. 71A-5-008.
Phase diagram p vs. Θ: Fig. 71A-5-009.

b Effect of E_{bias} and measuring electric field on dielectric constant: Fig. 71A-5-010, Fig. 71A-5-011, Fig. 71A-5-012, Fig. 71A-5-013, Fig. 71A-5-014.

c Spontaneous polarization: Fig. 71A-5-015, Fig. 71A-5-016.

(B) $C_nH_{2n+1}O$–⬡–⬡–$OCOCHBrCH(CH_3)C_2H_5$

n = 6: 3M2BPHOB
n = 8: 3M2BPOOB
n = 10: 3M2BPDOB
n = 12: 3M2BPDDOB

1b	phase		III	II	I	I′	87Oza1
			crystalline solid	smectic C* (Sm C*)	smectic A (Sm A)	isotropic liquid	
	state			F	P		
	Θ [°C]	n = 6	47	55			
		8	29	47	55		
		10	35	49	58		
		12	42	47	59		

(C) $C_nH_{2n+1}O$–⬡–⬡–$OCOCHClCH(CH_3)_2$

n = 7: 3M2CBHpOB
n = 8: 3M2CBOOB
n = 10: 3M2CBDOB

1b	phase		III	II	I	I′
			crystalline solid	smectic C* (Sm C*)	smectic A (Sm A)	isotropic liquid
	state			F	P	
	Θ [°C]	n = 7	67	73	77	
		8	63	71	80	
		10	66	69	81	
5a	Dielectric constant: Fig. 71A-5-017.					
c	Spontaneous polarization: see Fig. 71A-5-015.					

87Oza1

(D) $C_nH_{2n+1}O$–⬡–⬡–$OCOCHBrCH(CH_3)_2$

n = 6: 3M2BBHOB
n = 8: 3M2BBOOB
n = 10: 3M2BBDOB

1b	phase		III	II	I	I′
			crystalline solid	smectic C* (Sm C*)	smectic A (Sm A)	isotropic liquid
	state			F	P	
	Θ [°C]	n = 6	64	67		
		8	35	48	56	
		10	55	57	68	

87Oza1

(E) $C_nH_{2n+1}O$–⬡–⬡–$OCOCHClCH_2CH(CH_3)_2$

n = 6: 4M2CPHOB
n = 7: 4M2CPHpOB
n = 8: 4M2CPOOB

1b	phase		III	II	I	I′
			crystalline solid	smectic C* (Sm C*)	smectic A (Sm A)	isotropic liquid
	state			F	P	
	Θ [°C]	n = 6	62	65	74	
		7	56	63	64	
		8	61	64	68	

87Oza1

(F) $C_nH_{2n+1}O$– 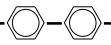 –$OCOCH(CH_3)C_2H_5$

n = 10: 2MBDOB
n = 11: 2MBUDOB
n = 12: 2MBDDOB

1b	phase		III	II	I	87Oza1
			crystalline solid	smectic C* (Sm C*)	smectic A (Sm A)	
	state			F	P	
	Θ [°C]	n = 10	73	74		
		11	70	72		
		12	68	69		

(G) $C_nH_{2n+1}O$–  –$OCOCHClC_2H_5$

n = 6: 2CBHOB
n = 8: 2CBOOB
n = 10: 2CBDOB

1b	phase		III	II	I	I′	87Oza1
			cystalline solid	smectic C* (Sm C*)	smectic A (Sm A)	isotropic liquid	
	state			F	P		
	Θ [°C]	n = 6	86	102	103		
		8	86	92	100		
		10	86	87	96		

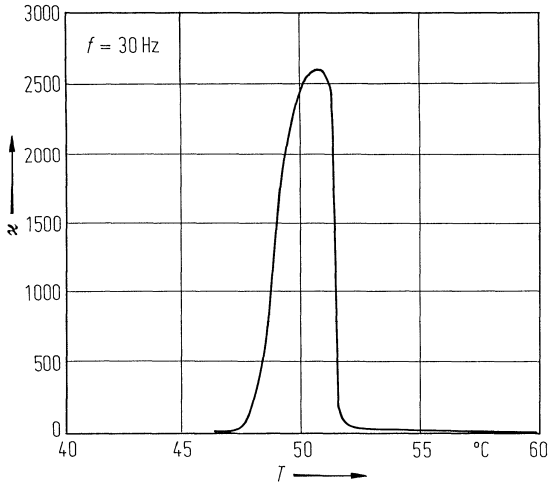

Fig. 71A-5-001. 3M2CPDOB. κ vs. T [87Yos1]. Cell thickness: 100 µm. f = 30 Hz.

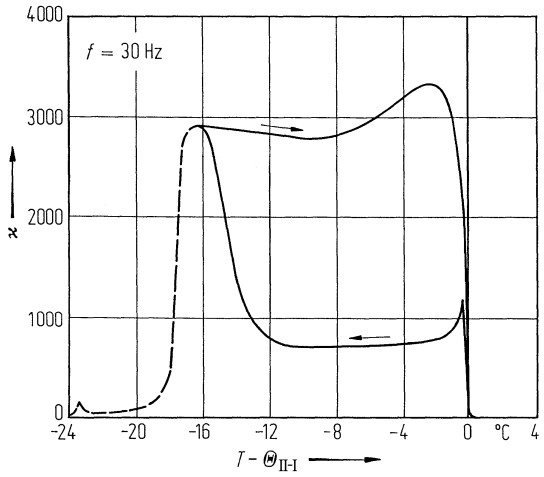

Fig. 71A-5-002. 3M2CPOOB. κ vs. $T - \Theta_{II-I}$ during cooling and heating cycle [87Oza1]. Cell thickness: 50 µm. f = 30 Hz.

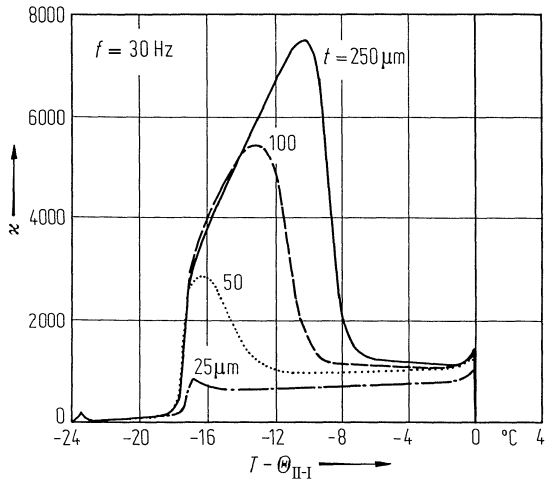

Fig. 71A-5-003. 3M2CPOOB. κ vs. $T - \Theta_{II-I}$ [87Oza1]. Parameter: t, sample thickness. f = 30 Hz. $E_{ac} = 5 \cdot 10^2$ V m^{-1}.

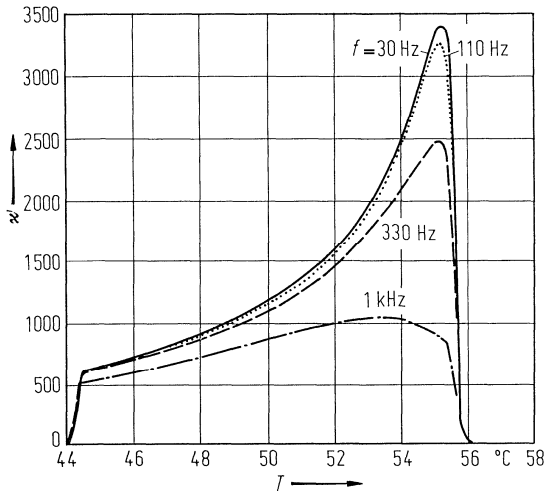

Fig. 71A-5-004. 3M2CPHpOB. κ' vs. T [87Oza1]. Parameter: f. Cell thickness: 100 µm.

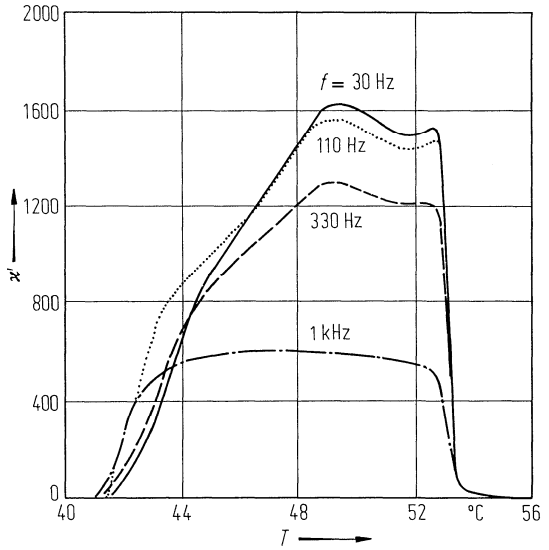

Fig. 71A-5-005. 3M2CPNOB. κ' vs. T [87Oza1]. Parameter: f. Cell thickness: 100 µm.

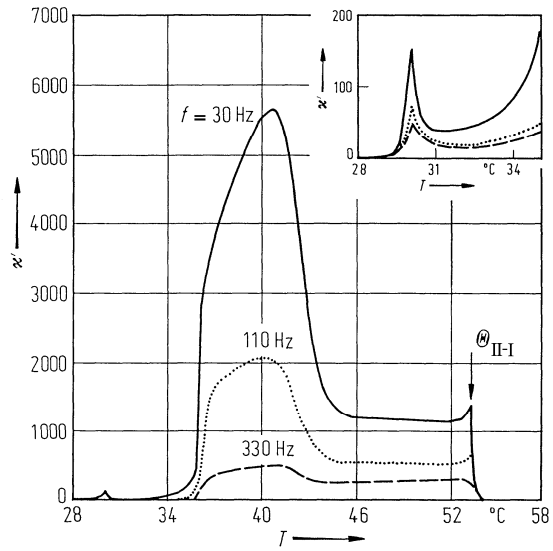

Fig. 71A-5-006. 3M2CPOOB. κ' vs. T [87Oza1]. Parameter: f. Cell thickness: 100 µm.

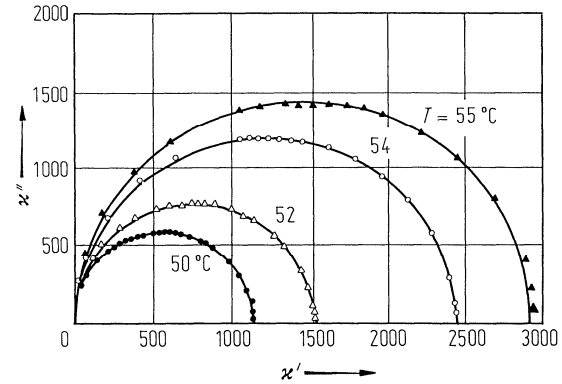

Fig. 71A-5-007. 3M2CPHpOB. κ' vs. κ'' (Cole-Cole plot) [87Oza1]. Parameter: T. Cell thickness: 100 µm.

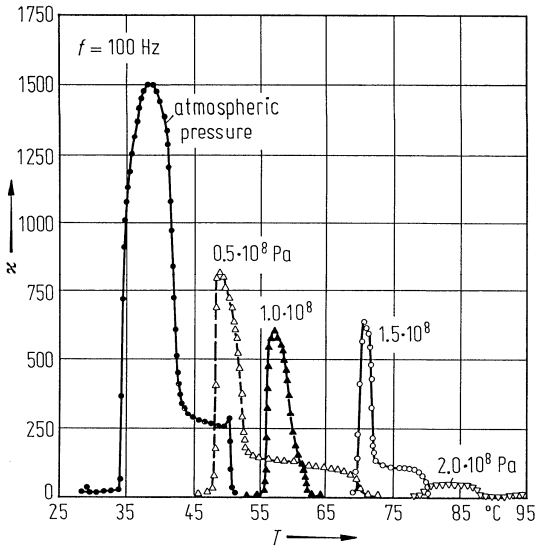

Fig. 71A-5-008. 3M2CPOOB. κ vs. T [87Oza2]. Parameter: p, hydrostatic pressure. Cell thickness: 150 µm. f = 100 Hz.

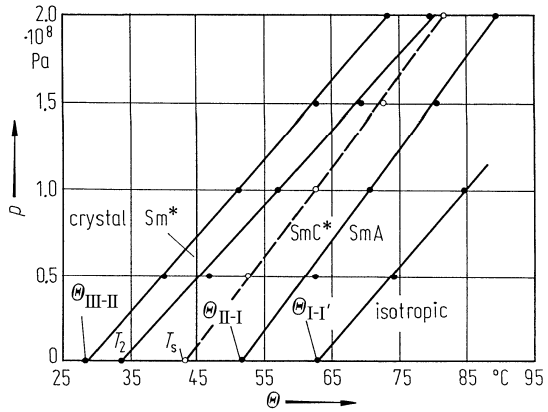

Fig. 71A-5-009. 3M2CPOOB. p vs. Θ determined by dielectric measurement [87Oza2]. p: hydrostatic pressure. Cell thickness: 150 µm.

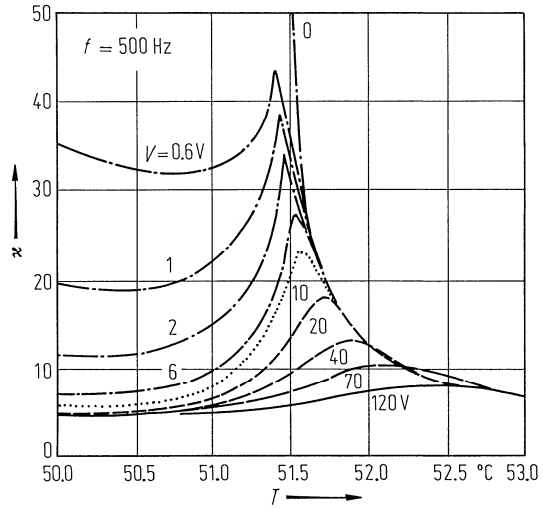

Fig. 71A-5-010. 3M2CPOOB. κ vs. T [87Yos2]. Parameter: V, applied dc voltage. Cell thickness: 16 µm. f = 500 Hz.

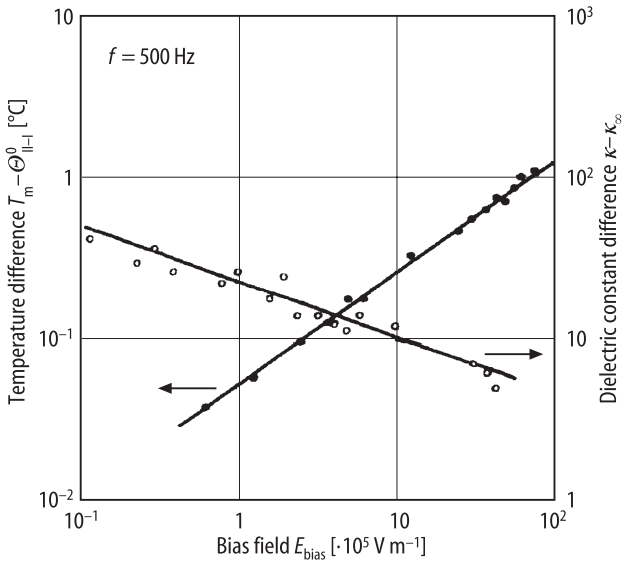

Fig. 71A-5-011. 3M2CPOOB. $T_m - \Theta^0_{II-I}$, $\kappa - \kappa_\infty$ vs. E_{bias} [87Yos2]. T_m: peak temperature of dielectric constant. Θ^0_{II-I}: Θ_{II-I} without E_{bias}. Cell thickness: 16 µm. f = 500 Hz. κ_∞: κ in Sm A phase.

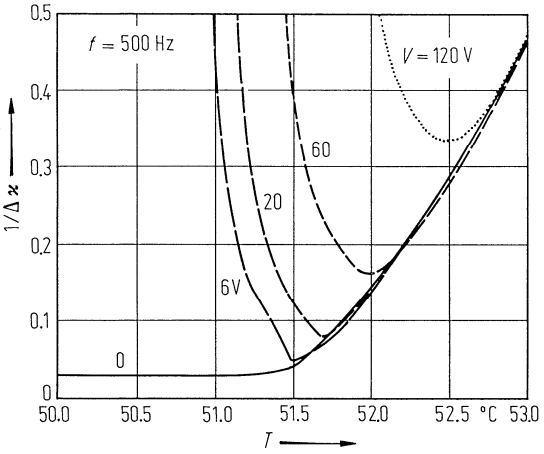

Fig. 71A-5-012. 3M2CPOOB. $1/\Delta\kappa$ vs. T [87Yos3]. Parameter: V, applied dc voltage. $\Delta\kappa = \kappa(C^*) - \kappa(A)$, where $\kappa(C^*)$ and $\kappa(A)$ are dielectric constants in the Sm C^* phase and Sm A phase, respectively. Cell thickness: 16 μm. f = 500 Hz.

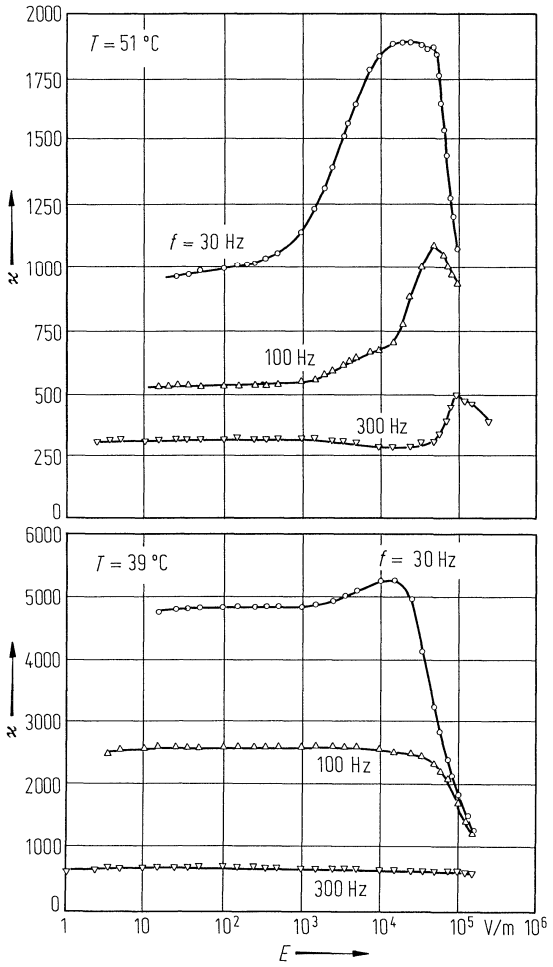

Fig. 71A-5-013. 3M2CPOOB. κ vs. E [87Oza1]. Parameter: f. E: measuring electric field. Cell thickness: 100 μm.

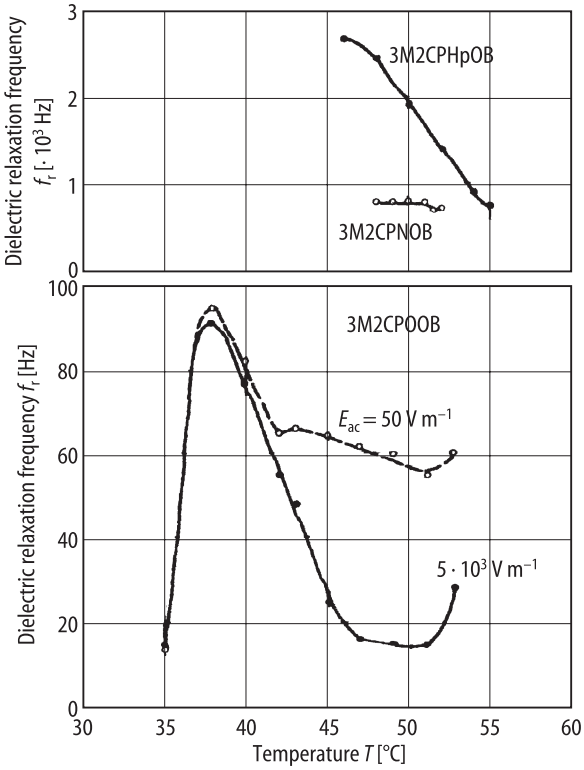

Fig. 71A-5-014. 3M2CPHpOB, 3M2CPOOB, 3M2CPNOB. f_r vs. T [87Oza1]. Parameter: E_{ac}, measuring electric field. f_r: dielectric relaxation frequency. Cell thickness: 100 µm.

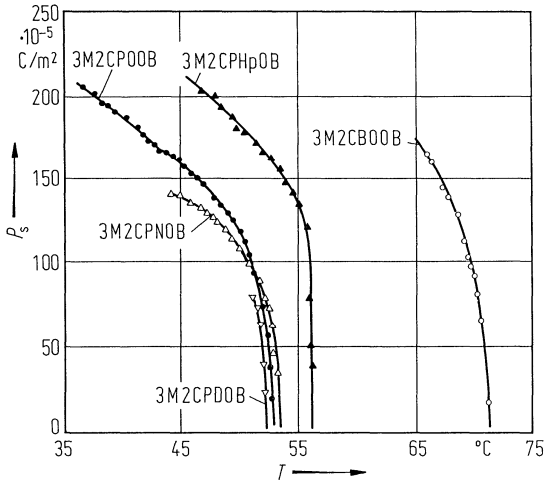

Fig. 71A-5-015. 3M2CPHpOB, 3M2CPOOB, 3M2CPNOB, 3M2CPDOB, 3M2CBOOB. P_s vs. T [87Yos1].

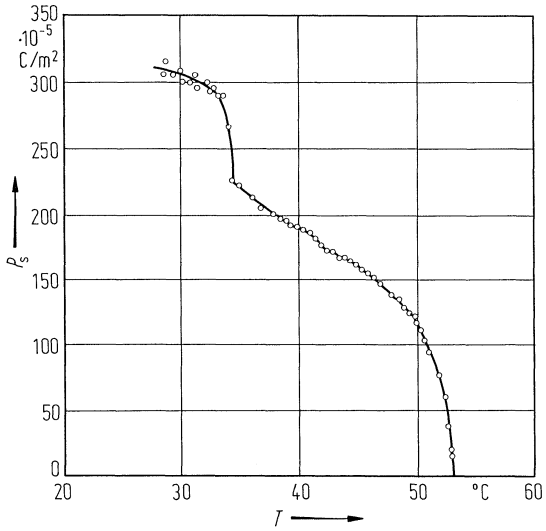

Fig. 71A-5-016. 3M2CPOOB. P_s vs. T [87Yos1].

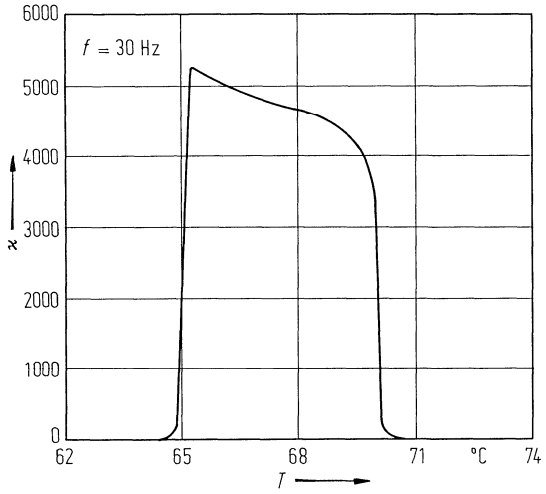

Fig. 71A-5-017. 3M2CPOOB. κ vs. T [87Yos1]. Cell thickness: 100 µm. f = 30 Hz.

References

87Oza1 Ozaki, M., Yoshino, K., Sakurai, T., Mikami, N., Higuchi, R.: J. Chem. Phys. **86** (1987) 3648.
87Oza2 Ozaki, M., Yasuda, N., Yoshino, K.: Jpn. J. Appl. Phys. **26** (1987) L1927.
87Yos1 Yoshino, K., Ozaki, M., Kishino, S., Sakura, T., Mikami, N., Higuchi, R., Honma, M.: Mol. Cryst. Liq. Cryst. **144** (1987) 87.
87Yos2 Yoshino, K., Nakao, K., Taniguchi, H., Ozaki, M.: Jpn. J. Appl. Phys. **26** (1987) Suppl. 26–1, p. 97.
87Yos3 Yoshino, K., Nakao, K., Taniguchi, H., Ozaki, M.: J. Phys. Soc. Jpn. **56** (1987) 4150.

No. 71A-6 4′-((S)-2-methylbutyloxy)phenyl-4-alkoxy-benzoate and analogues

(A) $C_nH_{2n+1}O$–⬡–COO–⬡–$OCH_2CH(CH_3)C_2H_5$
4′-((S)-2-methylbutyloxy)phenyl-4-alkoxy-benzoate

1b	phase	III	II	I	I′	I″	84Kel
		crystalline solid	smectic C* (Sm C*)	smectic A (Sm A)	chiral nematic	isotropic liquid	
	state		F	P	P		
	Θ [°C] n = 8	42	43.5	58.5	62		
	9	44	(43.5)	60			
	10	44	50.2	65			
	11	49.5	(48)	63			
	12	49	52	65		( ): cooling	
	See also						84Dec
3b	Tilt angle: Fig. 71A-6-001.						
5c	Spontaneous polarization: Fig. 71A-6-002, Fig. 71A-6-003, Fig. 71A-6-004; see also Fig. 71A-6-001.						
6a	Specific heat: Fig. 71A-6-005.						

(B) $C_nH_{2n+1}O$–⬡–COO–⬡–$O(CH_2)_3CH(CH_3)C_2H_5$
4′-((S)-4-methylhexyloxy)phenyl-4-alkoxy-benzoate

1b	phase	IV	III	II	I	I′	I″	84Kel
		crystalline solid	unidentified smectic (Sm X*)	smectic C* (Sm C*)	smectic A (Sm A)	chiral nematic	isotropic liquid	
	state		F	F	P	P		
	Θ [°C] n = 8	49		61		79		
	9	41		66		75.5		
	10	35	(30)	70.4	72.5	76		
	11	50		72	74	76		
	12	45.5		74.5	77	80		
							( ): cooling	
3b	Tilt angle: Fig. 71A-6-006. Smectic layer spacing: Fig. 71A-6-007.							
6a	DSC intensity: Fig. 71A-6-008.							

(C) $C_nH_{2n+1}O$–⬡–OCO–⬡–$O(CH_2)_5CH(CH_3)C_2H_5$
4′-alkoxyphenyl-4((S)-6-methyloctyloxy)-benzoate

1b	phase		III	II	I	I′
			crystalline solid	smectic C* (Sm C*)	chiral nematic	isotropic liquid
	state			F	P	
	Θ [°C]	n = 7	54	63.5	70.5	
		8	50	66.5	73	
		9	49	67.5	71.5	
		10	53.5	69.5	74	

84Kel

(D) $C_nH_{2n+1}O$–⬡–COO–⬡–$O(CH_2)_2CH(CH_3)(CH_2)_3CH(CH_3)_2$
4′-((S)-3,7-dimethyloctyloxy)phenyl-4-alkoxybenzoate

3b	Tilt angle: Fig. 71A-6-009.
5c	Spontaneous polarization: Fig. 71A-6-010.

(E) $C_nH_{2n+1}O$–⬡–OCO–⬡–$O(CH_2)_2CH(CH_3)(CH_2)_3CH(CH_3)_2$
4′-alkoxyphenyl-4((S)-3,7-dimethyloctyloxy)-benzoate

5c	Spontaneous polarization: Fig. 71A-6-011.

(F) $C_nH_{2n+1}O$–⬡–COO–⬡–$OCH_2CH(CH_3)OC_mH_{2m+1}$
4′-((S)-2-alkoxypropoxy)phenyl-4-alkoxy-benzoate
n = 12, m = 2: 4′-((S)-2-ethoxypropoxy)phenyl-4-dodecyloxy-benzoate
n = 12, m = 3: 4′-((S)-2-propoxypropoxy)phenyl-4-dodecyloxy-benzoate

3b	Tilt angle: Fig. 71A-6-012, Fig. 71A-6-013.
5c	Spontaneous polarization: Fig. 71A-6-014, Fig. 71A-6-015.
8a	Rotational viscosity: Fig. 71A-6-016, Fig. 71A-6-017.

(G) $C_nH_{2n+1}O$–⬡–COO–⬡–$O(CH_2)_mOCH_2CH(CH_3)OC_2H_5$
(S)-4′((2-ethoxy)propoxy)alkoxyphenyl 4-alkoxybenzoate

3b	Tilt angle: Fig. 71A-6-018, Fig. 71A-6-019, Fig. 71A-6-020. Helical pitch: Fig. 71A-6-021, Fig. 71A-6-022, Fig. 71A-6-023.
5c	Spontaneous polarization: Fig. 71A-6-024, Fig. 71A-6-025, Fig. 71A-6-026.

(H) 

(S)-3,7-dimethyloctyl 4-*n*-alkoxybenzoyloxybenzoate

1b	Transition temperatures: Table 71A-6-001; Fig. 71A-6-027.
3b	Tilt angle and helical pitch: Fig. 71A-6-028, Fig. 71A-6-029.
5c	Spontaneous polarization: Fig. 71A-6-030.
6a	Transition enthalpy: see Table 71A-6-001.

(I) 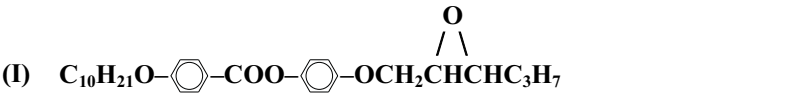

4′-((S,S)-2,3-epoxyhexyloxy)phenyl-4-(*n*-decyloxy)-benzoate

3b	Tilt angle: Fig. 71A-6-031.
5c	Spontaneous polarization: Fig. 71A-6-032.
8a	Rotational viscosity: Fig. 71A-6-033.

Table 71A-6-001. $C_nH_{2n+1}O$–  –COO––$COO(CH_2)_2CH(CH_3)(CH_2)_3CH(CH_3)_2$. Transition temperature Θ [°C], transition enthalpy ΔH [· 10^3 J kg], helical twist sense, direction of spontaneous polarization for various n [87Chi]. m.p.: mesophase-crystal boundary. Iso: isotropic liquid.

n	Twist	P_s (sign)		m.p [a])	Recrystal-lization	Sm C* - Sm A [b])	Sm A - Iso [b])	Sm C* - Iso
7	l(–)	(+)	Θ	35.6	18.0	-	49.6	-
			ΔH	63.4	40.2	-	12.2	
8	l(–)	(+)	Θ	38.5	14.9	30.2	51.1	-
			ΔH	64.1	51.5	0.04	13.8	
9	l(–)	(+)	Θ	39.4	21.1	40.3	50.0	-
			ΔH	52.0	46.3	0.04	13.8	
10	l(–)	(+)	Θ	38.8	22.5	46.0	51.3	-
			ΔH	47.8	43.6	0.17	13.0	
11	l(–)	(+)	Θ	42.3	28.5	47.4	50.4	-
			ΔH	66.2	51.5	0.38	12.2	
12	l(–)	(+)	Θ	37.5	20.5	49.0	51.8	-
			ΔH	62.9	38.5	0.08	12.2	
13	l(–)	(+)	Θ	47.4	28.2	48.6	49.8	-
			ΔH	64.1	59.9	0.04	15.5	
14 [c])	l(–)	(+)	Θ	41.5	38.3	50.0	51.0	-
			ΔH	-	-	-	-	-
16	l(–)	(+)	Θ	48.3	28.9	-	-	49.7
			ΔH	82.5	65.1	-	-	13.4

[a]) Temperatures obtained by DSC.
[b]) Temperatures obtained by thermal optical microscopy
[c]) Too small sample to measure enthalpies.

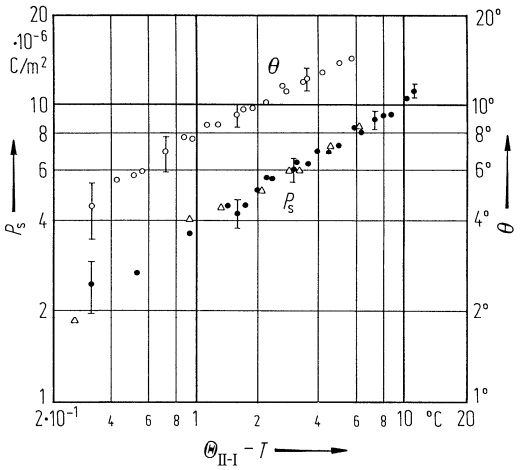

Fig. 71A-6-001. $C_nH_{2n+1}O$–⟨⬡⟩–COO–⟨⬡⟩–$OCH_2CH(CH_3)C_2H_5$ (n = 10). θ, P_s vs. $\Theta_{II-I} - T$ [78Los]. θ : tilt angle. Different symbols correspond to different runs.

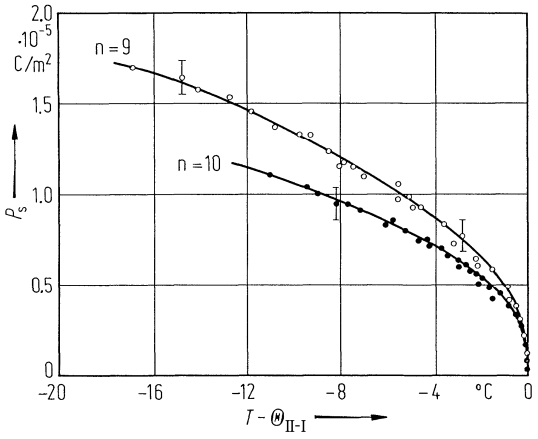

Fig. 71A-6-002. $C_nH_{2n+1}O$–⟨⬡⟩–COO–⟨⬡⟩–$OCH_2CH(CH_3)C_2H_5$ (n = 9, 10). P_s vs. $T - \Theta_{II-I}$ [80Ost].

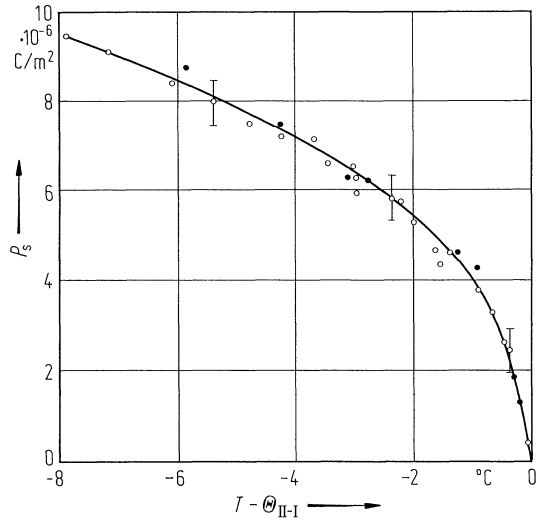

Fig. 71A-6-003. $C_nH_{2n+1}O$–⟨⟩–COO–⟨⟩–$OCH_2CH(CH_3)C_2H_5$ (n = 10). P_s vs. $T - \Theta_{II–I}$ [78Los]. Full circle, open circle: different runs of measurement.

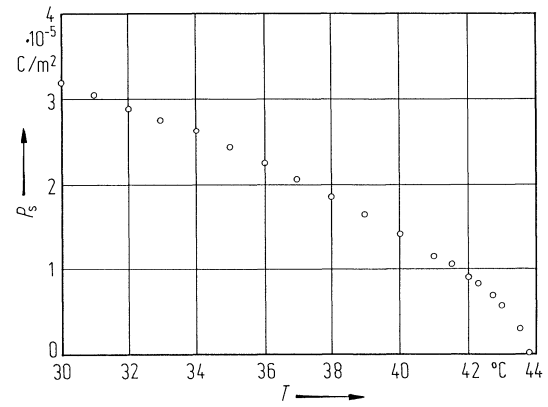

Fig. 71A-6-004. $C_nH_{2n+1}O$–⟨⟩–COO–⟨⟩–$OCH_2CH(CH_3)C_2H_5$ (n = 8). P_s vs. T [86Ska].

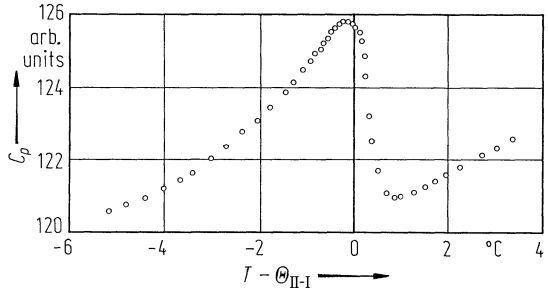

Fig. 71A-6-005. $C_nH_{2n+1}O$–⟨⟩–COO–⟨⟩–$OCH_2CH(CH_3)C_2H_5$ (n = 10). C_p vs. $T - \Theta_{II–I}$ [80Ost].

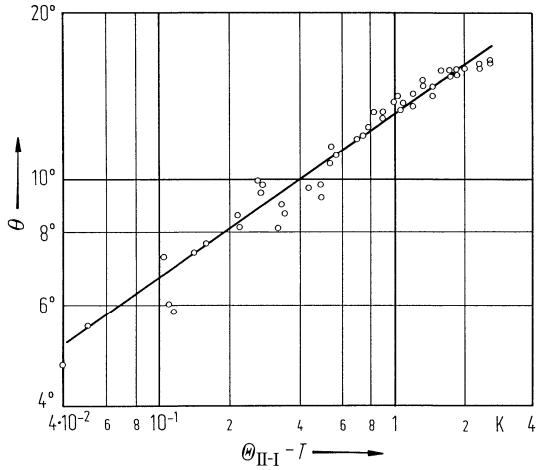

Fig. 71A-6-006. $C_nH_{2n+1}O$–⬡–COO–⬡–$O(CH_2)_3CH(CH_3)C_2H_5$ (n = 10). θ vs. Θ_{II-I}–T [85Kel]. θ: tilt angle.

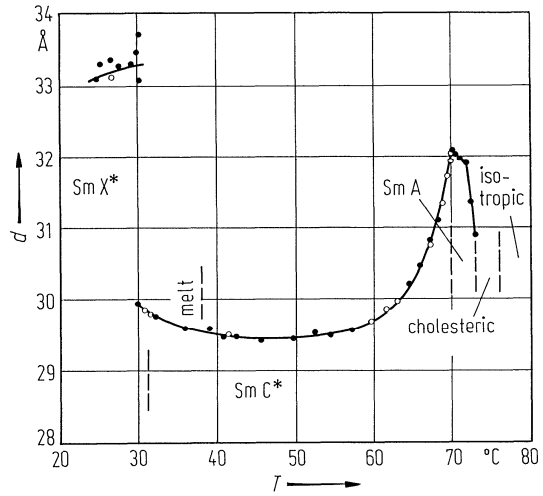

Fig. 71A-6-007. $C_nH_{2n+1}O$–⬡–COO–⬡–$O(CH_2)_3CH(CH_3)C_2H_5$ (n = 10). d vs. T [85Kel]. d: smectic layer spacing. Full circle, open circle: different runs of measurement.

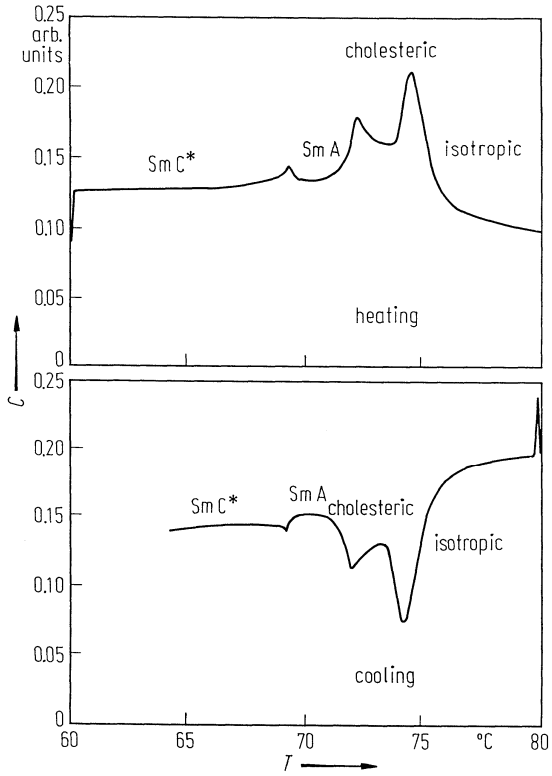

Fig. 71A-6-008. $C_nH_{2n+1}O$–⬡–COO–⬡–$O(CH_2)_3CH(CH_3)C_2H_5$ (n = 10). *C* vs. *T* [85Kel]. *C*: DSC intensity.

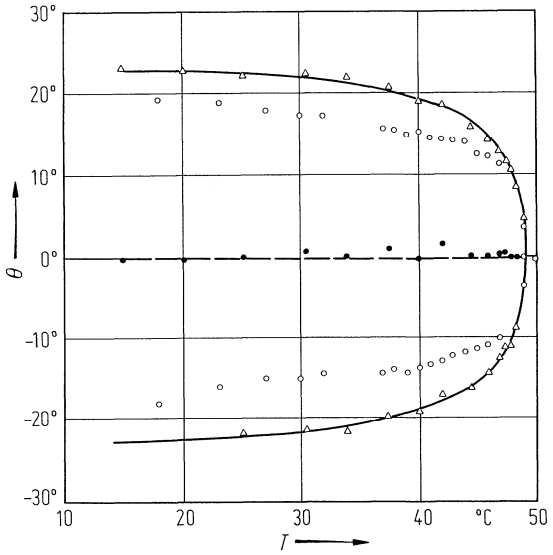

Fig. 71A-6-009. $C_nH_{2n+1}O$–⬡–COO–⬡–$O(CH_2)_2CH(CH_3)(CH_2)_3CH(CH_3)_2$ (n = 10). θ vs. *T* [87Pat]. θ: tilt angle. Open triangle: above saturation voltage. Open circle: below saturation voltage. Full circle: mean value.

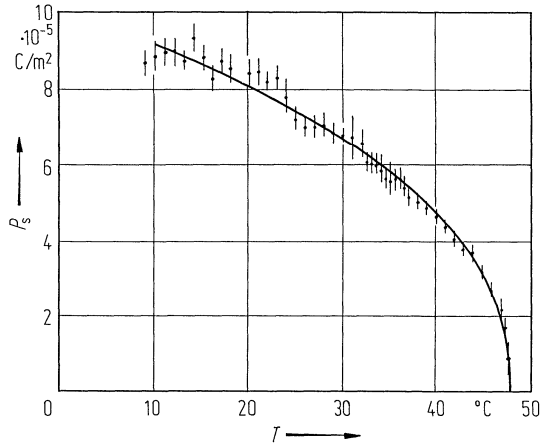

Fig. 71A-6-010. $C_nH_{2n+1}O$–⟨⟩–COO–⟨⟩–$O(CH_2)_2CH(CH_3)(CH_2)_3CH(CH_3)_2$ (n = 10). P_s vs. T [87Pat].

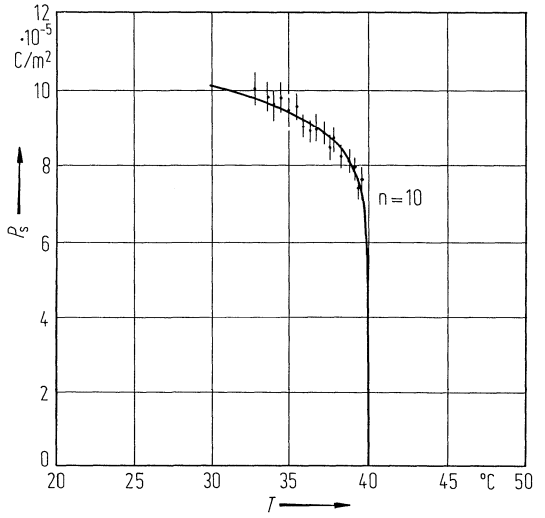

Fig. 71A-6-011. $C_nH_{2n+1}O$–⟨⟩–OCO–⟨⟩–$O(CH_2)_2CH(CH_3)(CH_2)_3CH(CH_3)_2$ (n = 10). P_s vs. T [87Pat].

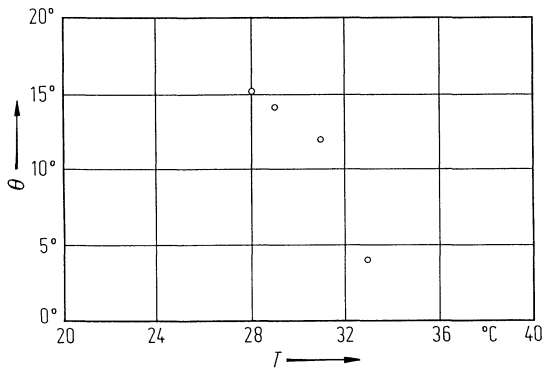

Fig. 71A-6-012. $C_nH_{2n+1}O$–⟨⟩–COO–⟨⟩–$OCH_2CH(CH_3)OC_mH_{2m+1}$ (n = 12, m = 2). θ vs. T [87And]. θ: tilt angle.

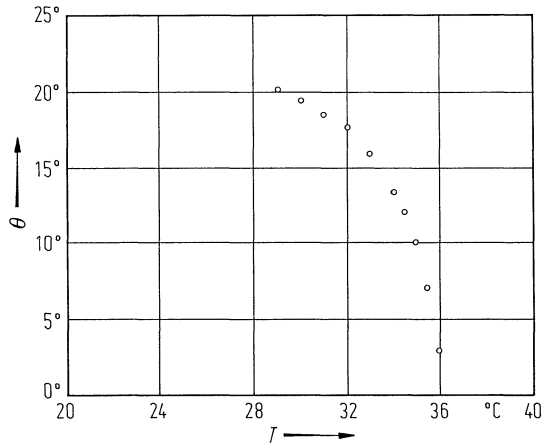

Fig. 71A-6-013. $C_nH_{2n+1}O$–⬡–COO–⬡–$OCH_2CH(CH_3)OC_mH_{2m+1}$ (n = 12, m = 3). θ vs. T [87And]. θ: tilt angle.

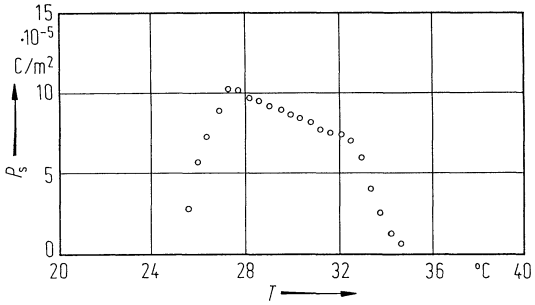

Fig. 71A-6-014. $C_nH_{2n+1}O$–⬡–COO–⬡–$OCH_2CH(CH_3)OC_mH_{2m+1}$ (n = 12, m = 2). P_s vs. T [87And].

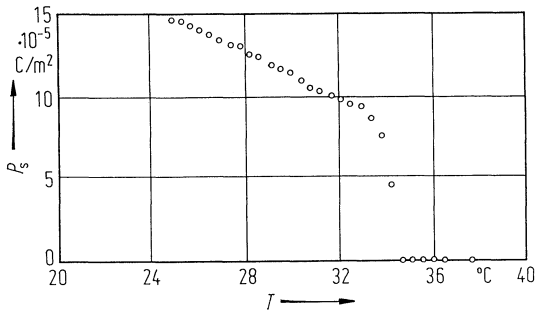

Fig. 71A-6-015. $C_nH_{2n+1}O$–⬡–COO–⬡–$OCH_2CH(CH_3)OC_mH_{2m+1}$ (n = 12, m = 3). P_s vs. T [87And].

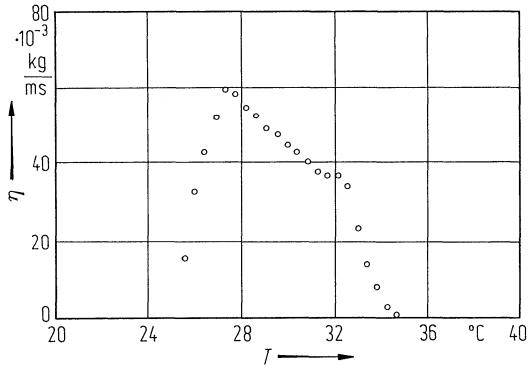

Fig. 71A-6-016. $C_nH_{2n+1}O$–⬡–COO–⬡–$OCH_2CH(CH_3)OC_mH_{2m+1}$ (n = 12, m = 2). η vs. T [87And]. η: rotational viscosity.

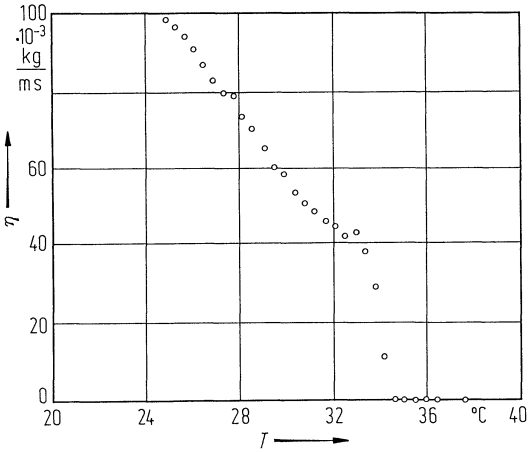

Fig. 71A-6-017. $C_nH_{2n+1}O$–⬡–COO–⬡–$OCH_2CH(CH_3)OC_mH_{2m+1}$ (n = 12, m = 3). η vs. T [87And]. η: rotational viscosity.

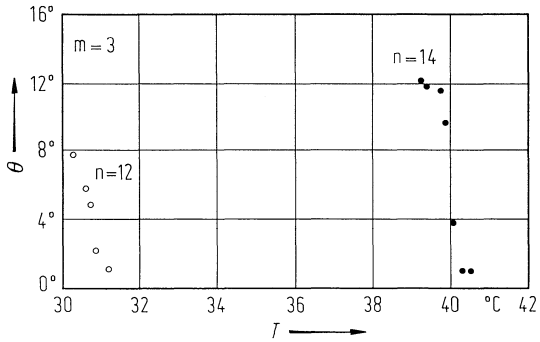

Fig. 71A-6-018. $C_nH_{2n+1}O$–⬡–COO–⬡–$O(CH_2)_mOCH_2CH(CH_3)OC_2H_5$ (n = 12, 14; m = 3). θ vs. T [87Ott]. θ: tilt angle.

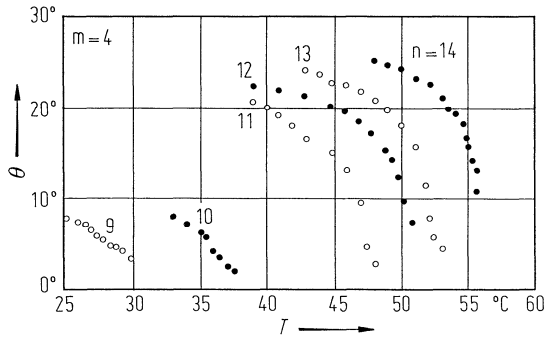

Fig. 71A-6-019. $C_nH_{2n+1}O$–⬡–COO–⬡–$O(CH_2)_mOCH_2CH(CH_3)OC_2H_5$ (n = 9...14; m = 4). θ vs. T [87Ott]. θ: tilt angle.

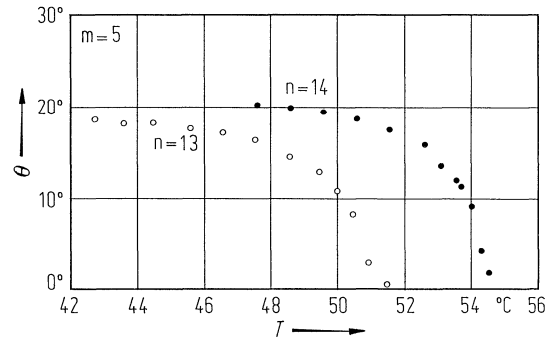

Fig. 71A-6-020. $C_nH_{2n+1}O$–⬡–COO–⬡–$O(CH_2)_mOCH_2CH(CH_3)OC_2H_5$ (n = 13, 14; m = 5). θ vs. T [87Ott]. θ: tilt angle.

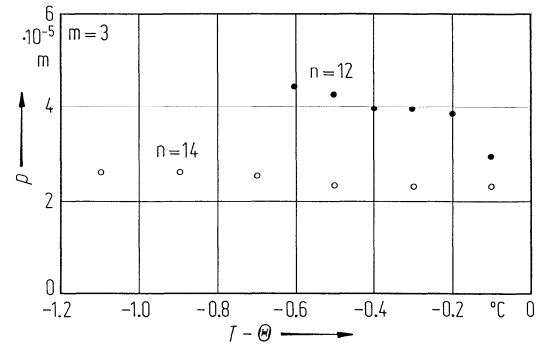

Fig. 71A-6-021. $C_nH_{2n+1}O$–⬡–COO–⬡–$O(CH_2)_mOCH_2CH(CH_3)OC_2H_5$ (n = 12, 14; m = 3). p vs. $T - \Theta$ [87Ott]. p: helical pitch. Θ: transition temperature between Sm A and Sm C* phases.

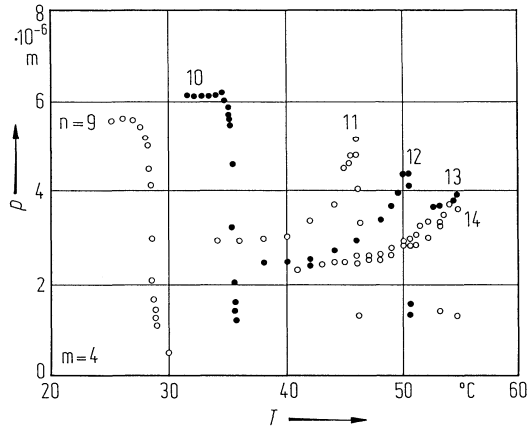

Fig. 71A-6-022. $C_nH_{2n+1}O$–⬡–COO–⬡–$O(CH_2)_mOCH_2CH(CH_3)OC_2H_5$ (n = 9...14; m = 4). p vs. T [87Ott]. p: helical pitch.

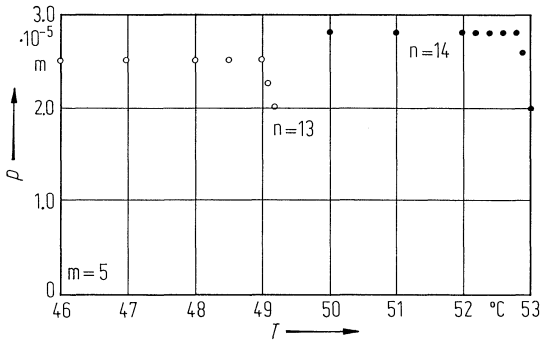

Fig. 71A-6-023. $C_nH_{2n+1}O$–⬡–COO–⬡–$O(CH_2)_mOCH_2CH(CH_3)OC_2H_5$ (n = 13, 14; m = 5). p vs. T [87Ott]. p: helical pitch.

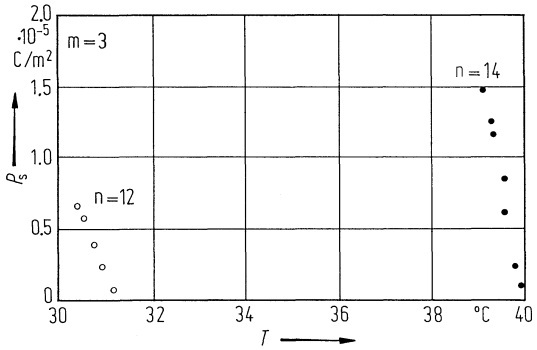

Fig. 71A-6-024. $C_nH_{2n+1}O$–⬡–COO–⬡–$O(CH_2)_mOCH_2CH(CH_3)OC_2H_5$ (n = 12, 14; m = 3). P_s vs. T [87Ott].

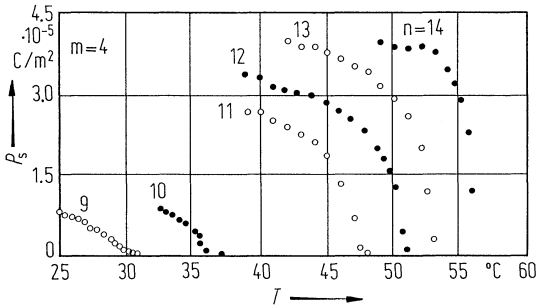

Fig. 71A-6-025. $C_nH_{2n+1}O$–⬡–COO–⬡–$O(CH_2)_mOCH_2CH(CH_3)OC_2H_5$ (n = 9...14; m = 4). P_s vs. T [87Ott].

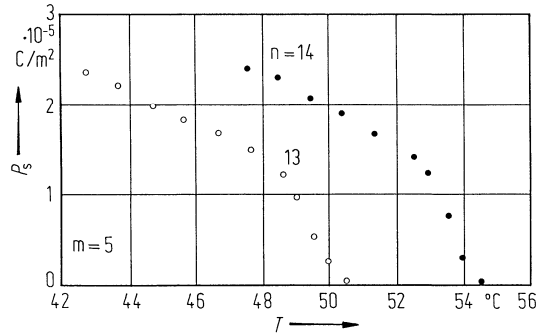

Fig. 71A-6-026. $C_nH_{2n+1}O$–⬡–COO–⬡–$O(CH_2)_mOCH_2CH(CH_3)OC_2H_5$ (n = 13, 14; m = 5). P_s vs. T [87Ott].

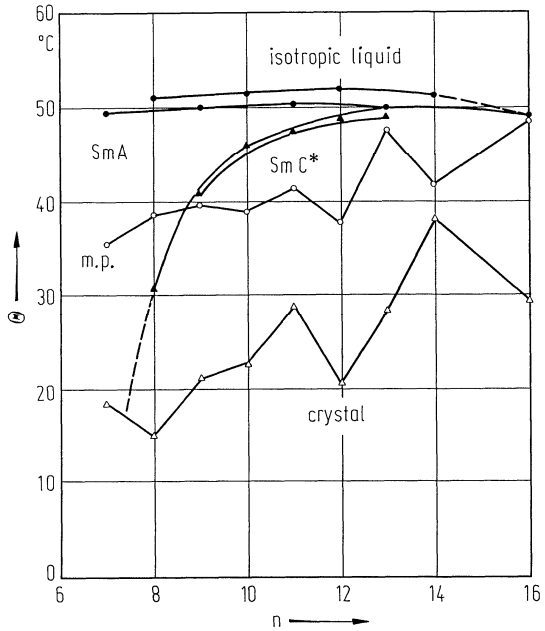

Fig. 71A-6-027. $C_nH_{2n+1}O$–⬡–COO–⬡–$COO(CH_2)_2CH(CH_3)(CH_2)_3CH(CH_3)_2$. Θ vs. n [87Chi]. m.p.: mesophase-crystal boundary.

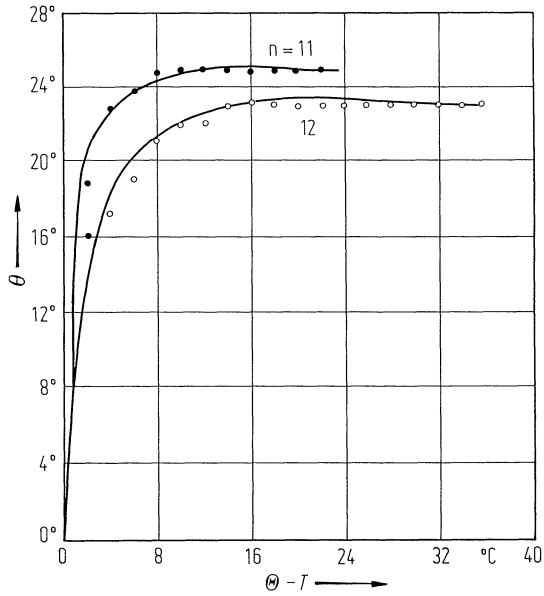

Fig. 71A-6-028. $C_nH_{2n+1}O$–⟨⬡⟩–COO–⟨⬡⟩–$COO(CH_2)_2CH(CH_3)(CH_2)_3CH(CH_3)_2$. θ vs. $\Theta - T$ [87Chi]. Parameter: n. θ: tilt angle. Θ: transition temperature between Sm A and Sm C* phases.

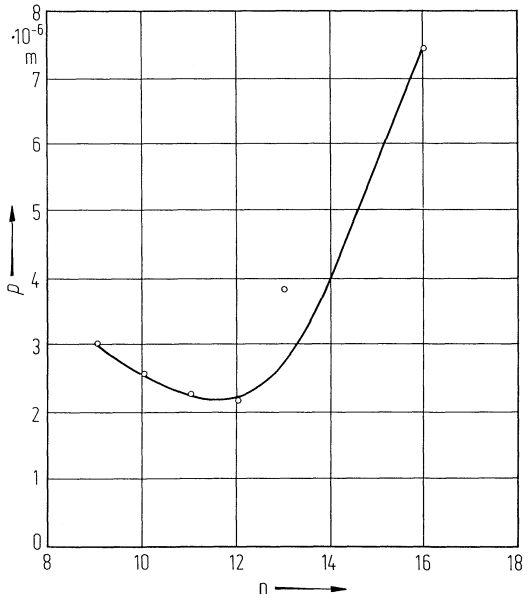

Fig. 71A-6-029. $C_nH_{2n+1}O$–⟨⬡⟩–COO–⟨⬡⟩–$COO(CH_2)_2CH(CH_3)(CH_2)_3CH(CH_3)_2$. p vs. n [87Chi]. p: helical pitch.

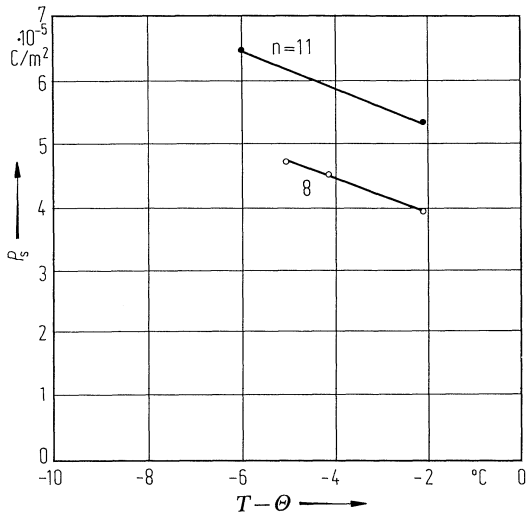

Fig. 71A-6-030. $C_nH_{2n+1}O$–⬡–COO–⬡–$COO(CH_2)_2CH(CH_3)(CH_2)_3CH(CH_3)_2$. P_s vs. $T-\Theta$ [87Chi]. Parameter: n. Θ: transition temperature between Sm A and Sm C* phases.

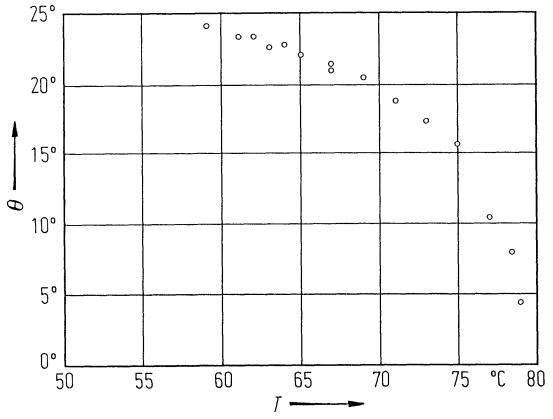

O
/ \

Fig. 71A-6-031. $C_{10}H_{21}O$–⬡–COO–⬡–$OCH_2CHCHC_3H_7$. θ vs. T [87And]. θ: tilt angle.

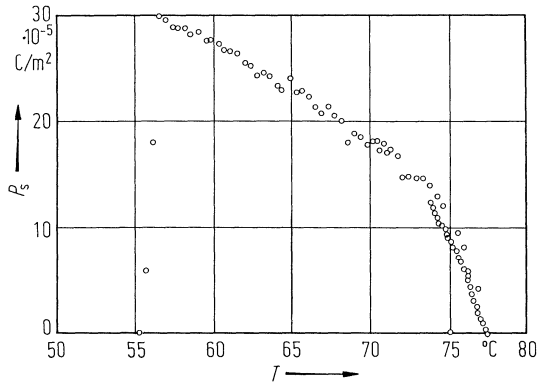

Fig. 71A-6-032. $C_{10}H_{21}O$–⬡–COO–⬡–$OCH_2CHCHC_3H_7$ (O). P_s vs. T [87And].

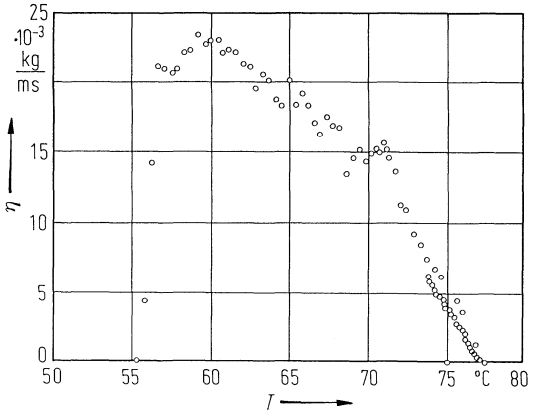

Fig. 71A-6-033. $C_{10}H_{21}O$–⬡–COO–⬡–$OCH_2CHCHC_3H_7$ (O). η vs. T [87And]. η: rotational viscosity.

References

78Los Loseva, M.V., Ostrovskii, B.I., Rabinovich, A.Z., Sonin, A.S., Strukov, B.A., Chernova, N.I.: Pis'ma Zh. Eksp. Teor. Fiz. **28** (1978) 404; JETP Lett. (English Transl.) **28** (1978) 374.

80Ost Ostrovskii, B.I., Rabinovich, A.Z., Sonin, A.S., Sorkin, E.L., Strukov, B.A., Taraskin, S.A.: Ferroelectrics **24** (1980) 309.

84Dec Decobert, G., Dubois, J.-C.: Mol. Cryst. Liq. Cryst. **114** (1984) 237.

84Kel Keller, P.: Ferroelectrics **58** (1984) 3.

85Kel Keller, P., Cladis, P.E., Finn, P.L., Brand, H.R.: J. Phys. (Paris) **46** (1985) 2203.

86Ska Skarp, K., Andersson, G.: Ferroelectric Lett. **6** (1986) 67.

87And Andersson, G., Dahl, I., Lagerwall, S.T., Skarp, K.: Mol. Cryst. Liq. Cryst. **144** (1987) 105.

87Chi Chin, E., Goodby, J.W., Patel, J.S., Geary, J.M., Leslie, T.M.: Mol. Cryst. Liq. Cryst. **146** (1987) 325.

87Ott Otterholm, B., Alstermark, C., Flatischler, K., Dahlgren, A., Lagerwall, S.T., Skarp, K.: Mol. Cryst. Liq. Cryst. **146** (1987) 189.

87Pat Patel, J.S., Goodby, J. W.: Mol. Cryst. Liq. Cryst. **144** (1987) 117.

No. 71A-7 4-(2-methylbutyloxy)phenyl-4′-*n*-alkoxy-cinnamate and analogues

(A) $C_nH_{2n+1}O$–⬡–CH=CHCOO–⬡–$OCH_2CH(CH_3)C_2H_5$

4-(2-methylbutyloxy)phenyl-4′-*n*-alkoxy cinnamate

1b Phase transition temperatures: Table 71A-7-001; Fig. 71A-7-001.

6a Transition enthalpy: see Table 71A-7-001.

(B) $C_nH_{2n+1}O$–⬡–CH=CHCOO–⬡–$COOCH_2CH(CH_3)C_2H_5$

4-(2-methylbutoxycarbonyl)phenyl-4′-*n*-alkoxy cinnamate

1b Phase transition temperatures: Table 71A-7-002; Fig. 71A-7-002.

6a Transition enthalpy: see Table 71A-7-002.

(C) $C_{11}H_{23}O$–⬡–CH=CHCOO–⬡–$OOCCHClCH(CH_3)C_2H_5$

4-(1-chloro-2-methylbutylcarbonyloxy)phenyl-4′-*n*-undecyloxy cinnamate

1b

phase	II	I	I′	91Pra
	smectic C* (Sm C*)	smectic A (Sm A)	isotropic liquid	
state	F	P		
Θ [°C]	83.5	99.5		

3b Helical pitch: Fig. 71A-7-003.
Tilt angle: Fig. 71A-7-004.

5c Spontaneous polarization: see Fig. 71A-7-004.

(D) $C_{12}H_{25}O$–⬡–CH=CHCOO–⬡–$COOCH_2CHClCH_2CH(CH_3)_2$

4-(2-chloro-4-methlpentyloxycarbonyl)phenyl-4′-*n*-dodecyloxy cinnamate

1b

phase	II	I	I′	91Pra
	smectic C* (Sm C*)	smectic A (Sm A)	isotropic liquid	
state	F	P		
Θ [°C]	65.5	81.0		

3b Helical pitch: Fig. 71A-7-005.
Tilt angle: Fig. 71A-7-006.

5c Spontaneous polarization: see Fig. 71A-7-006.

(E) $C_nH_{2n+1}O$–⬡–CH=CHCOO–⬡– $OOCCHClCH_2CH(CH_3)_2$

4′-(2-chloro-4-methylpentanoyloxy)phenyl trans-4″-*n*-alkyloxy cinnamate

1b	phase	II	I	I′	93Pra
		smectic C* (Sm C*)	smectic A (Sm A)	isotropic liquid	
	state	F	P		
	Θ [°C] n = 6	56.0	93.5		
	7	67.0	90.5		
	8	73.0	92.5		
3b	Tilt angle: Fig. 71A-7-007.				
5a	Dielectric dispersion: Fig. 71A-7-008, Fig. 71A-7-009.				
c	Spontaneous polarization: Fig. 71A-7-010.				

Table 71A-7-001. $C_nH_{2n+1}O-\bigcirc-CH=CHCOO-\bigcirc-OCH_2CH(CH_3)C_2H_5$. Transition temperature Θ [°C] and transition enthalpy ΔH [$\cdot 10^3$ J kg^{-1}] for several n [84Les]. m.p.: mesophase-crystal transition. Ch: cholesteric. [ ]: monotropic transition. ( ): ΔH.

n	Ch	Sm A	Sm C*	Sm I*	Sm J*	m.p.	Cryst I →Cryst. II	Recrystal-lization
6	103.4(3.2)	[94.7](1.0)	-	-	-	98.8(68.8)	-	77.8(–58.3)
7	100.8(3.0)	94.6(0.9)	[84.2] [a])	-	-	89.3(57.3)	-	76.8(–49.6)
8	103.2(4.7)	101.0(1.6)	89.5(0.2)	-	-	87.6(57.2)	-	66.4(–41.9)
9	102.3(9.5) [b])	101.7(-) [b])	92.7(0.2)	-	-	80.2(48.3)	-	55.5(–37.3)
10	-	103.4(11.6)	93.9(0.2)	[60.4](1.6)	-	81.0(51.7)	-	54.0(–24.3)
11	-	105.1(11.8)	94.5(0.3)	[61.9](4.1)	[52.2] [a])	80.0(50.1)	75.8(28.4)	52.2(–31.5)
12	-	103.8(12.8)	94.9(0.1)	[63.3](13.7)	[50.7] [a])	79.3(50.7)	69.5(17.7)	36 [c])
13	-	102.8(13.5)	94.0(0.3)	[64.8](5.0)	[47.3] [a])	76.3(81.7)	-	34 [c])
14	-	102.3(13.9)	94.4(0.1)	[66.3](5.0)	[45.8] [a])	74.5(76.6)	-	45 [c])

[a]) Too small to be detected by DSC; values obtained by optical microscopy entered.
[b]) Isotropic-cholesteric-SmA too close in temperature to be separated.
[c]) Recorded optically.

Table 71A-7-002. $C_nH_{2n+1}O-\bigcirc-CH=CHCOO-\bigcirc-COOCH_2CH(CH_3)C_2H_5$. Transition temperature Θ [°C] and transition enthalpy ΔH [$\cdot 10^3$ J kg^{-1}] for several n [84Les]. m.p.: mesophase-crystal transition. ( ): ΔH.

n [a])	Sm A	Sm C*	m.p	Recrystallization
6	95.9	-	78.4	56.2
7	93.0(7.5)	62.8 [b])	75.3(74.3)	45.5(–39.0)
8	95.5(8.2)	67.5 [b])	85.1(79.1)	27.5(–30.1)
9	92.9(8.1)	67.3 [b])	87.0(74.4)	18.8(–20.4)
10	95.2(9.3)	71.1(0.4)	60.2(62.3)	16.7(–29.0)
11	96.0(10.3)	73.0(1.3)	55.7(73.1)	29.5(–57.6)
12	95.4(9.9)	71.6 [b])	54.0(65.2)	8.7(–39.3)

[a]) DSC data not obtained.
[b]) Too small to be detected by DSC; values obtained by optical microscopy entered.

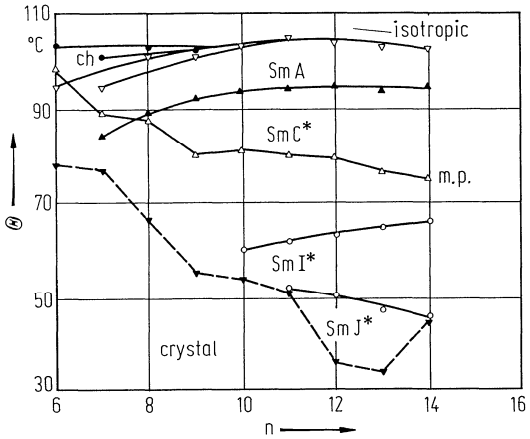

Fig. 71A-7-001. $C_nH_{2n+1}O$–⬡–CH=CHCOO–⬡–$OCH_2CH(CH_3)C_2H_5$. Θ vs. n [84Les]. m.p.: mesophase-crystal boundary on cooling. ch: cholesteric.

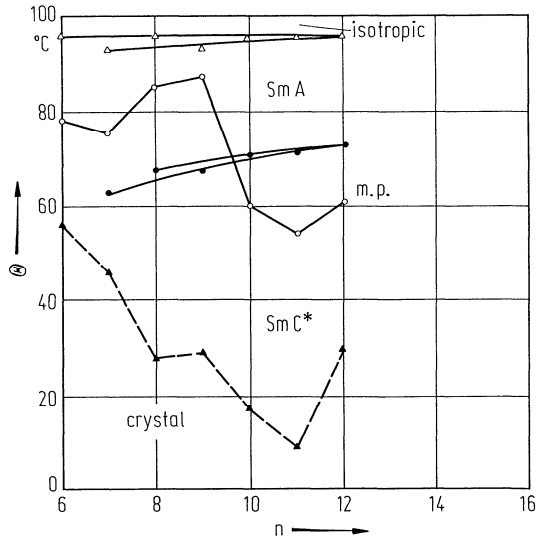

Fig. 71A-7-002. $C_nH_{2n+1}O$–⬡–CH=CHCOO–⬡–$COOCH_2CH(CH_3)C_2H_5$. Θ vs. n [84Les]. m.p.: mesophase-crystal boundary on cooling.

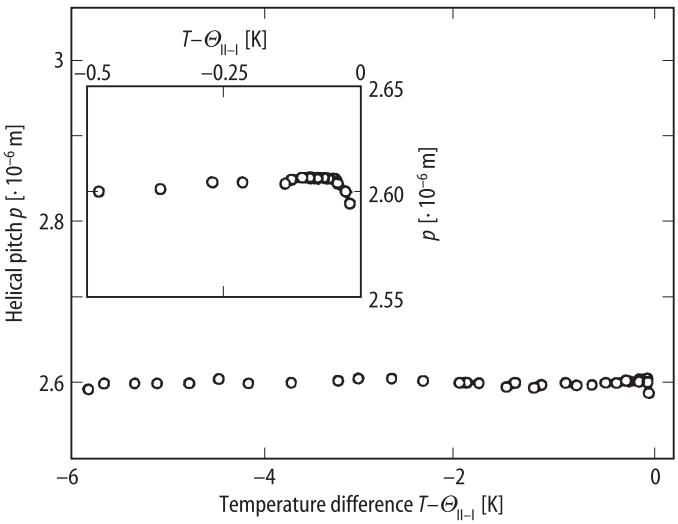

Fig. 71A-7-003. $C_{11}H_{23}O$–⬡–CH=CHCOO–⬡–$OOCCHClCH(CH_3)C_2H_5$. p vs. $T - \Theta_{I-I}$ [91Pra]. p: helical pitch.

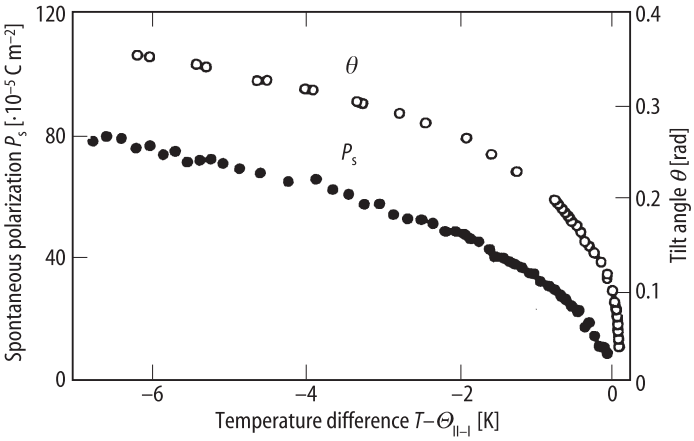

Fig. 71A-7-004. $C_{11}H_{23}O$–⬡–CH=CHCOO–⬡–$OOCCHClCH(CH_3)C_2H_5$. θ, P_s vs. $T - \Theta_{I-I}$ [91Pra]. θ: tilt angle.

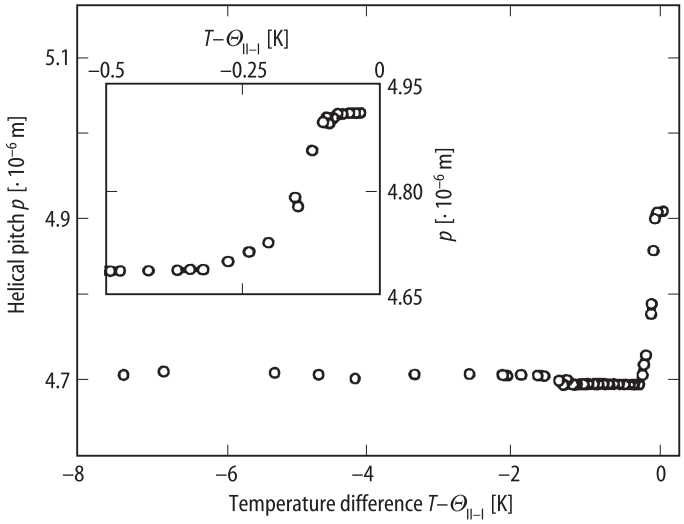

Fig. 71A-7-005. $C_{12}H_{25}O$–⬡–CH=CHCOO–⬡–$COOCH_2CHClCH_2CH(CH_3)_2$. p vs. $T - \Theta_{II-I}$ [91Pra]. p: helical pitch.

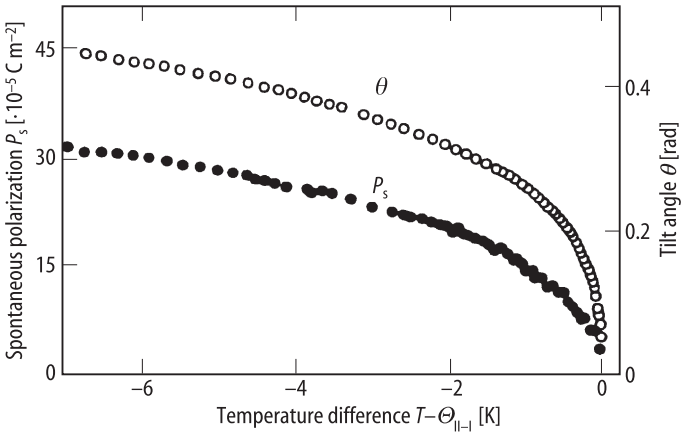

Fig. 71A-7-006. $C_{12}H_{25}O$–⬡–CH=CHCOO–⬡–$COOCH_2CHClCH_2CH(CH_3)_2$. θ, P_s vs. $T - \Theta_{II-I}$ [91Pra]. θ: tilt angle.

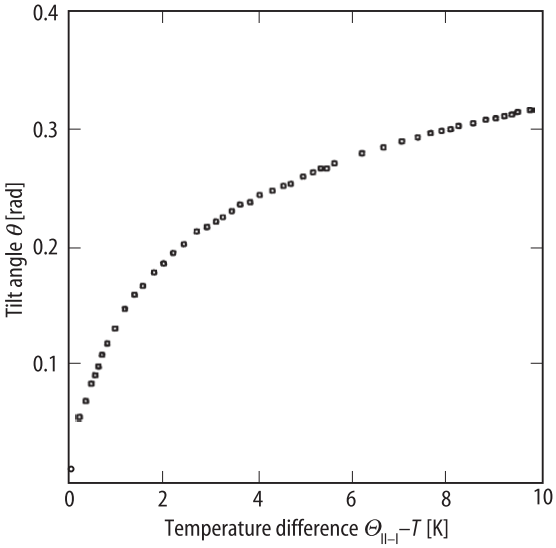

Fig. 71A-7-007. $C_nH_{2n+1}O-$⬡$-CH=CHCOO-$⬡$-OOCCHClCH_2CH(CH_3)_2$ (n = 6). θ vs. $\Theta_{II-I} - T$ [93Pra]. θ: tilt angle.

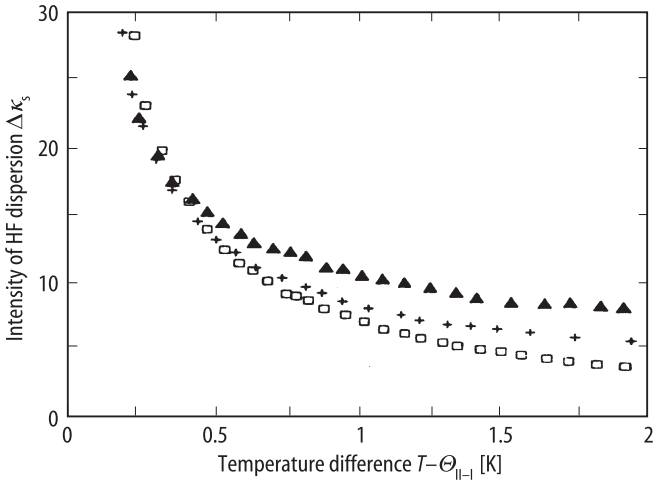

Fig. 71A-7-008. $C_nH_{2n+1}O-$⬡$-CH=CHCOO-$⬡$-OOCCHClCH_2CH(CH_3)_2$ (n = 6, 7, 8). $\Delta\kappa_s$ vs. $T - \Theta_{II-I}$ [93Pra]. Parameter: n. Square: n = 6, plus: n = 7, triangle: n = 8. $\Delta\kappa_s$: intensity of high frequency ("soft" mode) dispersion.

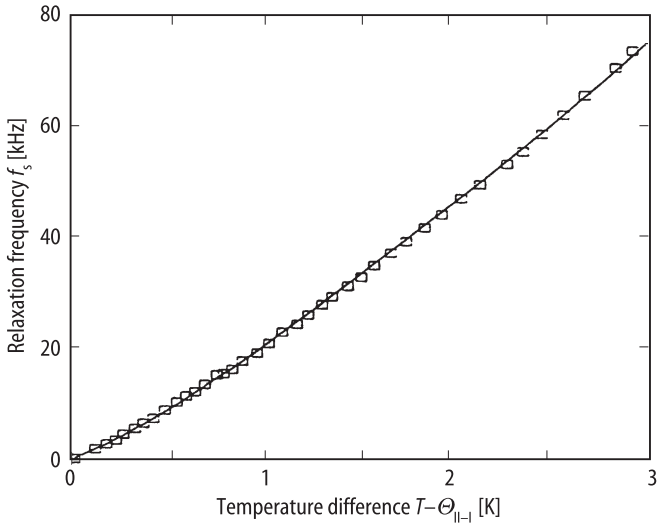

Fig. 71A-7-009. $C_nH_{2n+1}O$–⬡–CH=CHCOO–⬡–$OOCCHClCH_2CH(CH_3)_2$ (n = 6). f_s vs. $T - \Theta_{II–I}$ [93Pra]. f_s: relaxation frequency of high frequency ("soft" mode) dispersion.

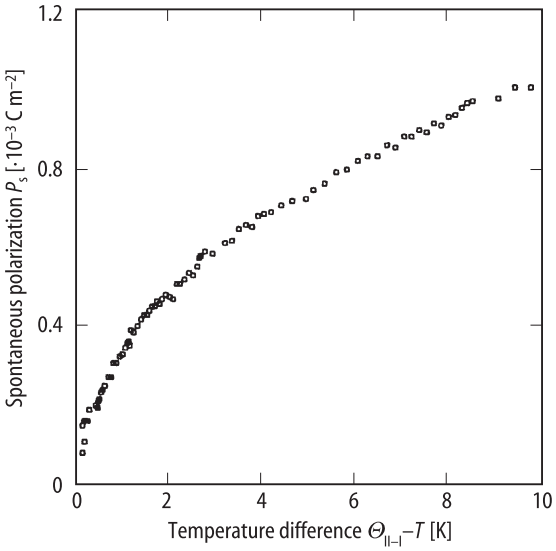

Fig. 71A-7-010. $C_nH_{2n+1}O$–⬡–CH=CHCOO–⬡–$OOCCHClCH_2CH(CH_3)_2$ (n = 6). P_s vs. $\Theta_{II–I} - T$ [93Pra].

References

84Les Leslie, T.M.: Ferroelectrics **58** (1984) 9.
91Pra Prasad, S.K., Nair, G.G.: Mol. Cryst. Liq. Cryst. **202** (1991) 91.
93Pra Prasad, S.K., Khened, S.M., Raja, V.N., Chandrasekhar, S., Shivkumar, B.: Ferroelectrics **138** (1993) 37.

No. 71A-8 8SI* and analogues

(A) C_nH_{2n+1}–⬡–⬡–COO–⬡–$CH_2CH(CH_3)C_2H_5$

(S)-(+)-4-(2′-methylbutyl)phenyl-4′-alkylbiphenyl-4-carboxylate

n = 8: 8SI*.

1b	phase	VI	V	IV	III	II	I	I′	I″	79Goo
		crystalline solid	smectic G (Sm G)	smectic H (Sm H)	smectic F* (Sm F*)	smectic C* (Sm C*)	smectic A (Sm A)	chiral nematic	isotropic liquid	
	state				F	F	P	P		
	Θ [°C] n = 8			(64)	69.5	84	135	141		
	9		(55)	(62)	69	83	134	138		
	10		(54)	62	69	83	132.5	134		

( ): monotropic transition temperature

3b	Smectic layer spacing: Fig. 71A-8-001. Tilt angle: Fig. 71A-8-002.
5c	Spontaneous polarization: Fig. 71A-8-003.
6a	DSC intensity: Fig. 71A-8-004.

(B) $C_nH_{2n+1}O$–⬡–⬡–COO–⬡–$CH_2CH(CH_3)C_2H_5$

(S)-(+)-4-(2′-methylbutyl)phenyl-4′-alkoxybiphenyl-4-carboxylate

n = 8: 8OSI*

1b	phase	VI	V	IV	III	II	I	I′	I″	79Goo
		crystalline solid	smectic G (Sm G)	smectic H (Sm H)	smectic F* (Sm F*)	smectic C* (Sm C*)	smectic A (Sm A)	chiral nematic	isotropic liquid	
	state				F	F	P	P		
	Θ [°C] n = 6			(84)		103	172	182		
	7		(66)	(70)	(79)	126	170	177		
	8		(61)	(72)	79	132	171	174		
	9		(61)	(70)	(78)	132	169	170		
	10		60	70	78	132	168			
	12			(68)	78	130	162			
	14			(66)	78	124	157			
	16			(65)	78	120	154			
	18			(64)	78	118	152			

( ): monotropic transition temperature

3b	Tilt angle: Fig. 71A-8-005.
5c	Spontaneous polarization: Fig. 71A-8-006.

(C) $C_nH_{2n+1}O$–⬡–⬡–COO–⬡–$COOCH(CH_3)COOC_mH_{2m+1}$

1AC1ECPAPB ((R)-4′-(1-alkoxycarbonyl-1-ethoxycarbonyl)phenyl-4-[4-(n-alkoxy)phenyl]-benzoate)

n = 8, m = 1: 1MC1ECPOPB
n = 8, m = 4: 1BC1ECPOPB
n = 8, m = 7: 1HpC1ECPOPB
n = 8, m = 8: 1OC1ECPDPB
n = 10, m = 1: 1MC1ECPDPB

5c Spontaneous polarization: Fig. 71A-8-007, Fig. 71A-8-008, Fig. 71A-8-009.

(D) $C_nH_{2n+1}O$–⬡–⬡–COO–⬡–$COOCH_2CH(CH_3)COOC_mH_{2m+1}$

2AC1PCPAPB ((S)-4′-(2-alkoxycarbonyl-1-propoxycarbonyl)phenyl-4-[4-(n-alkoxy)phenyl]-benzoate)

n = 8, m = 1: 2MC1PCPOPB

5c Spontaneous polarization: Fig. 71A-8-010; see also Fig. 71A-8-007.

(E) $C_nH_{2n+1}O$–⬡–⬡–COO–⬡–$COOCH(CH_3)CH_2COOC_mH_{2m+1}$

3AC2PCPAPB ((R)-4′-(3-alkoxycarbonyl-2-propoxycarbonyl)phenyl-4-[4-(n-alkoxy)phenyl]-benzoate)

n = 8, m = 2: 3EC2PCPOPB

5c Spontaneous polarization: see Fig. 71A-8-007.

(F) $C_nH_{2n+1}O$–⬡–⬡–COO–⬡–$COOCH(CH_3)CH_2OC_mH_{2m+1}$

3A2PCPAPB ((R)-4′-(3-alkoxy-2-propoxycarbonyl)phenyl-4-[4-(n-alkoxy)phenyl]-benzoate)

n = 8, m = 4: 3B2PCPOPB

5c Spontaneous polarization: Fig. 71A-8-011; see also Fig. 71A-8-009.

(G) $C_nH_{2n+1}O$–⬡–⬡–COO–⬡–$COOCH(CH_3)CH_2C(CH_3)_2OH$

4H4M2PeCPAPB ((R)-4′-(4-hydroxy-4-methyl-2-pentyloxycarbonyl)phenyl-4-(4-alkoxyphenyl)-benzoate)

n = 8: 4H4M2PeCPOPB

5c Spontaneous polarization: Fig. 71A-8-012.

(H) $C_nH_{2n+1}O$–⬡–⬡–COO–⬡–$OCH(CH_3)COOC_mH_{2m+1}$

1AC1EPAPB ((R)-4′-(1-alkoxycarbonyl-1-ethoxy)phenyl-4-[4-(n-alkoxy)phenyl]-benzoate)

n = 8, m = 1: 1MC1EPOPB
n = 8, m = 4: 1BC1EPOPB
n = 8, m = 7: 1HpC1EPOPB
n = 10, m = 1: 1MC1EPDPB
n = 11, m = 1: 1MC1EPUdPB

5a Dielectric constant: Fig. 71A-8-013.

c Spontaneous polarization: Fig. 71A-8-013; see also Fig. 71A-8-009.

(I) $C_nH_{2n+1}O$–⬡–⬡–COO–⬡–$OCH(CH_3)C_mH_{2m+1}$

***p*-(1-methyl-alkoxy)-phenyl ester of 4′-alkoxy-4-biphenyl carboxylic acid**

1b n = 8, m = 3: 86Inu

phase	IV	III	II	I	I′
	crystalline solid	undefined smectic (Sm X)	smectic C* (Sm C*)	smectic A (Sm A)	isotropic liquid
state		F	F	P	
Θ [°C]	66.5		80.5	122.5	162.5

Transition temperatures in m = 6 compounds: Fig. 71A-8-014.

3b Tilt angle: Fig. 71A-8-015.

5c Spontaneous polarization: Fig. 71A-8-016.

(J) $C_nH_{2n+1}O$–⬡–⬡–OCO–⬡–$OCH(CH_3)C_mH_{2m+1}$

4′-alkoxy-4-biphenyl ester of *p*-(1-methyl-alkoxy)-benzoic acid

1b m = 3: 86Inu

phase		III	II	I	I′
		crystalline solid	smectic C* (Sm C*)	chiral nematic	isotropic liquid
state			F	P	
Θ [°C]	n = 6	99.0	(84.3)	143.2	
	8	91.4	95.4	136.7	
	9	90.9	96.5	130.0	
	11	78.0	96.8	122.7	

( ): cooling

Transition temperatures in m = 6: Fig. 71A-8-017.

3b Tilt angle: Fig. 71A-8-018.

5c Spontaneous polarization: see Fig. 71A-8-018.

(K) C_nH_{2n+1}–⬡–⬡–OCO–⬡–$OCH(CH_3)C_6H_{13}$

4′-alkyl-4-biphenyl ester of *p*-(1-methyl-heptyloxy)-benzoic acid

1b	phase	III	II	I	I′	86Inu
		crystalline solid	smectic C* (Sm C*)	chiral nematic	isotropic liquid	
	state		F	P		
	Θ [°C] n = 7	53.1	58.9	106.2		
	8	50.0	62.5	87.2		

(L) $C_nH_{2n+1}O$–⬡–⬡–CH_2O–⬡–$COOCH(CH_3)COOCH_3$

1MC1EAPBB ((R)-1-methoxycarbonyl-1-ethyl-4-(4′-alkoxyphenyl)-benzyloxybenzoate)

n = 8: 1MC1EOPBB

5a Dielectric constant: Fig. 71A-8-019.

c Spontaneous polarization: Fig. 71A-8-020; see also Fig. 71A-8-008.

(M) $C_nH_{2n+1}O$–⬡–⬡–CH_2O–⬡–$COOCH_2CH(CH_3)COOCH_3$

2MC1PAPBB ((S)-2-methoxycarbonyl-1-propyl-4-(4′-alkoxyphenyl)-benzyloxybenzoate)

n = 8: 2MC1POPBB

5a Dielectric constant: see Fig. 71A-8-019.

c Spontaneous polarization: see Fig. 71A-8-020; see also Fig. 71A-8-010.

(N) $C_nH_{2n+1}O$–⬡–⬡–CH_2O–⬡–$COOCH(CH_3)CH_2COOCH_3$

3MC2PAPBB ((R)-3-methoxycarbonyl-2-propyl-4-(4′-alkoxyphenyl)-benzyloxybenzoate)

n = 8: 3MC2POPBB

5a Dielectric constant: see Fig. 71A-8-019.

c Spontaneous polarization: see Fig. 71A-8-020.

(O) $C_nH_{2n+1}O$–⬡–⬡–CH_2O–⬡–$COOCH(CH_3)CH_2OC_4H_9$

3B2PAPBB ((R)-3-butoxy-2-propyl-4-(4′-alkoxyphenyl)-benzyloxybenzoate)

n = 8: 3B2POPBB

5c Spontaneous polarization: see Fig. 71A-8-011.

(P) $C_nH_{2n+1}O$–⬡–⬡–CH_2O–⬡–$COOCH(CH_3)CH_2C(CH_3)_2OH$

4H4M2PePAPBB ((R)-4-hydroxy-4-methyl-2-pentyl-4-(4′-alkoxyphenyl)-benzyloxybenzoate)

n = 8: 4H4M2PeOPBB

5c Spontaneous polarization: see Fig. 71A-8-012.

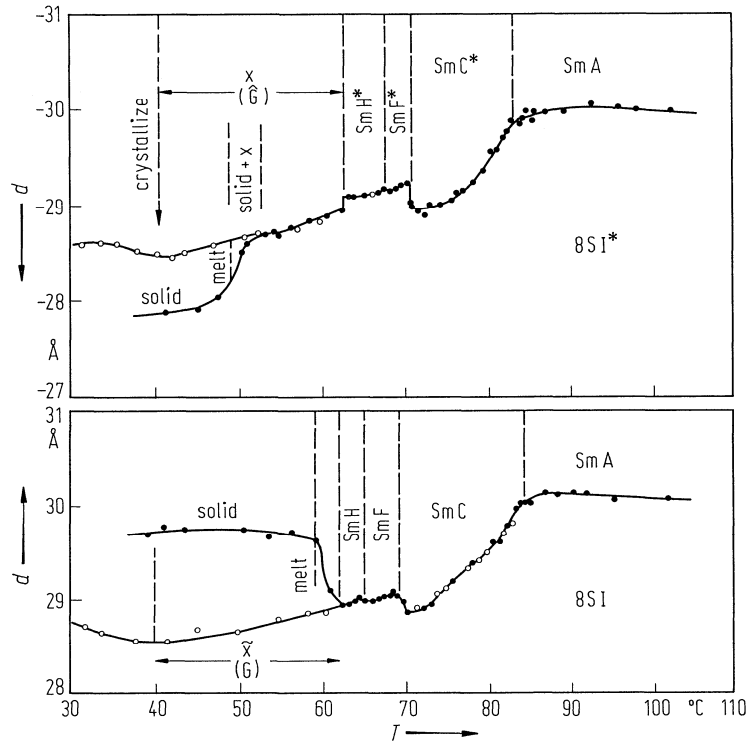

Fig. 71A-8-001. 8SI*, 8SI. d vs. T [84Bra]. d: smectic layer spacing. 8SI: racemic compound of 8SI*. Full circle: heating. Open circle: cooling.

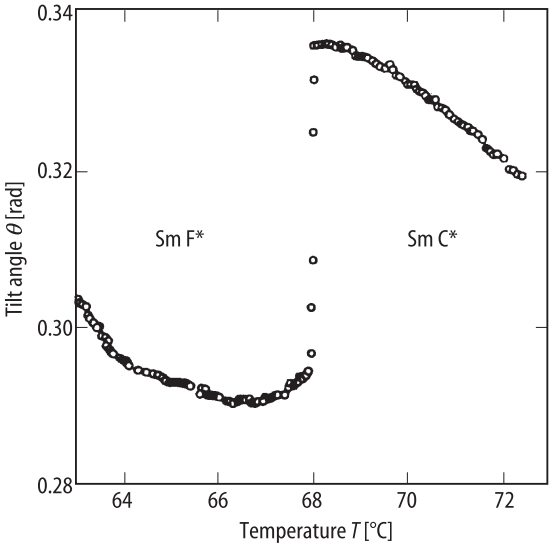

Fig. 71A-8-002. 8SI*. θ vs. T [91Raj]. θ: tilt angle.

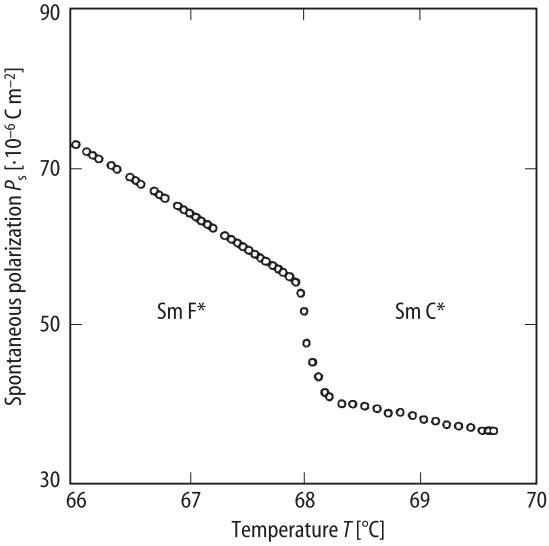

Fig. 71A-8-003. 8SI*. P_s vs. T [91Raj].

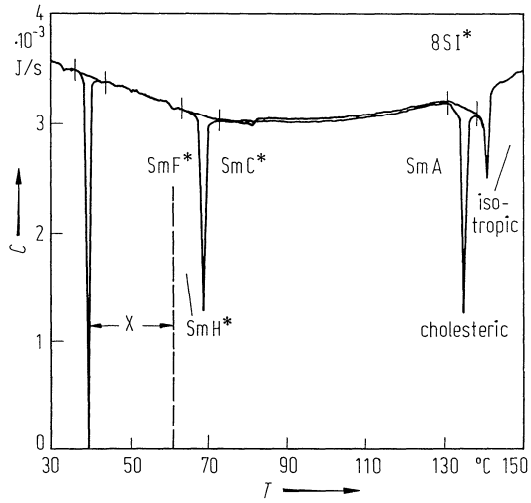

Fig. 71A-8-004. 8SI*. C vs. T [84Bra]. C: intensity of DSC.

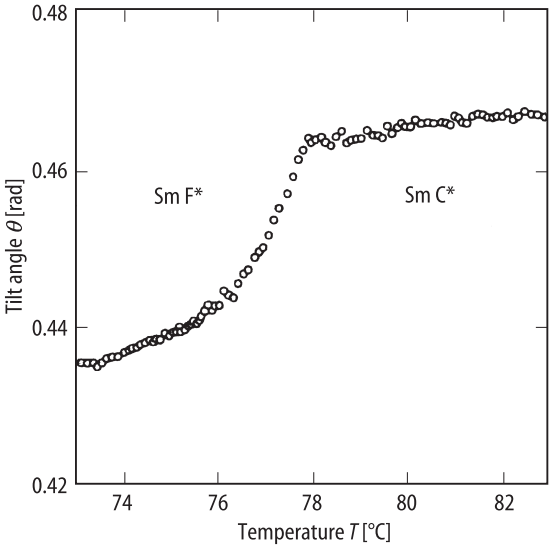

Fig. 71A-8-005. 8OSI*. θ vs. T [91Raj]. θ: tilt angle.

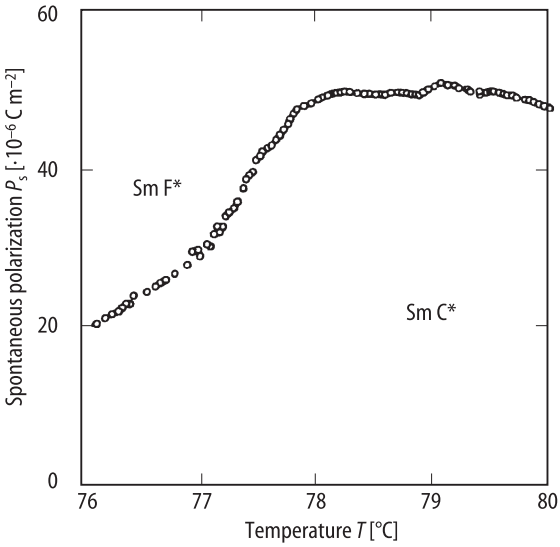

Fig. 71A-8-006. 8OSI*. P_s vs. T [91Raj].

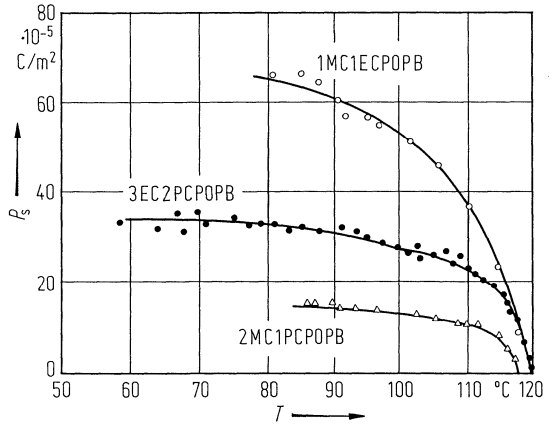

Fig. 71A-8-007. 1MC1ECPOPB, 2MC1PCPOPB, 3EC2PCPOPB. P_s vs. T [88Tan1].

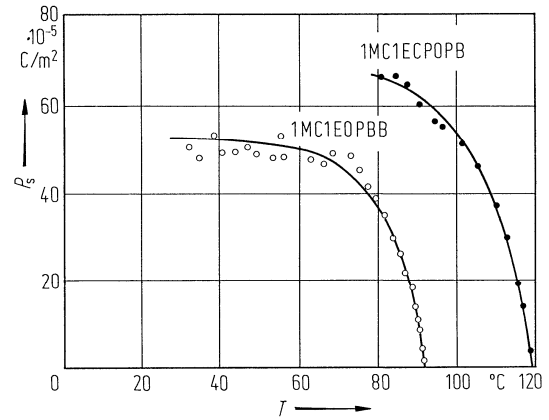

Fig. 71A-8-008. 1MC1ECPOPB, 1MC1EOPBB. P_s vs. T [88Tan2].

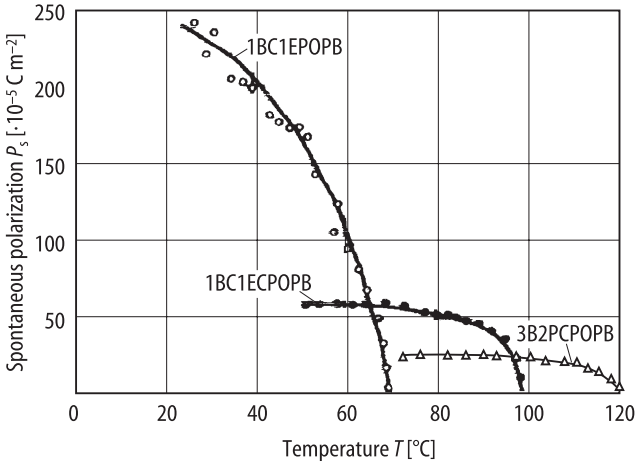

Fig. 71A-8-009. 1BC1EPOPB, 1BC1ECPOPB, 3B2PCPOPB. P_s vs. T [88Tan1].

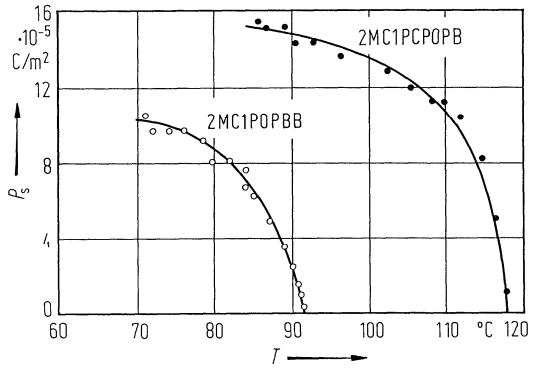

Fig. 71A-8-010. 2MC1PCPOPB, 2MC1POPBB. P_s vs. T [88Tan2].

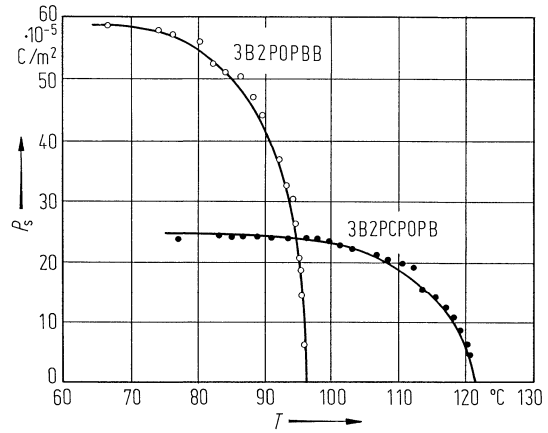

Fig. 71A-8-011. 3B2PCPOPB, 3B2POPBB. P_s vs. T [88Tan1].

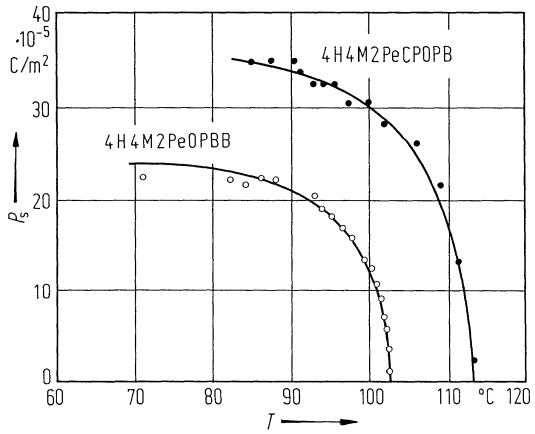

Fig. 71A-8-012. 4H4M2PeCPOPB, 4H4M2PeOPBB. P_s vs. T [88Tan2].

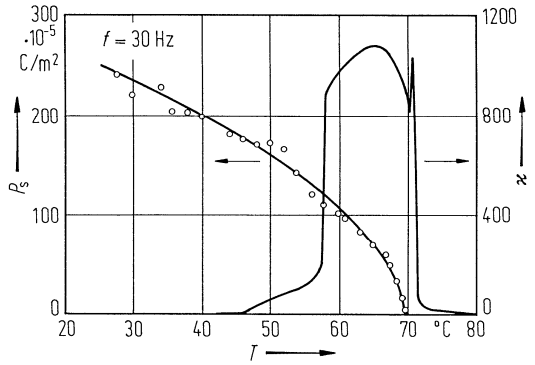

Fig. 71A-8-013. 1BC1EPOPB. κ; P_s vs. T [87Tan]. f = 30 Hz.

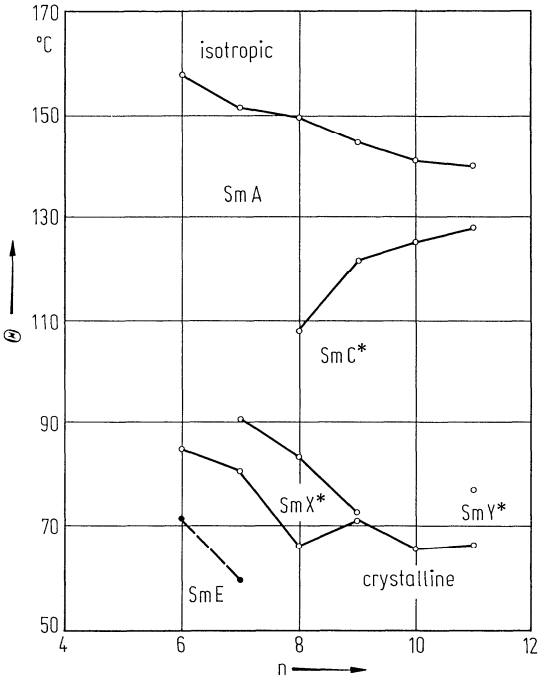

Fig. 71A-8-014. $C_nH_{2n+1}O$–⟨⟩–⟨⟩–COO–⟨⟩–$OCH(CH_3)C_6H_{13}$. Θ vs. n [86Inu].

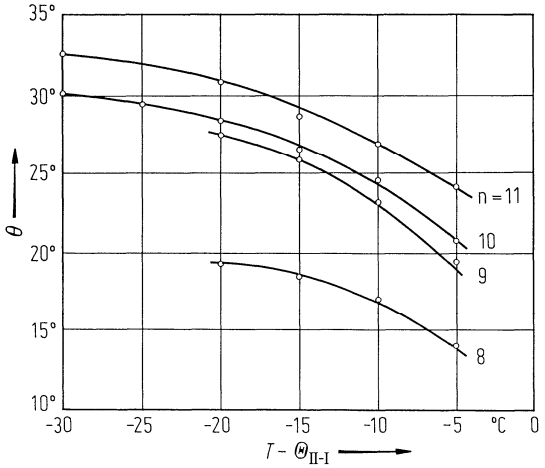

Fig. 71A-8-015. $C_nH_{2n+1}O$–⬡–⬡–COO–⬡–$OCH(CH_3)C_6H_{13}$. θ vs. $T - \Theta_{II-I}$ [86Inu]. θ: tilt angle. Parameter: n.

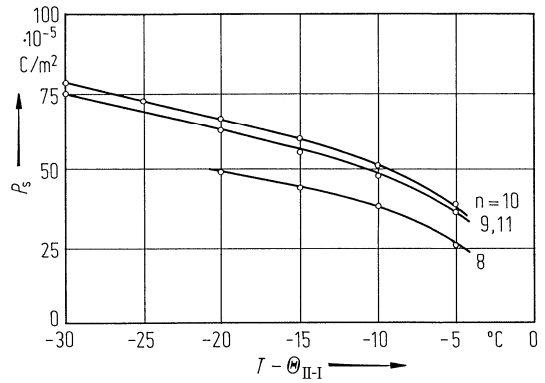

Fig. 71A-8-016. $C_nH_{2n+1}O$–⬡–⬡–COO–⬡–$OCH(CH_3)C_6H_{13}$. P_s vs. $T - \Theta_{II-I}$ [86Inu]. Parameter: n.

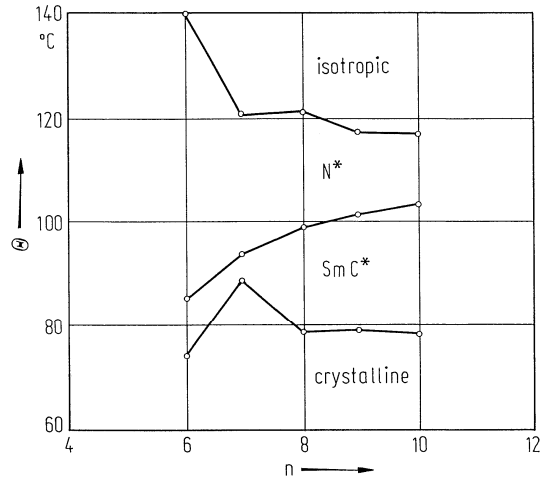

Fig. 71A-8-017. $C_nH_{2n+1}O$–⬡–⬡–OCO–⬡–$OCH(CH_3)C_6H_{13}$. Θ vs. n [86Inu]. N^*: chiral nematic.

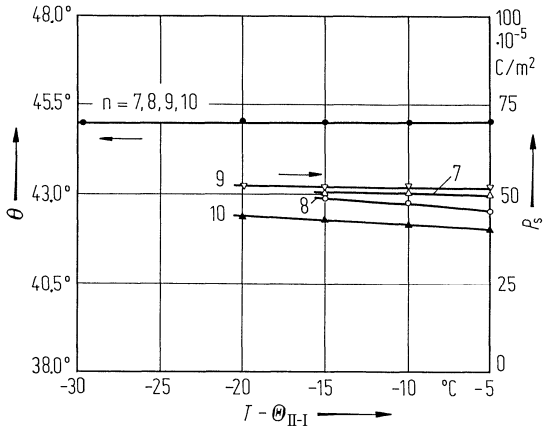

Fig. 71A-8-018. $C_nH_{2n+1}O$––OCO––$OCH(CH_3)C_6H_{13}$. θ, P_s vs. $T - \Theta_{II-I}$ [86Inu]. θ: tilt angle. Parameter: n.

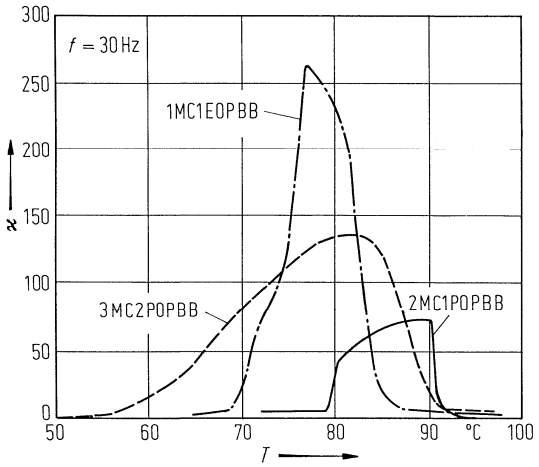

Fig. 71A-8-019. 1MC1EOPBB, 3MC2POPBB, 2MC1POPBB. κ vs. T [87Tan]. f = 30 Hz.

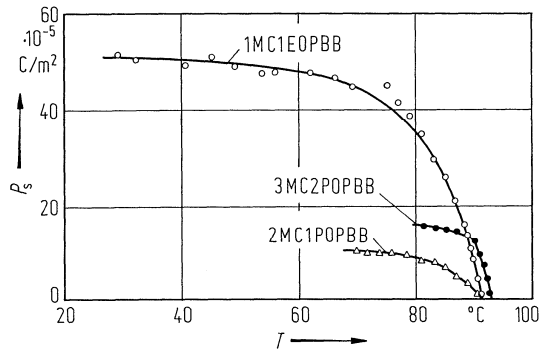

Fig. 71A-8-020. 1MC1EOPBB, 3MC2POPBB, 2MC1POPBB. P_s vs. T [87Tan].

References

79Goo Goodby, J.W., Gray, G.W.: J. Phys. (Paris) Colloq. **40** (1979) C3, 27.

84Bra Brand, H.R., Cladis, P.E.: Mol. Cryst. Liq. Cryst. **114** (1984) 207.

86Inu Inukai, T., Saitoh, S., Inoue, H., Miyazawa, K., Terashima, K., Furukawa, K.: Mol. Cryst. Liq. Cryst. **141** (1986) 251.

87Tan Taniguchi, H., Ozaki, M., Yoshino, K., Yamasaki, N., Satoh, K.: Jpn. J. Appl. Phys. **26** (1987) L1558.

88Tan1 Taniguchi, H., Ozaki, M., Yoshino, K., Satoh, K., Yamasaki, N.: Ferroelectrics **77** (1988) 137.

88Tan2 Taniguchi, H., Ozaki, M., Nako, K., Yoshino, K., Yamasaki, N., Satoh, K.: Jpn. J. Appl. Phys. **27** (1988) 452.

91Raj Raja, V.N., Krishna Prasad, S., Khened, S.M., Shankar Rao, D.S.: Ferroelectrics **121** (1991) 343.

No. 71A-9 *p-n*-alkylphenyl ester of 4′-(1-methyl-heptyloxy)-biphenyl-4-carboxylic acid and analogues

(A) C_nH_{2n+1}–⬡–OCO–⬡–⬡–$OCH(CH_3)C_6H_{13}$

***p-n*-alkylphenyl ester of 4′-(1-methyl-heptyloxy)-biphenyl-4-carboxylic acid**

1b Transition temperatures: Fig. 71A-9-001.

3b Tilt angle: Fig. 71A-9-002.

5c Spontaneous polarization: Fig. 71A-9-003.

(B) $C_nH_{2n+1}O$–⬡–OCO–⬡–⬡–$OCH(CH_3)C_mH_{2m+1}$

***p-n*-alkoxyphenyl ester of 4′-(1-methyl-alkoxy)-biphenyl-4-carboxylic acid**

1b n = 8, m = 3: 86Inu

phase	III	II	I	I′
	crystalline solid	smectic C* (Sm C*)	chiral nematic	isotropic liquid
state		F	P	
Θ [°C]		71.8	89.8	137.4

Transition temperatures in m = 6 compounds: Fig. 71A-9-004.

3b Tilt angle: Fig. 71A-9-005.

5c Spontaneous polarization: Fig. 71A-9-006.

(C) $C_nH_{2n+1}O$–⬡–OCO–⬡–OCO–⬡–$O(CH_2)_2CH(CH_3)(CH_2)_3CH(CH_3)_2$

4-*n*-alkoxyphenyl-4-(3′,7′-dimethyloctyloxy)benzoyloxy benzoate

1b Transition temperatures: Table 71A-9-001; Fig. 71A-9-007.

5c Spontaneous polarization: Fig. 71A-9-008.

6a Transition enthalpy: see Table 71A-9-001 in subsection 1b.

(D) C_nH_{2n+1}–⬡–COO–⬡–⬡–$OCH(CH_3)C_6H_{13}$

4-(1-methylheptyloxy)biphenyl 4-alkylbenzoate

1b n = 8: 86Inu

phase	III	II	I	I′
	crystalline solid	smectic C* (Sm C*)	chiral nematic	isotropic liquid
state		F	P	
Θ [°C]		64.5	67.4	90.9

Upon cooling transition from Sm C* to smectic B phase occurs at 57.2 °C.

(E) $C_nH_{2n+1}O$–⟨⟩–COO–⟨⟩–⟨⟩–$OCH(CH_3)C_6H_{13}$

4-(1-methylheptyloxy)biphenyl 4-alkoxybenzoate

1b	phase		III	II	I	I′
			crystalline solid	smectic C* (Sm C*)	chiral nematic	isotropic liquid
	state			F	P	
	Θ [°C]	n = 7	76.0	91.5	124.6	
		8	68.8	100.8	125.3	
		11	66.9	109.1	118.3	

86Inu

(F) $C_nH_{2n+1}O$–⟨⟩–COO–⟨⟩–⟨⟩(NO_2)–$OCH(CH_3)C_6H_{13}$

n = 10: W317

3b	Tilt angle: Fig. 71A-9-009, Fig. 71A-9-010.

Table 71A-9-001. $C_nH_{2n+1}O$–⟨⬡⟩–OCO–⟨⬡⟩–OCO–⟨⬡⟩–$O(CH_2)_2CH(CH_3)(CH_2)_3CH(CH_3)_2$. Transition temperature Θ [°C], transition enthalpy ΔH [$\cdot 10^3$ J kg^{-1}], helical twist sense and direction of spontaneous polarization [87Chi]. m.p.: mesophase-crystal boundary. Ch: cholesteric. Iso: isotropic liquid.

n	Twist	P_s (sign)		m.p [a])	Recrystal-lization	Sm C* - Ch [b])	Sm C* - Iso
6	d(+)	(–)	Θ	97.0	56.2	114	154.2
			ΔH	65.6	48.6	3.6	1.8
7	d(+)	(–)	Θ	79.5	55.5	116.6	150.0
			ΔH	49.4	38.1	3.7	1.4
8	d(+)	(–)	Θ	75.1	51.1	120.9	150.6
			ΔH	48.7	31.0	3.4	1.8
10	d(+)	(–)	Θ	67.3	40.5	119.5	143.5
			ΔH	45.7	33.9	3.9	1.7
11	d(+)	(–)	Θ	63.5	48.1	120.0	138.3
			ΔH	38.5	39.4	4.3	1.7
12	d(+)	(–)	Θ	70.5	52.4	120.2	138.6
			ΔH	33.9	44.8	3.6	1.5
14	d(+)	(–)	Θ	65.2	52.7	118.7	133.9
			ΔH	31.8	44.0	3.3	1.6
16	d(+)	(–)	Θ	70.1	65.8	115.8	129.3
			ΔH	59.5	61.6	2.5	1.6

[a]) Temperatures obtained by DSC.
[b]) Temperatures obtained by thermal optical microscopy.

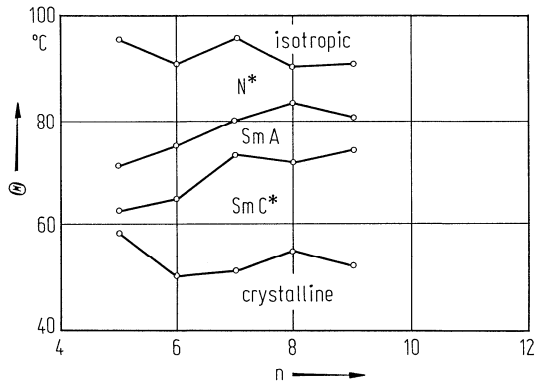

Fig. 71A-9-001. C_nH_{2n+1}–⟨◯⟩–OCO–⟨◯⟩–⟨◯⟩–$OCH(CH_3)C_6H_{13}$. Θ vs. n [86Inu]. N^*: chiral nematic.

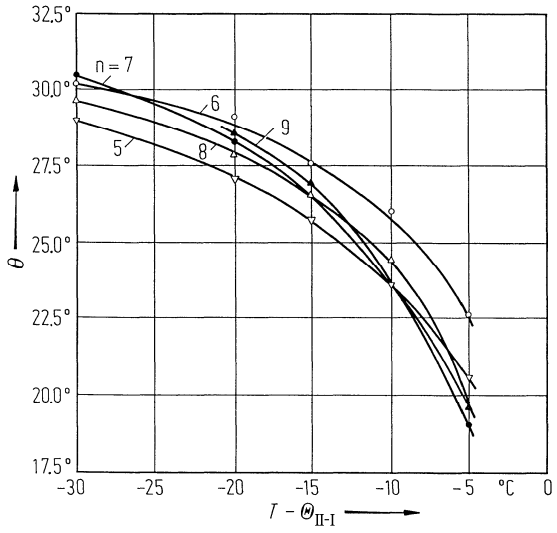

Fig. 71A-9-002. C_nH_{2n+1}–⟨◯⟩–OCO–⟨◯⟩–⟨◯⟩–$OCH(CH_3)C_6H_{13}$. θ vs. $T - \Theta_{II-I}$ [86Inu]. θ: tilt angle. Parameter: n.

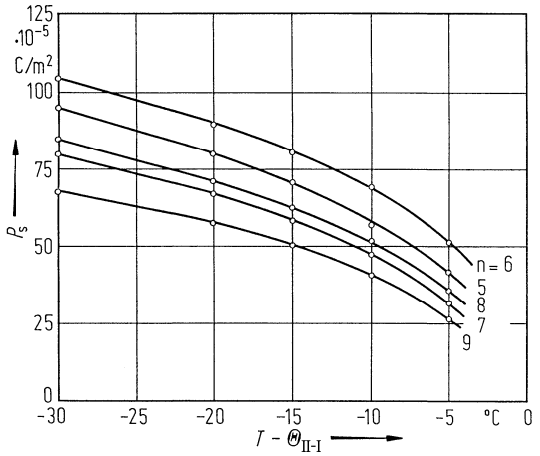

Fig. 71A-9-003. C_nH_{2n+1}–⟨◯⟩–OCO–⟨◯⟩–⟨◯⟩–$OCH(CH_3)C_6H_{13}$. P_s vs. $T - \Theta_{II-I}$ [86Inu]. Parameter: n.

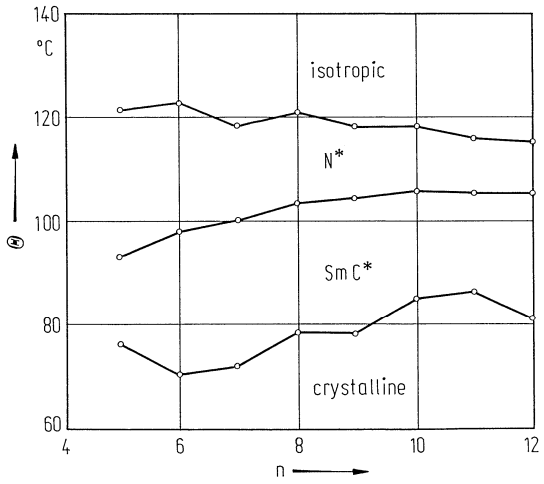

Fig. 71A-9-004. $C_nH_{2n+1}O$–⬡–OCO–⬡–⬡–$OCH(CH_3)C_6H_{13}$. Θ vs. n [86Inu]. N^*: chiral nematic.

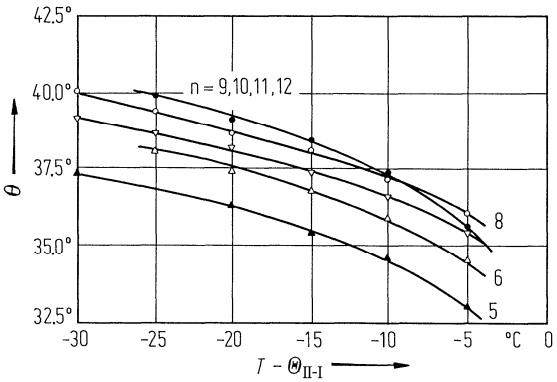

Fig. 71A-9-005. $C_nH_{2n+1}O$–⬡–OCO–⬡–⬡–$OCH(CH_3)C_6H_{13}$. θ vs. $T - \Theta_{II-I}$ [86Inu]. θ: tilt angle. Parameter: n.

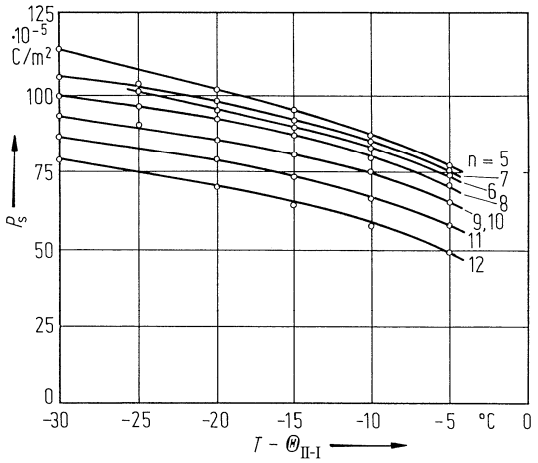

Fig. 71A-9-006. $C_nH_{2n+1}O$–⬡–OCO–⬡–⬡–$OCH(CH_3)C_6H_{13}$. P_s vs. $T - \Theta_{II-I}$ [86Inu]. Parameter: n.

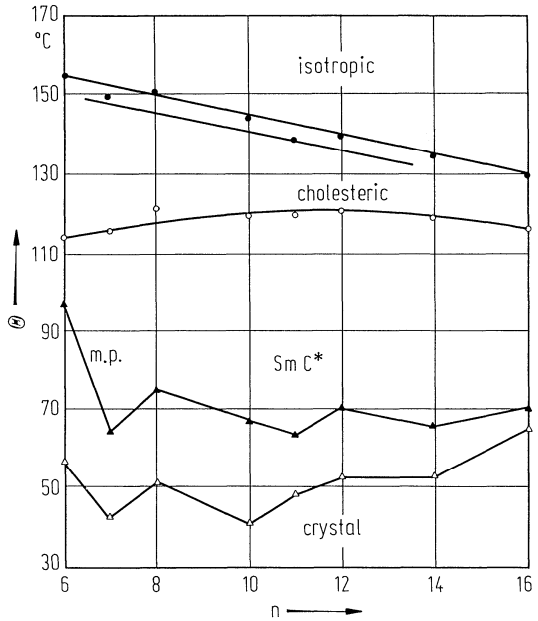

Fig. 71A-9-007. $C_nH_{2n+1}O$–⬡–OCO–⬡–OCO–⬡–$O(CH_2)_2CH(CH_3)(CH_2)_3CH(CH_3)_2$. Θ vs. n [87Chi]. m.p.: mesophase.

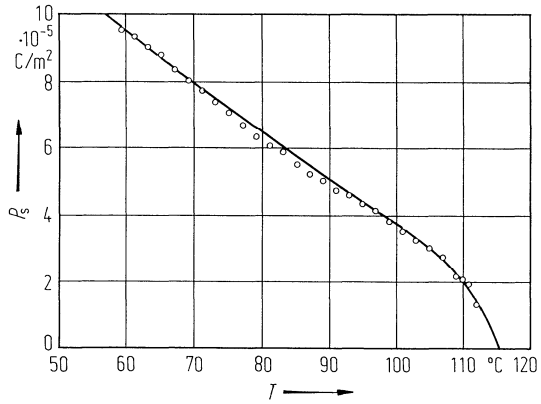

Fig. 71A-9-008. $C_nH_{2n+1}O$–⬡–OCO–⬡–OCO–⬡–$O(CH_2)_2CH(CH_3)(CH_2)_3CH(CH_3)_2$ (n = 7). P_s vs. T [87Chi].

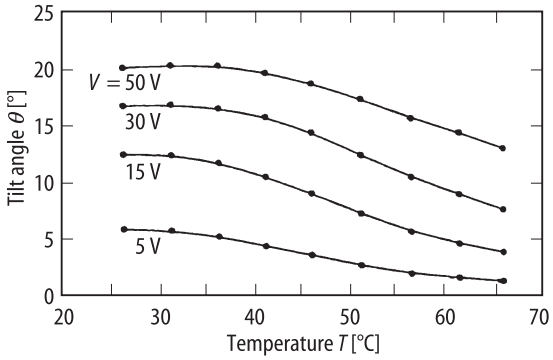

Fig. 71A-9-009. W317. θ vs. T [91Wil]. θ: tilt angle. Parameter: V, applied voltage.

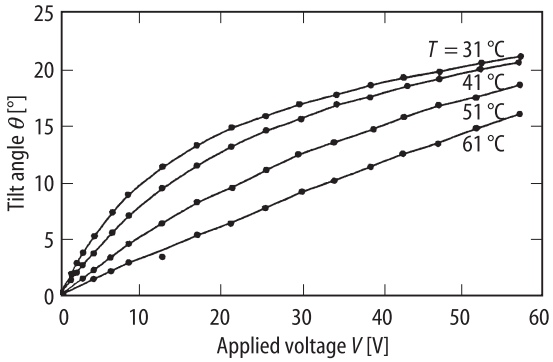

Fig. 71A-9-010. W317. θ vs. V [91Wil]. θ: tilt angle. V: applied voltage. Parameter: T.

References

86Inu Inukai, T., Saitoh, S., Inoue, H., Miyazawa, K., Terashima, K., Furukawa, K.: Mol. Cryst. Liq. Cryst. **141** (1986) 251.

87Chi Chin, E., Goodby, J.W., Patel, J.S., Geary, J.M., Leslie, T.M.: Mol. Cryst. Liq. Cryst. **146** (1987) 325.

91Wil Williams, P.A., Clark, N.A., Ros, M.B., Walba, D.M., Wand, M.D.: Ferroelectrics **121** (1991) 143.

No. 71A-10 ETFPPOPB and analogues

(A) $C_nH_{2n+1}O$–⬡–⬡–COO–⬡–$COOCH(CF_3)CH_2COOC_2H_5$

(–)-4′-(3-ethoxycarbonyl-1,1,1-trifluoro-2-propoxycarbonyl)phenyl 4-[4-(*n*-alkoxy)phenyl]-benzoate

n = 8: ETFPPOPB

3b Helical pitch: Fig. 71A-10-001

5a Dielectric constant: Fig. 71A-10-002.
Dielectric dispersion: Fig. 71A-10-003.

b Effects of applied electric field on κ: Fig. 71A-10-004, Fig. 71A-10-005, Fig. 71A-10-006.
Shift of the peak temperature of κ with E_{bias}: Fig. 71A-10-007.

c Spontaneous polarization: Fig. 71A-10-008.

(B) $C_nH_{2n+1}O$–⬡–⬡–COO–⬡–$COOCH(CF_3)CH_2CH_2$–⬡

(+)-4′-(1,1,1-trifluoro-4-phenyl-2-butoxycarbonyl)phenyl 4-[4-(*n*-alkoxy)phenyl]-benzoate

n = 8: TFPBPOPB

5c Spontaneous polarization: see Fig. 71A-10-008.

(C) $C_nH_{2n+1}O$–⬡–⬡–COO–⬡–$COOCH_2CF(CH_3)COOC_2H_5$

(–)-4′-(2-ethoxycarbonyl-2-fluoro-1-propoxycarbonyl)phenyl 4-[4-(n-alkoxy)phenyl]-benzoate

n = 8: EFPPOPB

5c Spontaneous polarization: see Fig. 71A-10-008.

(D) $(CH_3)_2CHCHClCOO$–⬡–⬡–OOC–⬡–R

(S)-4-(2-chloro-3-methyl-butanoyloxy)-4′-(4-subst.-benzoyloxy)-biphenyl

1b

phase	IV	III	II	I	I′	I″
	crystalline solid	smectic G* (Sm G*)	smectic C* (Sm C*)	smectic A (Sm A)	nematic	isotropic liquid
state		F	F	P	P	

87Moh

R: OC_nH_{2n+1}

	Θ [°C]					
n = 3	113		115			210
4	106		126			211
5	75		120			198
6	85		132			195
7	90		140			185
8	87		154			188
9	82		152			177
10	80		155			172
12	78		162	164		175

	R: C_6H_{13}					
		88	93	140		172
	R: CN					
		125			173	229
	R: OCH_2–CH=CH_2					
		97		104		207
3b	Tilt angle: Fig. 71A-10-009, Fig. 71A-10-010.					
5c	Spontaneous polarization: Fig. 71A-10-011.					

(E) **$(CH_3)_2CHCH_2CHClCOO$– 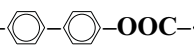 –OC_nH_{2n+1}**

(S)-4-(2-chloro-4-methyl-pentanoyloxy)-4′-(4-*n*-alkoxy-benzoyloxy)-biphenyl

1b	phase	III	II	I	I′	I″	87Moh
		crystalline solid	smectic C* (Sm C*)	smectic A (Sm A)	chiral nematic	isotropic liquid	
	state		F	P	P		
	Θ [°C] n = 5	100	116		158		
	6	86	122	144	156		
	7	81	132	145	160		
	8	80	137	154	160		

(F) **$C_2H_5CH(CH_3)CHClCOO$– 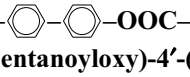 –OC_nH_{2n+1}**

(S)-4-(2-chloro-3-methyl-pentanoyloxy)-4′-(4-*n*-alkoxy-benzoyloxy)-biphenyl

1b	phase	III	II	I	I′	87Moh
		crystalline solid	smectic C* (Sm C*)	chiral nematic	isotropic liquid	
	state		F	P		
	Θ [°C] n = 8	90	177	195		
	12	90	159	190		

(G) **$(CH_3)_2CHCHClCOO$– 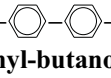 –R**

(S)-4-(2-chloro-3-methyl-butanoyloxy)-4′-subst.-biphenyl

1b	phase	III	II	I	I′	87Moh
		crystalline solid	smectic C* (Sm C*)	chiral nematic	isotropic liquid	
	state		F	P		

	R: H					
Θ [°C]		120				
	R: COOH					
		222		240		260
	R: COO–  –$OOCOC_6H_{13}$					
		130		150		212
	R: COO–  –$OOCOC_7H_{15}$					
		130		150		212

(H) **$(CH_3)_2CHCHClCOO$–  –OOC–  –R**

(S)-1-(2-chloro-3-methyl-butanoyloxy)-4-(4-subst.-benzoyloxy)-benzene

1b	phase	III	II	I	I′	I″	I‴	87Moh
		crystalline solid	smectic C* (Sm C*)	smectic A (Sm A)	chiral nematic	blue phase	isotropic liquid	
	state		F	P	P			
	R: OC_nH_{2n+1}							
	Θ [°C]							
	n = 5	93		(64)				
	6	88		(58)				
	7	75		(54)	(56)	(58)		
	8	49		62	71	73		
	9	65		(47)	67	70		
	10	66	(45)	68	70	72		
	11	77	(44)	(65)				
	12	63	(42)	69				
	R: C_nH_{2n+1}							
	n = 5	77						
	8	33		(23)				
	12	41		(39)				
	R: OCH_2–CH=CH_2							
		42		(40)	55			
							( ): cooling	

(I) $C_2H_5CH(CH_3)CHClCOO–C_6H_4–OOC–C_6H_4–OC_nH_{2n+1}$

(S)-1-(2-chloro-3-methyl-pentanoyloxy)-4-(4-*n*-alkoxy-benzoyloxy)-benzene

1b	phase	III	II	I	I′	I″	87Moh
		crystalline solid	smectic C* (Sm C*)	smectic A (Sm A)	chiral nematic	isotropic liquid	
	state		F	P	P		
	Θ [°C] n = 6	64		(42)	(45)		
	7	62		(33)	(38)		
	8	72	(20)	(48)	(49)		
	9	63		(52)			
	11	72		(57)			
						( ): cooling	

(J) $(CH_3)_2CHCH_2CHClCOO–C_6H_4–OOC–C_6H_4–OC_nH_{2n+1}$

(S)-1-(2-chloro-4-methyl-pentanoyloxy)-4-(4-*n*-alkoxy-benzoyloxy)-benzene

1b	phase	III	II	I	I′	87Moh
		crystalline solid	smectic C* (Sm C*)	smectic A (Sm A)	isotropic liquid	
	state		F	P		
	Θ [°C] n = 8	59		(54)		
	9	59	(30)	(52)		
	10	47	(36)	54		
	11	59		54		
					( ): cooling	

(K) $(CH_3)_2CHCHClCOO–C_6H_4–COO–C_6H_4–OOC–C_6H_4–OC_nH_{2n+1}$

(S)-4-(4-*n*-alkoxy-benzoyloxy)-phenyl-4′-(2-chloro-3-methyl-butanoyloxy)-benzene

1b	phase	III	II	I	I′	87Moh
		crystalline solid	smectic C* (Sm C*)	chiral nematic	isotropic liquid	
	state		F	P		
	Θ [°C] n = 6	90	95	208		
	7	95	100	191		
	8	94	108	198		
	9	106	110	190		
	10	99	123	193		

(L) **$(CH_3)_2CHCHClCOO$–  –COO–R**

(S)-4-(2-chloro-3-methyl-butanoyloxy)-benzoate

1b	phase	III	II	I	I′	87Moh
		crystalline solid	smectic C* (Sm C*)	chiral nematic	isotropic liquid	
	state		F	P		
	Θ [°C]	R: H				
		120				
		R: 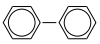				
		83				
		R: 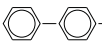 –CN				
		114			188	
		R: 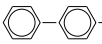 –OOC– 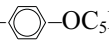 –OC_5H_{11}				
		180	202		340	
		R: 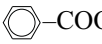 –COO–  –OC_8H_{17}				
		85	107		182	

(M) **$(CH_3)_2CHCHClCOO$–  –COO– 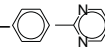 –C_nH_{2n+1}**

(S)-5-*n*-alkyl-2-(4-(4-(2-chloro-3-methyl-butanoyloxy)-benzoyloxy)-phenyl)-pyrimidine

1b	phase		III	II	I	I′	87Moh
			crystalline solid	smectic C* (Sm C*)	chiral nematic	isotropic liquid	
	state			F	P		
	Θ [°C]	n = 6	85		149		
		7	70	96	202		
		9	52	(69)	157		
						( ): cooling	

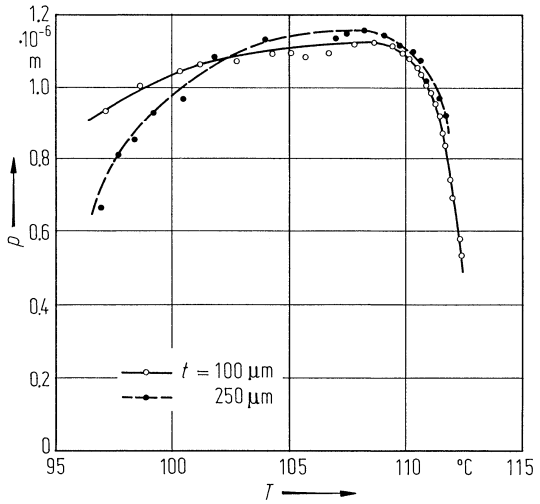

Fig. 71A-10-001. ETFPPOPB. p vs. T [87Tan]. p: helical pitch. Parameter: t, cell thickness.

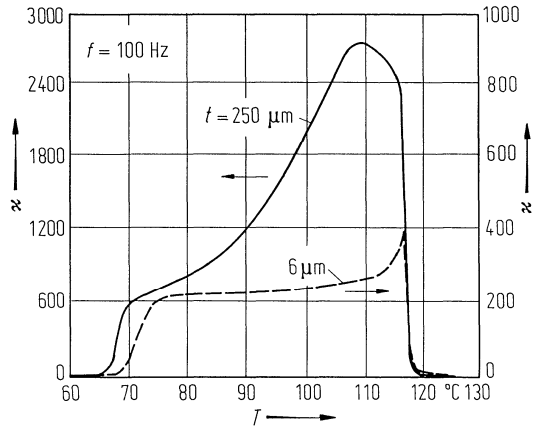

Fig. 71A-10-002. ETFPPOPB. κ vs. T [87Yos1]. Parameter: t, cell thickness. f = 100 Hz.

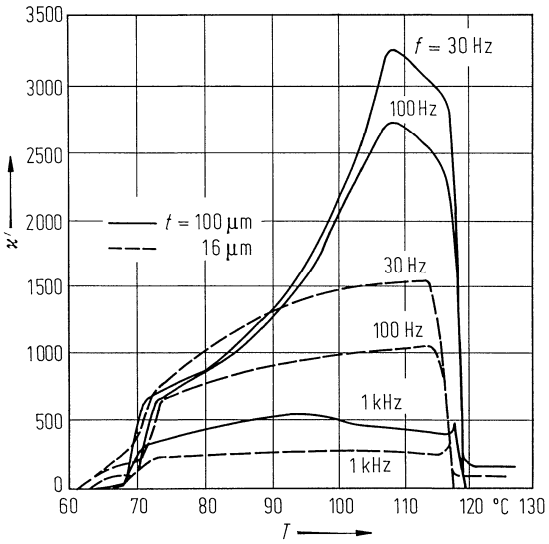

Fig. 71A-10-003. ETFPPOPB. κ' vs. T [87Yos2]. Parameter: *f*. *t*: cell thickness.

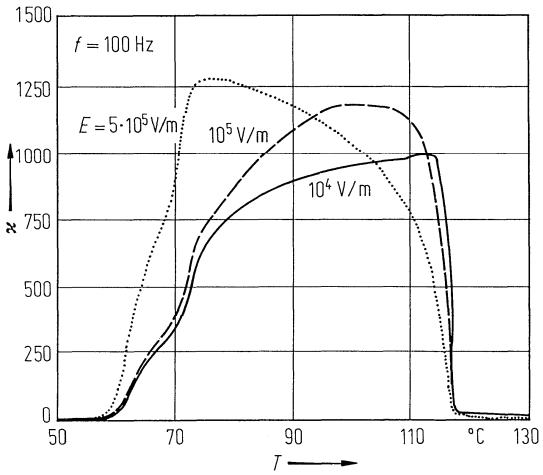

Fig. 71A-10-004. ETFPPOPB. κ vs. T [87Yos3]. Parameter: E, measuring ac electric field. f = 100 Hz.

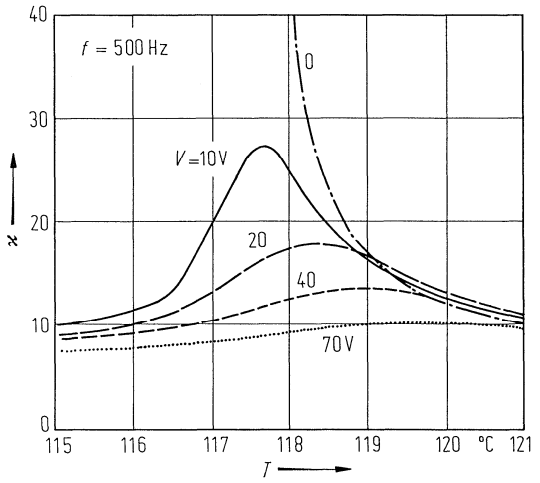

Fig. 71A-10-005. ETFPPOPB. κ vs. T [87Yos4]. Parameter: V, applied dc voltage. Cell thickness: 16 µm. f = 500 Hz.

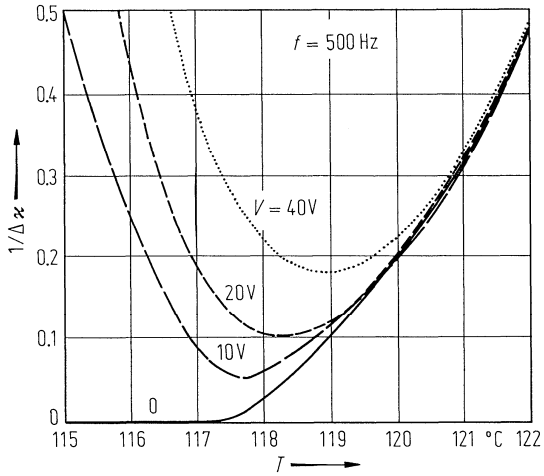

Fig. 71A-10-006. ETFPPOPB. $1/\Delta\kappa$ vs. T [87Yos4]. $\Delta\kappa = \kappa(C^*) - \kappa(A)$, where $\kappa(C^*)$ and $\kappa(A)$ are κ in the Sm C* phase and Sm A phase. Parameter: V, applied dc voltage. Cell thickness: 16 µm. f = 500 Hz.

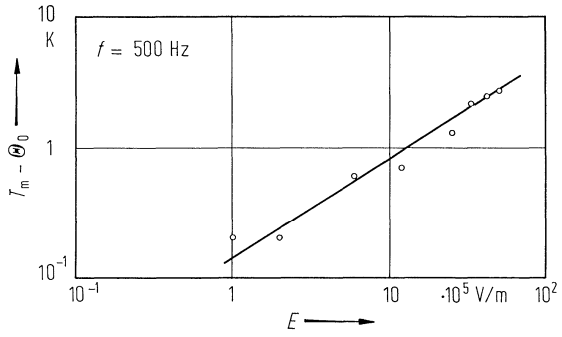

Fig. 71A-10-007. ETFPPOPB. $T_m - \Theta_0$ vs. E [87Yos4]. T_m: temperature at which dielectric constant shows maximum. Θ_0: phase transition temperature between Sm A and Sm C* under no bias field. Cell thickness: 6 µm. f = 500 Hz.

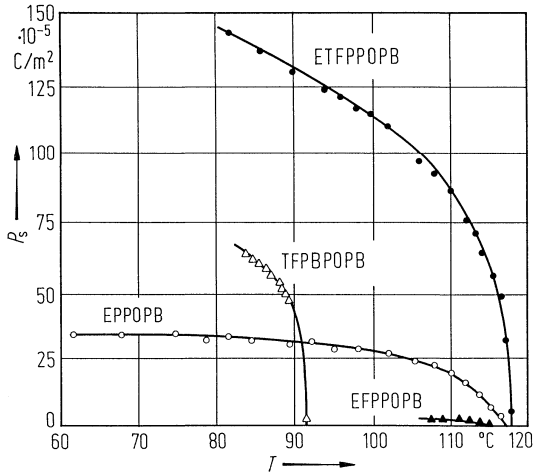

Fig. 71A-10-008. ETFPPOPB, TFPBPOPB, EFPPOPB, EPPOPB. P_s vs. T [87Tan]. EPPOPB: (–)-4′-(3-ethoxycarbonyl-2-propoxycarbonyl)-4-[4-(*n*-octyloxy)-phenyl]-benzoate.

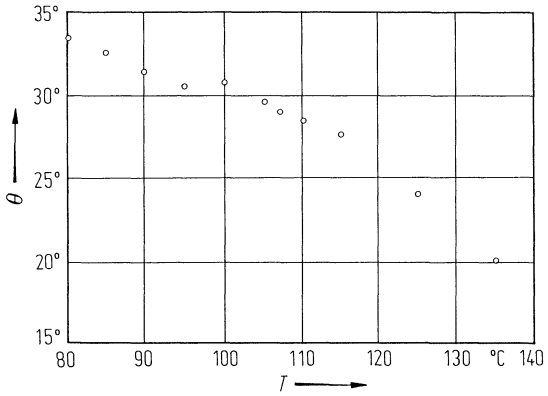

Fig. 71A-10-009. $(CH_3)_2CHCHClCOO$–⟨⟩–⟨⟩–OOC–⟨⟩–$OC_{10}H_{21}$. θ vs. T [87Moh]. θ: tilt angle determined by optical microscopic observation.

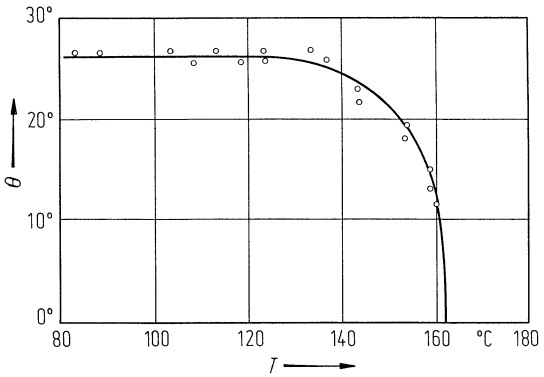

Fig. 71A-10-010. $(CH_3)_2CHCHClCOO$–⟨⟩–⟨⟩–OOC–⟨⟩–$OC_{12}H_{25}$. θ vs. T [87Moh]. θ: tilt angle determined by X-ray diffraction.

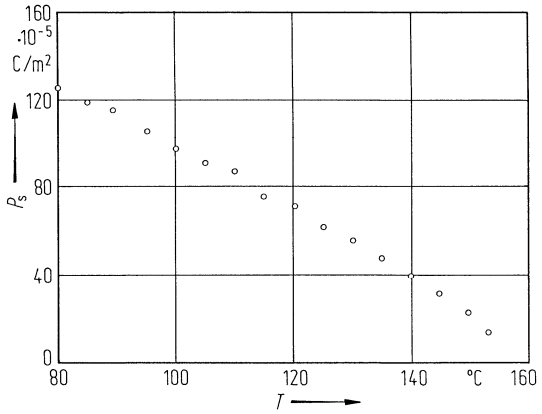

Fig. 71A-10-011. $(CH_3)_2CHCHClCOO$–⟨⟩–⟨⟩–OOC–⟨⟩–$OC_{12}H_{25}$. P_s vs. T [87Moh].

References

87Moh Mohr, K., Kohler, S., Worm, K., Pelzl, G., Diele, S., Zaschke, H., Demus, D., Andersson, G., Dahl, I., Lagerwall, S.T., Skarp, K., Stebler, B.: Mol. Cryst. Liq. Cryst. **146** (1987) 151.
87Tan Taniguchi, H., Ozaki, M., Yoshino, K.: Jpn. J. Appl. Phys. **26** (1987) Suppl. 26–2, p. 101.
87Yos1 Yoshino, K., Nakao, K., Taniguchi, H., Ozaki, M.: Jpn. J. Appl. Phys. **26** (1987) Suppl. 26–2, p. 97.
87Yos2 Yoshino, K., Ozaki, M., Taniguchi, H., Ito, M., Satoh, K., Yamasaki, N., Kitazume, T.: Chem. Express **2** (1987) 53.
87Yos3 Yoshino, K., Ozaki, M., Taniguchi, H., Ito, M., Satoh, K., Yamasaki, N., Kitazume, T.: Jpn. J. Appl. Phys. **26** (1987) L77.
87Yos4 Yoshino, K., Nakao, K., Taniguchi, H., Ozaki, M.: J. Phys. Soc. Jpn. **56** (1987) 4150.

No. 71A-11 Polymer ferroelectric liquid crystal

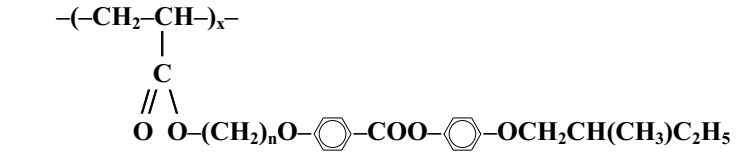

4-*n*-alkoxyphenyl-4′-(4″-methylhexyloxy)-benzoate based polymer

1b	Θ_f = 146 °C.	86Dec
3b	Smectic layer spacing: Fig. 71A-11-001.	

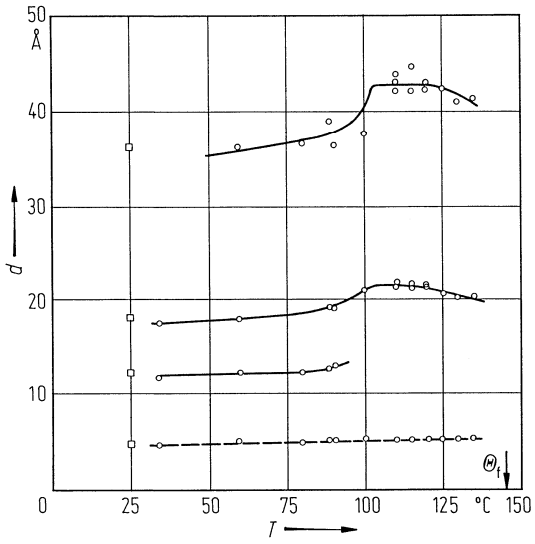

Fig. 71A-11-001. 4-*n*-alkoxyphenyl-4′-(4″-methylhexyloxy)-benzoate based polymer. *d* vs. *T* [86Dec]. *d*: smectic layer spacing. Dashed curve: intermolecular distance. Solid curve: layer spacing. Square: stretched orientated fiber.

Reference

86Dec Decobert, G., Dubois, J.-C., Esselin, S., Noël, C.: Liq. Cryst. **1** (1986) 307.